UNIVERSITEIT VAN PRETORIA
UNIVERSITY OF PRETORIA
YUNIBESITHI YA PRETORIA

Assessment of contaminant transport at a burial site in Middelburg (Mpumalanga, South Africa)

By:

Stephinah Lehlohonolo Aphane

27515819

Submitted in partial fulfilment of the requirements for the degree

M.Sc. Hydrogeology

In the Faculty of Natural and Agricultural Sciences

University of Pretoria

August 2018

DECLARATIONS:

I, Stephinah Lehlohonolo Aphane declare that the thesis/dissertation, which I hereby submit for the degree M.Sc. Hydrogeology at the University of Pretoria, is my own work and has not previously been submitted by me for a degree at this or any other tertiary institution.

SIGNATURE:
DATE:

ACKNOWLEDGEMENTS

I would like to take this opportunity and express my sincere gratitude and deep regard to firstly, heavenly father (God), who has made it possible for me to complete this work. I would then like to acknowledge the people who have embarked with me on this journey.

To my supervisor, Dr. Matthys Dippenaar and my co-supervisor Dr. Roger Diamond, I am truly thankful for the support and guidance they have given me throughout my research work.

I would like to acknowledge my fellow student Sarah Mahlangu for the help, encouragement and team work. To my parents Mr. & Mrs. Aphane, my siblings and my daughter Obonolo Aphane, I am truly thankful and appreciative of the constant love and support they have shown me.

Many thanks to the Water Research Commission & NRF for funding the project and the Steve Tswete Local Municipality of Middelburg, Mpumalanga, for access to the Municipal and Concentration Camp cemetery. Lastly, to Ms J Dykstra and Ms W Grote at the XRD & XRF facility of the Department of Geology, for expert guidance during sample preparation and laboratory analyses.

ABSTRACT

Most present cemeteries were sited without any consideration of the potential risks they may have to the local environment and community. The metals used in coffin-making may gradually weaken into harmful contaminants. These harmful contaminants may mobilize into the groundwater and surrounding soils. According to the literature reviewed, there has been inadequate research carried out on the contamination of groundwater by metals from cemeteries. In light of the aforesaid, the research study aims to assess the mobility of metals from graves that may leach into and contaminate the surrounding soils and groundwater. This study was conducted at the Fontein Street Cemetery in Middelburg (Mpumalanga, South Africa), where 5 boreholes were drilled for the investigation of hydrogeological, geochemical and geological characteristics of the site. The boreholes were monitored for a period of six months, with water samples collected on a monthly basis. Moreover, a total of thirty-eights soil samples and fourty-three water samples were collected for XRD & XRF and ICP-MS analyses, respectively. The analysis of XRD and XRF indicated that the geology of the area is composed of Loskop Formation Sandstones and Dwyka Group Shales, this was also observed on the geological logs of the drilled boreholes. The unsaturated zone of the study site has high concentrations of Zn^{2+}, Rb^{2+}, Sr^{2+} and Zr^{2+} which appeared to have not leached into the groundwater. This was primarily because the unsaturated zone of the area is composed of clay-sand material of low porosity. Water results indicated high concentrations of Cl^{-} and Ca^{2+} from one deep cemetery borehole and high concentrations of SO_4^{2-} from the stream near the cemetery, the municipal water, shallow cemetery boreholes and the Athlone dam. A hydrocensus was conducted for a comparison of water qualities between on-site and off-site boreholes downgradient to the study area. Upon analysis of the results, no correlation was established between water qualities of on-site and off-site boreholes. High concentrations of SO_4^{2-} from the stream, Athlone dam, shallow cemetery boreholes and the municipal water may have resulted from contamination of surface water by acid mine drainage from the surrounding mines within the B12D quaternary catchment. Nonetheless, soils below the grave area have high concentrations of metals than those away from the grave area. Accordingly, this proves that burial practices do indeed influence metal concentrations in cemetery soils, albeit it takes longer for them to reach deeper levels and eventually leach into the groundwater.

LIST OF ABBREVIATIONS

BH	:Borehole
DO	:Dissolved Oxygen
EC	:Electrical Conductivity
GPS	:Global Positioning System
GW	:Groundwater
GWB	:Geochemist's Workbench
ICP-MS	:Inductively Coupled Plasma Mass Spectroscopy
K	:Potassium
LOI	:Loss On Ignition
MCCSSO	:Moisture condition, Colour, Consistency, Structure, Soil texture, Origin
mg/L	:Milligrams per litre
Mun	:Municipal
mV	:Millivolts
SABS	:South African Bereau of Standards
SANS	:South African National Standards
*u*S/cm	:MicroSiemens per Centimetre
Ppm	:Parts Per million
WHO	:World Health Organisation
XRD	:X-Ray Diffraction
XRF	:X-Ray Fluorescence

TABLE OF CONTENTS

LIST OF FIGURES

LIST OF TABLES

1. INTRODUCTION

1.1. Project Background

Almost all present cemeteries were sited without giving regard to the potential risks they may have to the local community and environment. In their study, Zychowski and Tomasz (2014) have proven that cemeteries introduce chemical and biological pollutants into the surrounding earth, water and air, through the decomposition of human corpses. The development of new cemetery sites/graveyards or extensions to such sites has the potential to impact on the local water environment, particularly groundwater underlying the site. Therefore, it is important that when planning such sites, officials and relevant stakeholders consider the possible impacts and where necessary, ensure that adequate site investigation and risk assessment is undertaken.

During the process of decomposition, large quantities of nutrients (e.g. nitrogen) and chemicals (e.g. mercury) are released into the soil and may leach into the groundwater. As a consequence, this can negatively affect the environment and lead to human health problems, such as cancer, if the contaminants reach drinking water sources. The toxic chemicals from the buried coffins that may be released into groundwater include varnishes, sealers, preservatives, metal handles and ornaments used on wooden coffins. In addition, the burial of coffins can pose an environmental and health hazard since the metals that are used in coffin-making can corrode or degrade into harmful toxins.

In most instances, the end-products of a decomposition process are similar to those occurring naturally in the environment. In the case of cemeteries, decomposition of human corpses may cause groundwater pollution not because of any specific toxicity they possess but by increasing the concentrations of naturally occurring organic and inorganic substances to a level sufficient to render groundwater unusable or non-potable (WHO, 1998). As groundwater flows through the ground, metals such as iron and manganese are dissolved and may be found in high concentrations in water. Furthermore, human-induced contaminants also accumulate and migrate to the watertable.

In consideration of the foregoing, the protection of groundwater from the risk of possible contamination is important because, as previously alluded to, pollutants could cause health problems in human beings, reduce the quality of farming and agricultural products, make the water unsuitable for certain industrial processes and pose a threat to the countryside and environment, including rendering the concerned locations or sites unsuitable for recreational purposes. Therefore, the contamination of groundwater does not only have health and environmental impacts, but also serious economic consequences.

The vadose zone has been found to be the most important line of defence against transport of degradation products into aquifers, in the past research studies (WHO, 1998). It was established that the vadose zone acts as both a filter and an adsorbent. The prevailing assumption is that the most functional soil type to increase retention of degradation products is a low porosity clay-sand mix with a small to fine grain size. The study therefore, focuses on assessing the transport of contaminants through the vadose zone and determining whether the vadose zone is the defence mechanism against the transportation of degradation products into aquifers. The study particularly pays attention on the mobility of metals in cemetery soils and their concentrations.

1.2. The South African Context

Within the South African context, Jonker and Olivier (2012) investigated the mineral contamination of cemetery soils in Zandfontein Cemetery (Pretoria). Being of comparative nature in approach, their study compared the mineral concentrations of soils within the cemetery to those off-site, as well as those in zones with high burial loads with zones with fewer burials. They found that mineral concentrations of soils within the Zandfontein cemetery were considerably higher than those off-site. The soil samples in multiple burial blocks also had elevated metal concentrations. However, the researchers pointed out that the results did not necessarily reflect the situation at other cemeteries in Pretoria and the surroundings. According to the final report, “the fact that this cemetery is located on the slopes of a mountain may cause leaching of minerals into groundwater and aggravate potential health risks”.

Similarly, Van Alleman et al. (2018) conducted a laboratory study on the pollution of formaldehyde in cemeteries (South Africa). The findings of their study indicated a percolation

of formaldehyde through the soil between week 6 and week 14 of interment, with a greater amount being leached from sand. However, different environmental conditions such as soil type, pH, temperature, and rainfall did not appear to affect the amount of leachate or the mobility rate through soils, although sand allowed more effective leaching. Considering the fact that burials take place on a weekly basis in operational cemeteries in South Africa, the accumulated amount of formaldehyde reaching the groundwater may be a matter of concern.

Prior to the implementation of environmental legislation, most cemeteries were sited by chiefs and kings in black communities, who neither had scientific knowledge of the potential hazardous impact of burials on the environment nor access to pertinent expert wisdom. As a result, most cemeteries were poorly sited and currently poses potential health hazards on groundwater in many rural parts of South Africa. Groundwater is a hidden treasure for sustainable development and plays a vital role in communities, especially in rural areas. A significant increase in the number of deaths due to various factors, including the HIV/AIDS pandemic, is recognised as causing problems for already stretched cemetery facilities throughout many parts of South Africa. As a consequence of the growing death rate, it is patently obvious that more burial sites would be needed in the near future. It is precisely because of this consideration, amongst others, that a proper planning for cemetery siting is necessary.

1.3. Objectives

The study aims to:

- Review metal mobility, notably those emanating from burial sites, in changing redox conditions at variable saturation in South African context
- Conduct a case study at the Fontein Street Cemetery in Middelburg, Mpumalanga, by sampling and running hydraulic tests within the cemetery

2. LITERATURE REVIEW

2.1. Subsurface Water

The hydrological cycle involves the continual movement of water between the atmosphere, surface water and the ground (Muldoon & Payton, 1993). The groundwater system should be understood in relation to both surface water and the atmospheric moisture. Groundwater recharge mostly comes from the atmosphere in the form of precipitation. However, surface water in streams, rivers, ponds, lakes and artificial impoundments moves into the groundwater system wherever the hydraulic head of the water surface is higher than the water table (Boulding & Ginn, 2004). Water typically enters the vadose zone in the form of rainfall or irrigation, or by means of industrial and municipal spills. Some of the rainfall or irrigation water may be intercepted on the leaves of vegetation. In an instance where the rainfall or irrigation intensity is larger than the infiltration capacity of the soil, water will be removed by surface runoff, or will accumulate at the soil surface until it evaporates back to the atmosphere or infiltrates into the soil.

Moreover, some of the water that infiltrates into the soil profile may be taken up by plant roots and eventually returned to the atmosphere by plant transpiration. The processes of evaporation and transpiration are often combined into the single process of evapotranspiration. Only water that is not returned to the atmosphere by evapotranspiration may percolate to the deeper vadose zone and eventually reach the watertable. If the watertable is close enough to the soil surface, the process of capillary rise may move water from the groundwater table through the capillary fringe toward the root zone and the soil surface (Simunek& Van Genuchten, 2006).

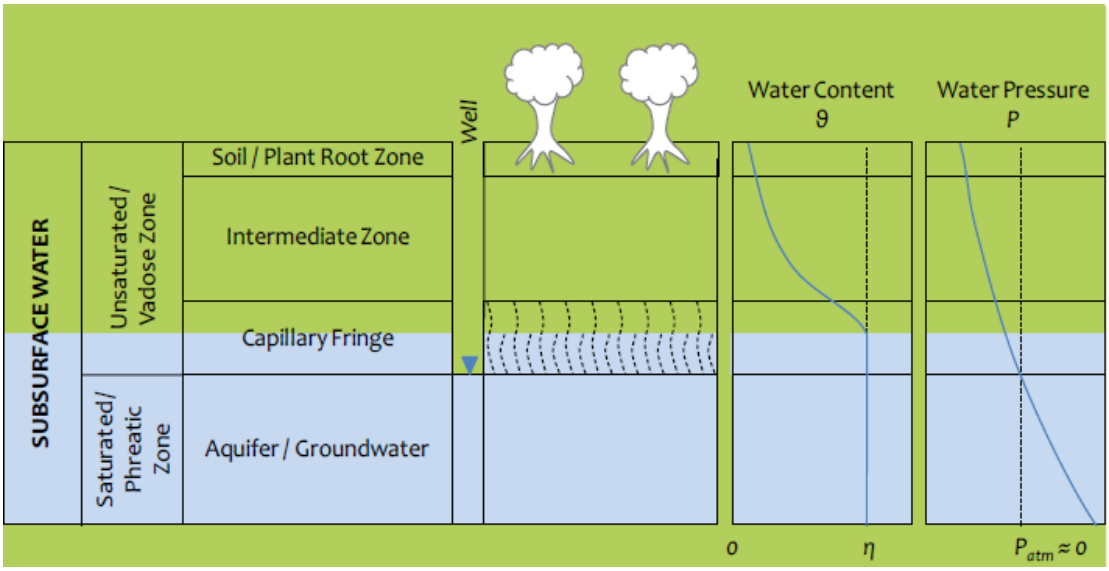

Figure 1: Classification of subsurface water (Adapted from (Fitts 2002) (Fetter 1994) (Todd & Mays 2005).

2.1.1. The vadose zone

The term vadose is derived from the Latin *vadosus*, meaning shallow. The vadose zone, which is also termed the unsaturated zone or the zone of aeration, is the part of the Earth which extends from the land surface to the water table (the lowest water table if there is more than one). The pore space of the vadose zone is usually filled with air and water. The vadose zone overlies the saturated zone or any aquifer. Typically, there is a contaminant release; the contaminants must pass through this region to get to the aquifer. Although this region is not saturated (i.e. having all available pore space filled with fluid), areas may be locally saturated, while elsewhere fluid moves in response to tension and capillary forces. The vadose zone is also typically where volatile contaminant gases or vapours will arise and move from contaminant releases. The vadose zone is geologically a very heterogeneous region. Generally, soil formation occurs at the surface and soils may be buried sequentially in fluvial and alluvial depositional processes. Vadose zones may vary in thickness from several kilometres to hundred kilometres (Palmer, 1996).

Rates of transport of water and other substances within the vadose zone influence infiltration, runoff, erosion, plant growth, microbiota, contaminant transport, and aquifer recharge and discharge to surface water. The flow of the vadose zone is complicated due to non-linearity and hysteresis of unsaturated hydraulic properties, and extreme sensitivity to materials and hydraulic conditions (Nimmo, 2009). Boulding and Ginn (2004) are of the opinion that the vadose zone is also a significant reservoir for the capture, storage and release of contaminants

and therefore cannot be ignored in the study of contaminant hydrogeology. Although the term unsaturated zone is often used loosely to refer to the vadose zone, part or all of this zone may be irregularly saturated and may contain several important subdivisions.

The vadose zone has three major subdivisions (Van Schalkwyk & Vermaak, 2000):

- Soil water or root zone

  This zone lies between the ground surface and the maximum depth to which roots penetrate. It is characterised by large fluctuations in the quantity and quality of moisture in response to transpiration and evaporation.

- Intermediate vadose

  This zone contains a residual moisture content determined by the matric potential. In coarse-grained (sand and gravel), the amount of water held by matric potential is low; in fine-grained materials, particularly clays, the amount of water held may be very high. Since this zone also contains a significant amount of air in pore spaces, gravitational water reaching this zone moves relatively slowly to the saturated zone by unsaturated flow until it reaches the capillary fringe.

- Capillary fringe

  The capillary fringe, which is also known as the zone of tension saturation, is the transition zone between the saturated and unsaturated regions. It is the layer in which groundwater seeps up from a water table by capillary action to fill pores. Pores at the base of the capillary fringe are filled with water due to tension saturation. This saturated portion of the capillary fringe is less than the total capillary rise because of the presence of a range in pore sizes. If the pore size is small and relatively uniform, it is possible that soils can be completely saturated with water for several metres above the water table.

Contaminants entering the vadose zone will tend to move more slowly than in the saturated zone because of the processes described above that retard the rate of water movement. For instance, in the root zone, contaminants may be removed from the soil and incorporated into plant tissue or they may remain in the soil after water is removed by transpiration until more water enters the soil and moves them farther down the soil profile (Boulding & Ginn, 2004).

2.1.2. The phreatic zone

The phreatic zone, which is also known as the zone of saturation, is the area below the watertable, in which all pores and fractures are saturated with water. The upper boundary of the phreatic zone defines the lower boundary of the vadose zone. Pore water pressure in the phreatic zone is greater than that of the atmosphere. Water within the phreatic zone will readily flow out of the pores while the negative pressures within the capillary fringe tightly hold the water in place.

2.1.3. Chemical composition of groundwater

The chemical and biochemical interactions between groundwater and the geological materials of soils and rocks provide a wide variety of dissolved inorganic and organic constituents. Other important considerations include the varying composition of rainfall and atmospheric dry deposition over groundwater recharge areas. The principal dissolved components of groundwater are the six major ions sodium (Na^{+}), calcium (Ca^{2+}), magnesium (Mg^{2+}), chloride (Cl^{-}), bicarbonate (HCO_3^{-}) and sulphate (SO_4^{2-}). These cations and anions comprise over 90% of the total dissolved solids content, regardless of whether the water is dilute rainwater or has a salinity greater than seawater. Minor ions include potassium (K^{+}), dissolved iron (Fe^{2+}), strontium (Sr^{2+}) and fluoride (F^{-}). The introduction of contaminants into groundwater by human activities can result in some normal minor ions reaching concentrations equivalent to major ions (Hiscock & Bense, 2014).

General water quality indicators are parameters used to indicate the presence of harmful contaminants. Testing for indicators can eliminate costly tests for specific contaminants. Generally, if the indicator is present, the supply may contain the contaminant as well. For example, turbidity or lack of clarity in a water sample usually indicates that bacteria might be present. The pH value is also considered a general water quality indicator. High or low pHs can indicate how corrosive the water is. Corrosive water may further indicate that metals like lead or copper are being dissolved in the water as it passes through the distribution pipes (Hiscock & Bense, 2014).

2.2. Contaminant Transport

Soils, whether in urban or agricultural areas, represent a major sink for metals released into the environment from a wide variety of anthropogenic sources (Nriagu, 1990). Once in soil, some of these metals would be persistent because of their immobile nature. Other metals are more mobile, and therefore are transferred either through the soil profile down to groundwater, or via plant-root uptake (bio available). Pollution problems arise when metals are mobilized into the soil solution and taken up by plants or transported to the surface water or groundwater. The properties of the soil are thus very important in the attenuation of metals in the environment. The solubility of metals in soil is controlled by reactions with solid phases (Sherene, 2010).

Increased attention has recently been paid to the vadose zone where much of the subsurface contamination originates, passes through, or can be eliminated before it contaminates surface and subsurface water resources. Sources of contamination often can be more easily remediated in the vadose zone, before contaminants reach the underlying groundwater. The concentration of metals in an uncontaminated soil is primarily related to the geology of the parent material from which the soil was formed. Metals associated with the aqueous phase of soils are subject to movement with soil water, and may be transported through the vadose zone to groundwater (McLean & Bledsoe, 1992).

Metals in the soil solution are subject to a net movement of mass out of the system by leaching to groundwater, plant uptake, or volatilization, a potentially important mechanism for Hg, Se, and As. The concentrations of metals in the soil solution are governed by interrelated processes such as inorganic and organic complexation, redox reactions, precipitation/dissolution reactions, and adsorption/desorption reactions. Immobilization of metals, by mechanisms of adsorption and precipitation, prevents movement of metals to groundwater. Metals, unlike organics, cannot be degraded. Some metals, such as Cr, As, Se, and Hg, can be transformed to other oxidation states in soil, changing their mobility and toxicity (McLean & Bledsoe, 1992).

The rate of travel of water and pollutants through the vadose zone depends largely on the type of soil present and the infiltration rate, this was discovered by soil scientists (Selker et al., 1999). However, just because water moves well through a soil does not mean that pollutants will move at the same rate. Each type of pollutant will interact with the soil in its own way.

The mobility of inorganics, metals, or organic pollutants is compound-specific and depends on the soil matrix. Nevertheless, metals and microorganisms are more likely to adsorb, or stick, to soil particles (Pitt et al., 1996).

2.2.1. Transport mechanisms

Most groundwater contaminants are reactive in nature and infiltrate through the vadose zone, reach the watertable and continue attenuate with groundwater flow. Contaminants are introduced into groundwater through a variety of mechanisms, which include advection, dispersion, molecular diffusion and retardation. Each of these mechanisms plays a significant role in the amount of contamination that may reach the aquifer. Advection is the movement caused by the flow of groundwater. Dispersion is the movement caused by the irregular mixing of waters during advection. Molecular diffusion is the process by which molecules show a net migration. Retardation occurs through a variety of processes attenuating contaminants (Verral et al., 2008).

2.2.1.1. *Advection*

The term advection refers to the transport of solutes by the bulk movement of groundwater, the movement of particles within flowing water. For a contaminant to rapidly progress away from its source, advection along with dispersion is required. If a positive hydraulic gradient is present, advection will take place in the direction of the flow of the hydraulic gradient. However, advection like dispersion, also depends on physical properties of the aquifer as well as chemical properties of the contaminant. Contaminants such as metals from graves will move through the groundwater, if reached, in the form of advection. A smaller amount of dispersion may take place, depending on the aquifer properties, and even less diffusion depending on the contamination state of the groundwater and the adsorptive properties of the aquifer material. This can only take place if groundwater is moving under a hydraulic gradient (Verral et al., 2008).

Groundwater flow/advection is calculated using Darcy's law (Eq. 1).

$$Q = KiA \quad [1]$$

Where:
Q = quantity of flow per unit of time, in gpd
K = hydraulic conductivity, in gpd/ft^2
i = hydraulic gradient
A = cross-sectional area through which the flow moves, in ft^2 (Boulding & Ginn, 2004).

2.2.1.2. *Hydrodynamic dispersion*

Hydrodynamic dispersion is the net effect of a variety of microscopic, macroscopic and regional conditions that influence the spread of a solute concentration front through an aquifer (Anderson, 1984). Mechanical dispersion and molecular diffusion cannot always be distinguished, and are subsequently termed hydrodynamic dispersion together.

Mechanical dispersion

The water molecules and dissolved species making up flowing groundwater do not pass through the subsurface in an orderly fashion. Instead of following simple trajectories, they branch continually into threads, moving around grains, into and out of areas of high conductivity, or along fractures. The threads may combine with threads of distant origin, or recombine with those from which they have previously split. Some threads move ahead of the average flow, others are retarded relative to it; a thread may follow the centreline of the flow or stray far to the side. In this way, groundwater continually mixes by mechanical means, an effect known as hydrodynamic dispersion (Freeze & Cherry, 1979).

Dispersion on the microscopic scale is caused by (1) external forces acting on the groundwater fluid, (2) variations in pore geometry, (3) molecular diffusion along concentration gradients, and (4) variations in fluid properties such as density and viscosity. Dispersion at this scale, also called mechanical dispersion, is generally less accurate than estimated advective flow and, for this reason, is often ignored (Boulding & Ginn, 2004).

Dispersion on the macroscopic scale is caused by variations in hydraulic conductivity and porosity, which create irregularities in velocity and consequent additional mixing of the solute.

Over large distances, regional variations in hydrogeologic units can affect the amount of dispersion that occurs. Macroscopic dispersion may result in substantially faster travel times of contaminants than those predicted by equations for mechanical dispersion (Boulding & Ginn, 2004).

Molecular diffusion

Molecular diffusion (or self-diffusion) is the process by which molecules show a net migration, most commonly from areas of high to low concentration, as a result of their thermal vibration, or Brownian motion. Molecular diffusion is best described by Fick's law. This law states that a substance put into solution close to a dissolving material will tend to diffuse towards constant concentration throughout the solution (Mondofacto, 1997). Fick's first law relates the diffusion flux, *J*, to the steepness of the concentration gradient.

$$J = -D\frac{dC}{dx'} \qquad [2]$$

Where:

J = The mass flux i.e. the movement of matter from one point to another per time unit

D = diffusion coefficient

C = concentration of the ion in question

X = the distance that the material is diffusing

2.2.1.3. *Retardation*

Retardation refers to the process by which chemical reactions slow the transport of a contaminant plume through the subsurface, relative to the average groundwater solids, or from precipitation. A sorbing contaminant introduced to an aquifer, for example, traverses the aquifer more slowly that the flowing groundwater, because some of the contaminant is continually removed from solution. The contaminant will arrive at a point along the aquifer sometime after the water that originally contained it. If clean water is introduced to a contaminated area, conversely, a sorbing contaminant is flushed from the aquifer more slowly than water migrates along it. Even under ideal circumstances, groundwater in an aquifer containing a sorbing pollutant may need to be replaced many times before the aquifer is clean (Bethke, 2008).

In groundwater contaminant transport, several chemical and physical mechanisms retard or slow the movement of constituents in groundwater. Four major mechanisms that retard contaminant movement are; filtration, sorption, precipitation and transformation or degradation. ***Figure 2*** illustrates the movement of a concentration front by advection only (A), advection plus dispersion (A + D), and with the addition of sorption, a partitioning process (A + D + S). The greatest retardation, however, results from the combined effects of advection, dispersion, sorption, and biotransformation (A + D + S + B). The amount of retardation resulting from sorption, other partition processes, and biotransformation depends on physical and chemical properties of the aquifer, including populations, and chemical properties of the contaminant (Boulding & Ginn, 2004).

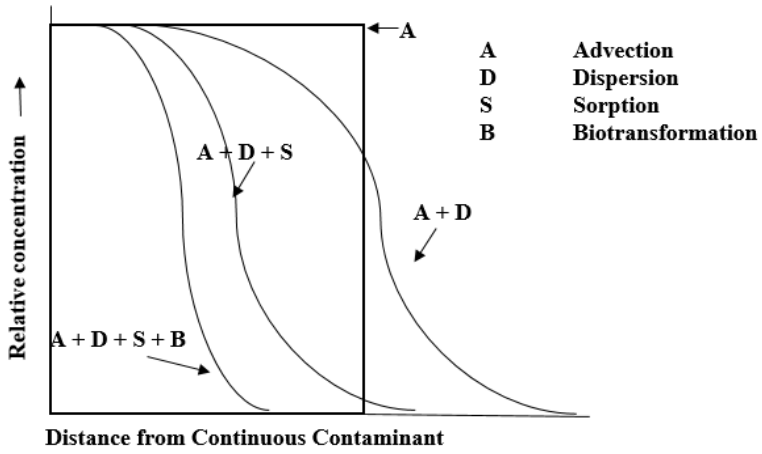

Figure 2: Effect of dispersion and retardation on movement of a contaminant front from a continuous source (Boulding & Ginn, 2004).

2.3. Groundwater Pollution

Groundwater pollution usually results from a variety of anthropogenic sources. The sources of groundwater pollution are many and varied, and include waste disposal facilities, industrial pollution, wastewater treatment works, on site sanitation, cemeteries and many others (Tredoux et al., 2004), as shown in ***Table 1***. The alteration and degradation of the natural quality of groundwater result where groundwater pollution occurs. Sililo and Saymaan (2001) recognised a wide range of pollutants that occur in groundwater. These pollutants included bacteria and other micro-organisms, major inorganic ions (NO_3, Cl, SO_4, etc.), trace ions, and a varied range of organic chemicals (Sililo & Saymaan, 2001).

The potential of groundwater pollution by cemeteries has been disregarded in South Africa (Engelbrecht, 1998). In the past groundwater pollution was not taken into consideration when siting cemeteries. Engelbrecht (1998) undertaken a research study on groundwater pollution at a local cemetery and the study results shown how the rising water tables in winter can lead to significant impacts.

Table 1: Groundwater pollution sources with some of their main characteristics (Tredoux et al., 2004).

Pollution Category	Pollution Source	Main Pollutant	Potential Impact
Municipal	Sewer leakage	Nitrate Viruses and Bacteria	Health risk to users, eutrophication of water bodies, odour and taste
	Septic tanks, cesspools, privies		
	Sewage effluent and sludge	Nitrate, Minerals, organic compounds, Bacteria and Viruses	
	Storm water runoff	Bacteria and Viruses	Health risk to water users
	Landfills	Inorganic minerals, Organic compounds, Heavy metals, Bacteria and Viruses	Health risk to users, eutrophication of water bodies, odour and taste
	Cemeteries	Nitrates, Bacteria and Viruses	Health risk to water users
Agriculture	Feedlot wastes	Nitrate-nitrogen-ammonia, Viruses and Bacteria	Health risk to water users (e.g. Metahemoglobinemia)
	Pesticides and herbicides	Organic compounds	Toxic/Carcinogenic
	Fertilizers	Nitrogen, Phosphorus	Eutrophication of water bodies
	Leached salts	Dissolved salts	Increased TDS in groundwater
Industrial	Process water and plant effluent	Organic compounds Heavy metals	Carcinogens and toxic elements (As, Cn)
	Industrial landfills	Inorganic minerals, Organic compounds, Heavy metals, Bacteria and Viruses	Health risk to users, eutrophication of water bodies, odour and taste
	Leaking storage tanks (e.g. Petrol stations)	Hydrocarbons, Heavy metals	Odour and taste
	Chemical transport	Hydrocarbons, chemicals	Carcinogens and toxic compounds
	Pipeline leaks		
Atmospheric Deposition	Coal fired power stations	Acidic precipitation	Acidification of groundwater and toxic leached heavy metals
	Vehicle emissions		
Mining	Mine tailings & stockpiles	Acid Drainage	
	Dewatering of mine shafts	Salinity, inorganic compounds, metals	May increase concentrations of some compounds to toxic levels
Groundwater Development	Salt and water intrusion	Inorganic minerals Dissolved salts	Steady water quality deterioration

2.4. Metal Mobility in Soil

Trace metals found in the soil can contribute to the surface water and groundwater contamination through runoff and vertical transportation, respectively (Wu et al., 2014). Once deposited in soil, the mobility of trace metals is controlled by their chemical speciation including chemical fraction, surface complex, and surface precipitation, etc., which are further affected by various environmental conditions (Grafe et al., 2014).

In contaminated soils, many geochemical conditions like pH, Eh, and coexisting chemical components influence the behaviors of redox-sensitive elements (Borch et al., 2010). Arsenic is found to be one of the most intensively studied elements due to its high toxicity and frequent occurrence in soil and groundwater originating from both natural and anthropogenic sources. In the study of the geochemical behaviour of As, the effect of competitively adsorbing ions, particularly oxyanions, has been identified as an important controlling factor in mineral and soil suspensions (Campbell & Nordstrom, 2014). In their study, Pettry and Switzer (2001) observed that the concentration of arsenic in soil may correlate with clay content, pH, cation exchange capacity, organic matter content, and most significanctly Fe and Al concentration.

Trace metals in soil are associated with various risks that depend mainly on their chemical forms (Kirpichtchikowa et al., 2006). An accurate assessment of trace metals, their forms in soil and their dependence on soil properties is the foundation for proper soil management, hence, will reduce drastically their negative impacts on the environment (Aydinalp & Marinova, 2003).

Concentrations of metals in soils help in determining the vertical and horizontal extent of contamination and for measuring any net change (leaching to groundwater, surface runoff, erosion) in soil metal concentration over time (Mehes-Smith et al., 2014). In the environment, heavy metals (metals of relatively high density, or high relative atomic weight) are generally more persistent than organic contaminants such as pesticides or petroleum by-products (Hashim et al., 2011). It is important to have a better understanding about the fractionation and speciation of toxic metals in soils in order to assess contamination of soil by metals more accurately (Ghayoraneh & Qishlaqi, 2017).

The unsaturated zone does not always attenuate and immobilise contaminants (Silillo, 1997). Only few chemicals will be attenuated, others will rapidly leach into and contaminate groundwater. The fate of inorganic contaminants in soils are usually affected by factors such as contaminant characteristics, the presence of other reactive species, the physical and chemical conditions in solution, the presence of complexing ligands, and the nature and surface area of solid particles and adsorbing surfaces (Silillo & Saayman, 2001).

Surface area, particle size, structure, mineralogy, organic and mineral coatings are the important soil properties that control contaminant attenuation (Silillo & Saayman, 2001). Silillo and Saayman (2001) further noted texture and surface area to be closely related, in a manner that as particle size decreases, the surface area per unit mass increases. Elements tend to be less mobile in soils with large quantity of sorption sites, eg. Clays. Soil organic matter provides cation adsorption sites and is also involved in hydrophobic sorption of organic compounds (Silillo & Saayman, 2001).

2.5. Factors affecting adsorption and metal mobility in soils

Some of the different soil properties that influence the attenuation capacity of soil are; soil pH, soil organic matter, clay content, Fe and Mn oxides, and will be discussed in the sections that follow.

2.5.1. Soil pH

Vangheluwe et al. (2005) consider the soil pH as the primary soil property that controls every chemical and biological process in the soil environment. The pH of the soil applies to the H^+ concentration in solution present in soil pores which is in dynamic equilibrium with the mainly negatively charged surfaces of the soil particles. The soil pH therefore controls the number of negatively charged binding sites for cations (Vangheluwe et al., 2005). Metal speciation, solubility from mineral surfaces, movement and bioavailability is also strongly influenced by soil pH (Zhao et al., 2010) The soil pH is therefore considered as a very important soil variable in the attenuation of metals (Sparks, 2003).

Accordingly, soil pH will only affect the mobility of some contaminants. For instance, with the exception of selenium, chromium, and arsenic at some valence states, the mobility of trace

elements and heavy metals increases with a decrease in pH (Brusseau & Wilson, 1995). For metal cations, high pH promotes sorption and precipitation as oxides, hydroxides and carbonates. Although pH is regarded as the primary variable, there are instances where well-buffered soils can resist pH changes whether acidity or alkalinity is introduced in one form or another (McBride, 1994).

In a study by Bang and Hesterberg (2004) a decrease in pH revealed an increase in desorption of Cd, Pb and Zn and thus an increase in the mobility and bioavailability of these metals (Wang et al., 2006. The soil pH can range from pH < 3 in pyritic soils, to pH > 9 in sodium affected or black-alkali soils. Soils with pH values less than 4 and greater than 8.5 are usually considered to be impacted by human activities (Sparks, 2003). In general heavy metals cations are most mobile under acid conditions (Alloway, 1995).

2.5.2. Soil organic matter

Organic matter is in a stable state in the soil. This is the state where it has been decomposed until it is resistant to further decomposition. Only about 5% of it usually mineralizes on a yearly basis (Herselman et al., 2013). That rate increases only if temperature, oxygen, and moisture conditions favour decomposition (Brady, 2002). Organic substances play a vital role in geochemical cycling and biochemical weathering of trace elements (Kabata-Pendias & Pendias, 2001).

Organic matter serves as a reservoir of nutrients, trace elements and water in the soil, aids in reducing compaction and surface crusting, and increases infiltration of water into the soil. Organic matter has many negative charges which result from the dissociation of organic acids, which have a high affinity to adsorb metal cations and reduce its availability (Vangheluwe et al., 2005). These elements are gradually released into the soil solution and made available to plants throughout the growing season (Brady, 1999).

Soil organic matter plays a vital role in metal attenuation. Apart from soil pH, it is viewed as the most important soil factor controlling metal movement. Studies conducted by Sauvé (2000) indicated that the majority of dissolved metals in soil were found in metal-organic complexes.

Consequently, any factor that has an influence on the organic matter will have an influence on the metal solubility.

2.5.3. Clay content

The percentage of clay, silt and sand in the soil control the soil textural class. Clays are soil particles less than 2µm in size, having a higher surface area than other soil particles like sand and silt (Vangheluwe et al., 2005). These small particles have a permanent charge which is mainly negative but in some instances a positive charge can develop (Coyne & Thompson, 2006). Cations are attracted to the mostly negative charged surfaces which render them less mobile than in situations where these charges are not available, i.e. where there are less clay particles.

Clay minerals are the products of weathered rock and affect both soil physical and chemical properties. The amount and type of clay minerals present affects soil factors such as the shrink-swell behaviour, plasticity, water holding capacity as well as the exchange capacity of the soil (Brady & Weil, 2002). Clay minerals may contain small amounts of trace elements as structural components, but their sorption capacities to trace elements play an important role.

2.5.4. Fe and Mn oxides

Fe and Mn oxides have significant effects on many soil chemical processes such as sorption and redox due to their high specific surface area (Sparks, 2003). They are also referred to as accessory minerals owing to their intimate association with the layer silicates and occur in the clay size fraction of soils, usually mixed with the clays. Metal oxides are able to mask the surface properties of layer silicates (Essington, 2004). The metal oxides have a pH dependent charge and can therefore develop a negative or positive charge subject to the soil chemical properties (negative charge in alkaline conditions and positive in acid conditions).

Ferric and Mn oxides co-precipitate and adsorb cations including Co, Cr, Mn, Mo, Ni, V and Zn from the soil solution due to a pH dependent charge (Kabata-Pendias & Pendias, 2001). Fe and Mn oxides have a much greater adsorption capacity for trace element cations than Al oxides and other clay minerals (Basta et al., 2005). Quantities of hydrous oxides in the soil as well as the adsorptive capacity of the soil are controlled by variations in redox conditions. The onset

of reducing conditions result in the dissolution of the oxides and the release of their adsorbed ions (Alloway, 1995).

2.6. Metal Contamination from Cemeteries

The opportunity for seepage reduction during decomposition of corpses is controlled by the unsaturated zone underneath the cemetery (WHO, 1998). Sites where the groundwater is shallow and protected by a thin unsaturated zone which is composed of coarse grained materials, should be avoided when siting cemeteries because their groundwater is potentially vulnerable to contamination. Such particular sites usually have high permeability and low capacity of retention of contaminants. Also, fine grained soils where anaerobic conditions are superior, even if the filtration zone is above the water table, should not be considered when siting cemeteries (Engelbrecht, 1998). It is assumed that the most functional soil type to increase retention of degradation products is a low porosity clay-sand mix with a small to fine grain size (WHO, 1998).

In their study, Fisher and Croukamp (1993) stated that inappropriately located or insufficiently protected cemeteries may pose a significant health problem for people. Cemeteries have been a matter of debate since the early 1950s (Van Haaren, 1951) in terms of the risk they pose to the environment. Decomposition products (e.g. gaseous products: CO, CO2, CH4, NO3) are released into the environment or accumulate in the grave area when corpses and grave contents decompose (Fielder et al., 2004a). Artefacts like metal coffin fittings might contain heavy metals and the textiles used to clothe and bed the deceased are made of barely degradable polyester and are also treated with chemical moisture binders (Williams et al., 2009). Graveyard-specific soil conditions (filter and buffer capacity of the soil) influence whether potentially toxic breakdown products of body or coffin substances enter the environment (Dent, 2002).

Van Haaren (1951) investigated the influence of cemeteries on the groundwater regime. In this investigation, Van Haaren measured, though without an assessment of soil properties, high concentrations of some ions in shallow groundwater (e.g. 500 mg/l chloride, 300 mg/l sulphate, 450 mg/l bicarbonates) and high electrical conductivity (2300 µS/cm). Schraps (1972) then confirmed high concentrations of ions in the immediate neighbourhood of graves (Germany), especially 50 cm below the interment level. Schraps focused on the variability of ion

concentrations depending on the distance from the burial ground and the inclination of its surface, with respect to chemical oxygen demand (COD), nitrate and ammonium concentrations, carbon dioxide and gaseous ammonia. Concentrations of these contaminants decreased with distance from the burial sites. A decrease of contamination levels with distance from cemeteries was also measured by Gray et al. (1974). Schraps (1972) also found evidence of bacteria in groundwater near cemeteries.

This kind of contamination was not seen in studies in Hamburg (Germany), where the lower contaminant concentrations resulted from a thicker (0.7 m) unsaturated zone under the graves and lower permeability of the soil (Hanzlick, 1994). A slow decrease in ion concentrations between 100 and 200 m from a cemetery in Britain and a rapid decrease beyond 200 m was noted by British researchers. Studies conducted in England and Wales revealed high concentrations of chlorides close to and under burial sites (Zychowski, 2012). A study at Carter Cemetery in Germany demonstrated low groundwater contamination with sulphates, chlorides, sodium ions, and higher concentrations locally of carbolic acid and zinc, which was associated with the considerable thickness of the unsaturated zone (maximum 9.4 m at the time of study) (Trick et al., 1999).

Young et al. (1999) drew attention to the rarely studied occurrence of pesticides, natural fertilizers and herbicides in the cemetery environment when they revealed high concentrations of formaldehyde (8.6 mg/l) close to a recent interment site in Northwood cemetery. Studies by Zychowski et al. (2000, 2002, 2005, 2007) stress the significance of local geology and topography, weather conditions and water table oscillations on the adverse impact from cemeteries on groundwater. The highest levels of contamination indicators are found in the cemeteries located in humid and warm climatic conditions e.g. in Brazil. Ammonia is considered the principle product of decomposition. Most researchers regard nitrogen and phosphorus containing ions, as well as bacteria and viruses, as the greatest threat posed by the presence of cemeteries (Zychowski, 2012).

Engelbrecht (1993) showed that the leachate from the cemetery appears to be a nutrient source for the micro-organisms, rather than a poison. Pathogenic bacteria, viruses and helminths that survive will consequently reach the groundwater. The most vulnerable groundwater occurs in areas with high rainfall and high watertables. Serious groundwater pollution can also result where cemeteries are underlain by fractured or cavernous rock.

The risk of groundwater contamination is increased where (Engelbrecht, 2000):

- Burial occurs near groundwater abstraction point (such as a borehole); this reduces the time needed for mobile waste production to degrade completely, and for the geological subsurface material to purify the potential contaminants, before they reach the abstraction point.
- Corpses are buried in direct contact with the groundwater, resulting in reducing the time taken for mobile degradation products to reach the groundwater.
- The more burial in an area, the greater the concentration of contaminants that are generated.

Outfront (2005) emphasizes the fact that soil contains micro-organisms and that if, and when these elements find their way into the soil they are consumed and become part of the live cycle of the soil. For example, ammonia and nitrogen based chemicals are absorbed and become fixed nitrogen and part of the soil's nitrogen cycle. Soil contains all the major groups of micro-organisms: bacteria, fungi, algae, protozoa and viruses. Soil contains bacteria that digest special substances such as cellulose, protein, pectin, butyric acid, anole urea as well as nitrogen fixing, nitrifying and denitrifying bacteria. Soil has a pH ranging from 2 to 9 and this pH aids in determining how well micro-organisms will grow in it.

Contaminants from burial sites may migrate into:

- The soil zone surrounding the burial
- The unsaturated zone
- The saturated zone of the aquifer.

Soils are complex in composition and are the site of biochemical reactions, so contaminants may change while passing through them. Air access is generally good (unless the soil is waterlogged), encouraging the rapid oxidation of pollutants. The main process contributing to the attenuation of pollutants are hydrolysis, absorption, dispersion, cationic exchange, chelation and biochemical transformation. In the unsaturated zone, less chemical and biological activity takes place than in the overlying soils. Oxygen diffusion from the surface is low and anoxic conditions may develop. However, chemical and biochemical reactions may continue to attenuate pollutants. Filtration and sorption may continue to de-mobilise particulates and some dissolved pollutants (Environment Agency, 2004).

Pacheco et al. (1991) concluded that groundwater samples from three Brazilian cemeteries of different soil types were "*unsatisfactory from a hygienic and sanitary point of view*". Faecal coliform, proteollytic and lipolytic bacteria were abundant in some water samples. These bacteria dominate during decomposition of organic material. Also, water samples collected had a '*nauseating´* smell. However, not all the samples analysed had high levels of contamination. This was attributed to the different lithologies and watertable levels. A deep water table and fine-grained soil, preferably clay-sand mixture, were concluded to be ideal conditions to prevent leaching of organic contamination.

Schraps (1978) analysed groundwater from a West German cemetery 50 cm below grave level at various distances down slope from the cemetery. High levels of bacteria (60x background), chemical oxygen demand (2x background), ammonia and nitrate were identified in the immediate vicinity, dropping off quickly with distance. Schraps (1978) noted that cemeteries should not be sited in permeable soils or soils so fine that anaerobic conditions prevail.

Van Allemann et al. (2018) conducted a laboratory study on the pollution of formaldehyde in cemeteries (South Africa). In their study, they wanted to determine whether formaldehyde becomes mobile and leaches into groundwater and, if so, then estimate the rate of leaching. Assessment of the amount of rainfall and its pH, soil type and temperature was also undertaken in order to determine how they affect the rate of leaching. Contrary to what was expected, their results showed the persistence of formaldehyde in soils and a slow percolation through the soil for a period of at least 14 weeks.

Different environmental conditions such as rainfall and its pH, soil type and temperature also did not appear to have an effect on the amount of leachate or the mobility rate through soils, although sand allowed more effective leaching. The study have, however, indicated a total of 2.6 % of formalin that was introduced into the experimental soil columns to have leached from the soil over a period of 6 months. The remaining ~97 % was assumed to have either broken down or would have only mobilized out of the soil column at a later stage (Van Allemann et al., 2018)

3. MATERIALS AND METHODS

3.1. Site Description

3.1.1. Locality

As part of the research study, site visit was conducted to familiarise ourselves with the site and to evaluate the geology, hydrogeology and potential receptors of pollution emanating from the cemetery. The selected site for this study was the Fontein Street Cemetery which is situated on the south-eastern corner of Samora Machel Street (previously known as Fontein Street after which the cemetery was named) and Verdoorn Street, in Middelburg (Mpumalanga, South Africa), as illustrated in ***Figure 3***. The study area falls within the Steve Tshwete Local Municipality of the Nkangala District. The coordinates for the study area are 25˚45'789" S, 29˚26'811 E. The first funeral to take place at the Fontein Street Cemetery was in the year 1959. Between the years 1959 and 2015, about 32 846 graves were recorded. The site is bounded to the south by a historical landfill which is presently used as a sports ground, ***Figure 4***. Residential developments occur to the east of the site and a drainage channel occurs 231 m away from the north-western corner.

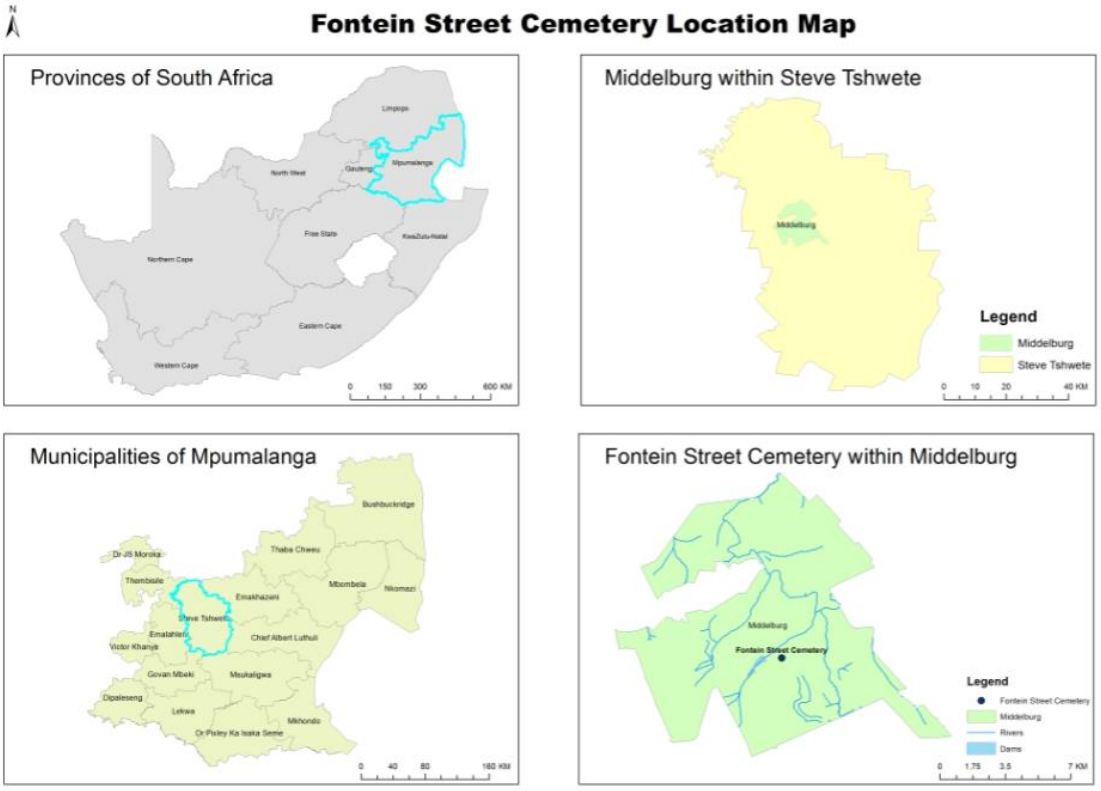

Figure 3: Fontein Street Cemetery location map.

Figure 4: Google Earth © satellite imagery of the Fontein St Cemetery, as well as the adjacent drainage feature and historical landfill.

3.1.2. Climate

The Steve Tshwete Local Municipality in Middelburg received 657 mm of rain in the year 2016, with most rainfall having occurred in March and November. The municipality received no rain in January but the highest rainfall of 194 mm subsequently occured in March, as illustrated in ***Figure 5***. The average midday temperature for Middelburg in the year 2016 ranged from 15°C in June to 27°C in January.

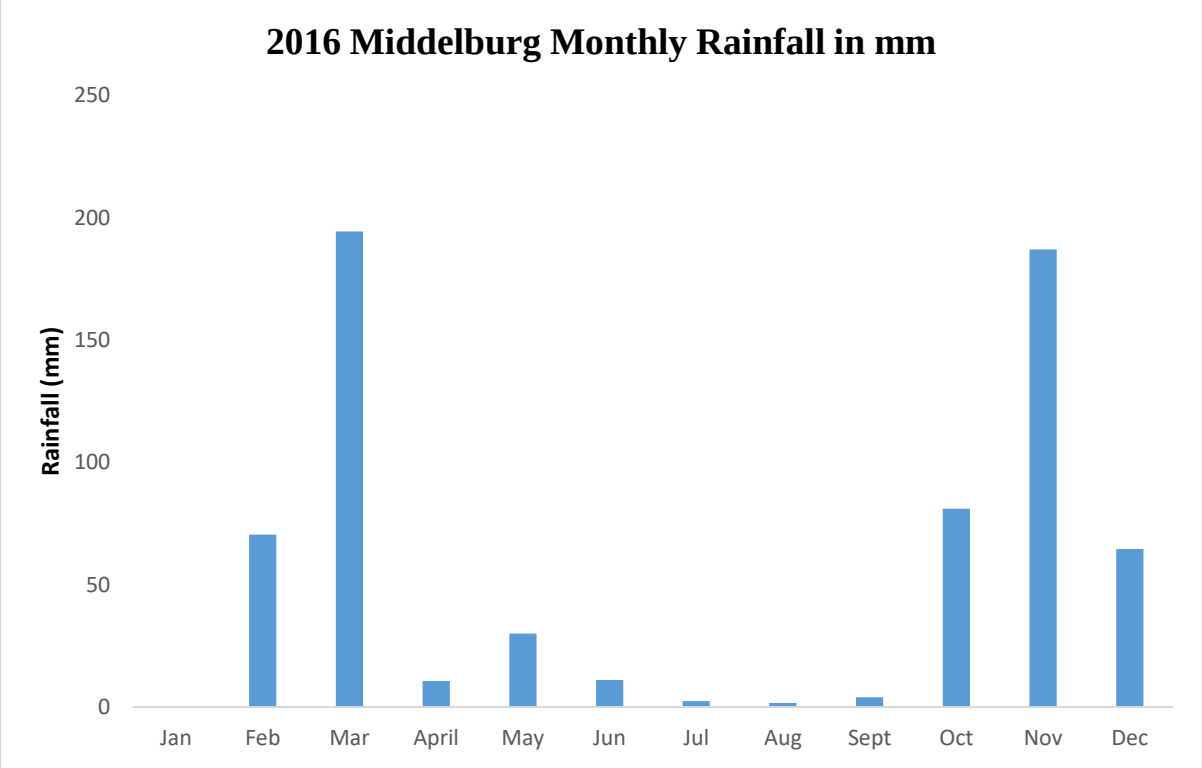

Figure 5: Monthly rainfall (mm) from Jan 2016 – Dec 2016 in Middelburg as measured by the SAWS weather station.

3.1.3. Regional geology

The geology of the study area is shown on the 1: 250 000 geology map 2528 Pretoria (Council for Geoscience; ***Figure 6***). The Geological Map (Survey, 1973) indicates that the study area (Fontein Street Cemetery) is underlain by the Dwyka Group (Pd) of the Karoo Supergroup and the Loskop Formation (Vls) of the Transvaal Supergroup. The Dwyka Group (Pd) is characterised by tillite and shale whereas on the other hand, the Loskop Formation (Vls) is characterised by shale, sandstone, conglomerate and volcanic rocks.

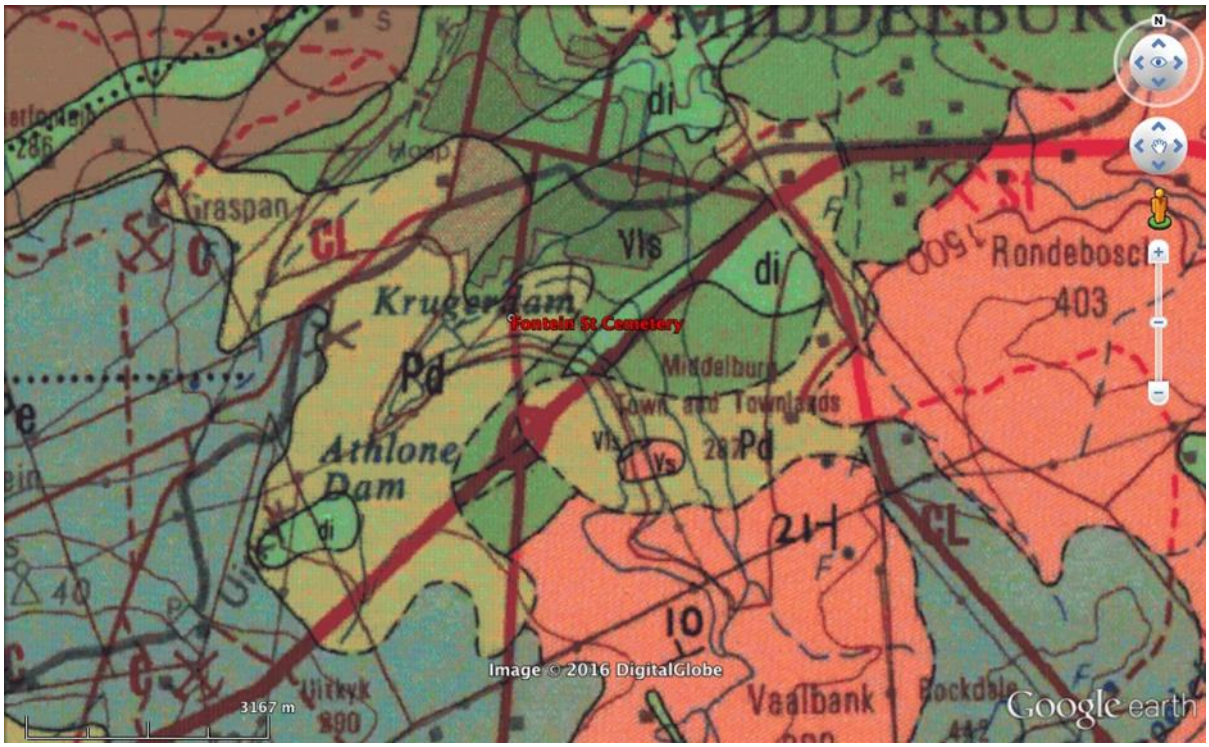

Figure 6: Geological Map of the study area and surroundings (adapted from the 2528 PRETORIA 1: 250 000 Geology Map, Geological Survey, 1978).

LEGEND		
Geological Unit Name		**Map Description**
Pe	Ecca Group, Karoo Supergroup	Shale, Shaly Sandstone, Sandstone, Grit, Conglomerate, Coal in places near base and top
Di		Diabase
Pd	Dwyka Group, Karoo Supergroup	Tillite, Shale
Vls	Loskop Formation	Shale, Sandstone, Conglomerate, Volcanic rocks
Vs	Selonsrivier Formation, Rooiberg Group	Volcanic rocks

3.1.4. Regional surface hydrology

Figure 7 shows the drainage map of the Middelburg area. The Fontein Street Cemetery falls within the B12D quaternary catchment of the Upper Olifant's water management area. The quality of water at upper Olifant's sub-area is under threat from coal mines. The eco-status of the B12D quaternary catchment is classified as D which is highly modified. The Klein-Olifant's river is the closest perennial surface water body to the study site. Based on the data obtained from Groundwater Resources of South African map series (1995), total recharge in the catchment ranges from 50-75 mm/a and total dissolved solids range between 300 and 1500 mg/L.

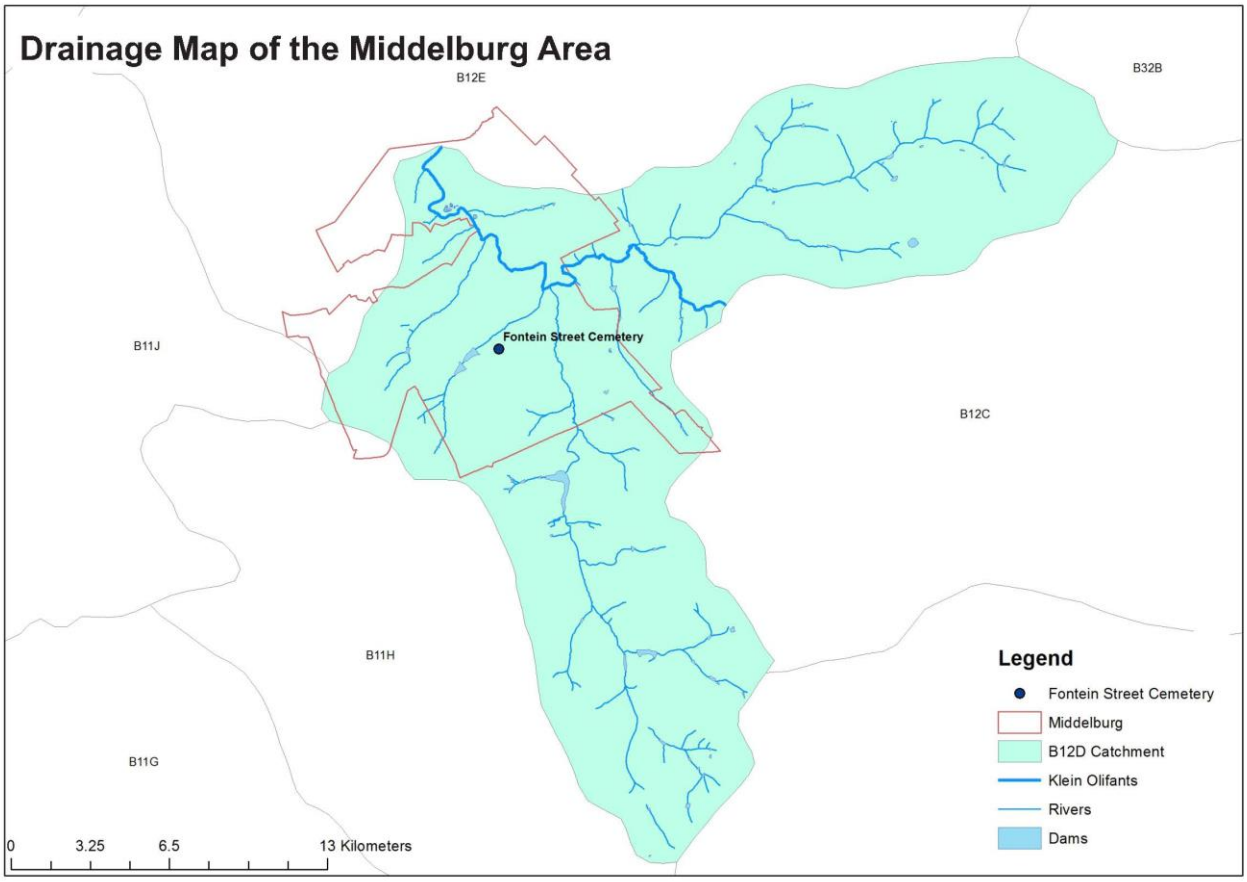

Figure 7: Drainage map of the Middelburg area.

3.2. Methodology

3.2.1. Hydrocensus

A hydrocensus was conducted on 8 November 2016 in Middelburg at a radius of 1 km around cemetery. The main aim of conducting a hydrocensus was to identify legitimate groundwater users and get a comparison of the water quality results between cemetery boreholes and off-site boreholes (hydrocensus boreholes). Only three boreholes could be located downslope to the cemetery within the delineated 1 km radius. Field parameters such as temperature, pH, redox potential (Eh), and dissolved oxygen (DO) content all change once the groundwater sample is exposed to ambient conditions at the ground surface, during storage and laboratory analysis. On-site measurement of electrical conductivity (EC) also needs to be conducted to limit the exsolution of gases from the groundwater. Therefore, all field parameters had to be measured during sampling. These parameters fall within acceptable limits of the South African National Standards of drinking water (SANS 241:2015). No boreholes were found within the 1 km radius in an upslope direction, however two boreholes were found at 3.7 km (Middelburg Mall) from the cemetery.

The groundwater of the four boreholes in the area where the hydrocensus was conducted is generally used for garden irrigation and to a lesser extent as potable water. Most people use municipal water from their taps for drinking.

Figure 8: Google Earth © satellite imagery indicating hydrocensus borehole locations (yellow placemarks) with reference to the study site (red polygon).

Table 2: Hydrocensus data from Middelburg.

Date	Borehole ID	Depth (m)	Year Drilled	Location	Water usage	Field Parameters				
						Temperature (°C)	Eh (*u*S/cm)	pH	EC (mV)	DO (mg/L)
08-Nov-16	BH5A	42	2014	5 Morkel street, Middelburg	Irrigation & Drinking (Filtered)	24.1	176	7.28	289	3.72
08-Nov-16	BH17	30	2016	17 Jeppe street, Middelburg	Irrigation	23.2	152	6.95	158	3.88
08-Nov-16	Mall BH1	Unknown	2014	Middelburg Mall	Irrigation	25.3	172	7.11	134	4.5
08-Nov-16	BH14A	Unknown	Over 20 years old	14 Hoog street, Middelburg	Irrigation & Drinking (Unfiltered)	22.1	189	6.88	567	3.71

3.2.2. Rotary percussion drilling

A total of five vertical boreholes (***Figure 9***) of 170 mm in diameter were drilled in February 2016 at Fontein Street Cemetery to (i) evaluate subsurface stratigraphic and hydrogeologic conditions, (ii) determine groundwater quality and (iii) serve as future monitoring boreholes. The deepest borehole (BH2D) was drilled to a depth of 5 m but eventually sunk to 8.05 m due to the wet clay material below the land surface. All the five boreholes were equipped with 63 mm solid-slotted PVC casings. Soil samples were collected for analyses of X-Ray Diffraction and X-Ray Fluorescence to determine the mineralogy and the distribution of metals in the cemetery. The vadose zone and the underlying aquifer were hydraulically tested to provide an understanding of the hydraulic properties and to obtain flow and contaminant transport properties. Groundwater monitoring and a hydrocensus were also conducted in and around the cemetery (at a delineated radius of 1 km).

Figure 9: Google Earth © satellite imagery indicating borehole positions at Fontein Street Cemetery.

Table 3: Drilled borehole conditions.

Borehole ID	Depth (mbgl)	Water Level (mbgl)	Location	Elevation (m)
BH1D	2,11	1,46	25°47'17,22"S 29°27'38,1"E	1488
BH2D	5,15	4,22	25°47'24,8"S 29°27'51,7"E	1500
BH3D	4,90	Dry	25°47'26,6"S 29°27'42,7"E	1499
BH4S	1,20	Dry	25°47'19,6"S 29°27'40,6"E	1494
BH1S	1,27	Dry	25°35'57,6"S 28°27'04,8"E	1388

Rotary percussion drilling was employed for soil sampling and hydrogeological investigations at Fontein Street Cemetery as shown in ***Figure 10***. Soil profiling for each hole was conducted and described according to the Moisture, Colour, Consistency, Structure, Soil texture, Origin system (SABS, 2009). 38 soil samples were collected from three of the five drilled boreholes and then taken to Stoneman lab for analyses. Samples were numbered accordingly; the number of each sample included each hole and the depth from the surface that each sample was obtained.

Figure 10: Rotary percussion drilling at Fontein Street Cemetery on 10 February 2016.

Borehole diameters (170 mm) allow easy access to the aquifer, for the purpose of sampling and for lowering other test instruments (pumps, bailers, a dipmeter etc.). The borehole casings also allow easy access for monitoring purposes and do not block the flow of water through the borehole. The collar height of the casing cap was 0.4 m above the ground surface to ensure that surface run-off does not flow into the borehole during flood conditions. A concrete block was built around the top of the casing to protect the casing and the borehole, as well as to prevent surface pollution from flowing down the side of the casing. Gravel-packed portions were used to backfill the borehole. Slotted casings were used to allow a flow of fresh groundwater into the borehole.

3.2.3. Geological profile

Geological logs from the Fontein Street Cemetery provide an accurate and comprehensive record of the geological conditions encountered together with some relevant information obtained during drilling. The logs show nodular ferricrete gravel material at or near the surface which overlies the Loskop Formation medium-grained residual Sandstone, which is in return overlain by the Dwyka Group silty-clay Shale, as illustrated in Appendix 5. The logs also provide information about the depths of boreholes and those of watertables. The watertable was intersected at different depths by boreholes BH1D and BH2D, whereas no watertable was intersected by borehole BH3D.

3.2.4. Percolation testing

Hand auger drilling was performed to conduct percolation tests in the study area, as illustrated in ***Figure 11***. This method was chosen as it is cost effective and provides a generalised profile of different materials within the cemetery. Four holes were hand augured at different locations within the study area to run percolation tests, see ***Figure 12***. Percolation tests were conducted to determine the absorption rate of the soil and to infer hydraulic properties.

A series of percolation tests were conducted at various locations within the cemetery. To perform this experiment in four locations through inverted auger hole method, a hole with 100 mm diameter was digged to the depth of refusal in a flat surface by auger. While digging the hole, it was considered that the inner wall of the hole was not compacted or destroyed, the hole was also digged completely vertical in order not to make any disturbance for water infiltration into soil.

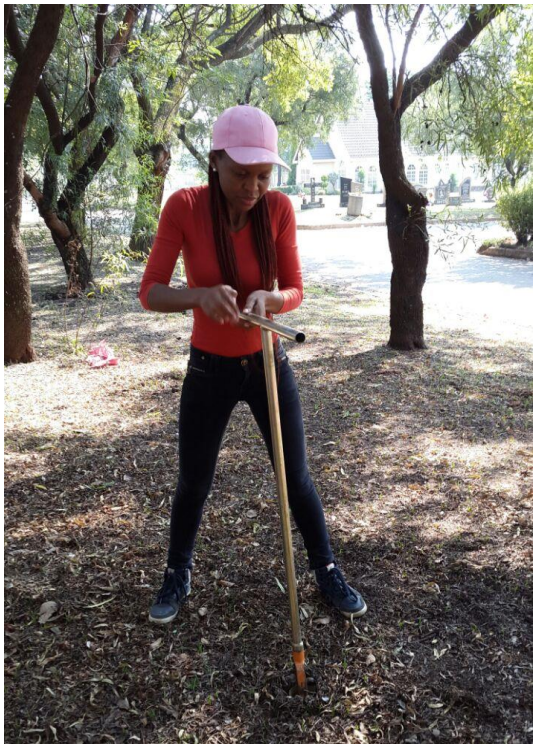

Figure 11: Hand Auger drilling at Fontein Street Cemetery.

Below are the steps that were undertaken to conduct percolation tests in the cemetery; -

- The hole was hand augured to a depth of refusal
- The hole was then pre-soaked with water by maintaining a high-water level
- The test was run by filling the hole with water to a specific level and then timing the drop of the water level (as illustrated in ***Figure 13***), measured with a steel ruler placed in the hole
- Water was allowed to drain down before the next test was conducted

Figure 12: Google Earth © satellite imagery indicating augured borehole positions at Fontein Street Cemetery.

Figure 13: Sarah Mahlangu and Chantelle Schmidt conducting a percolation test in one of the augured holes at the study site.

Table 4 is an illustration of percolation test results from the Fontein Street Cemetery. The results are presented in terms of saturated hydraulic conductivies (K-values) for each hole. Tests were run three times for each hole. Hydraulic conductivities increase with increasing soil water content until reaching a maximum rate in saturated conditions where the hydraulic gradient equals to 1, at which it is referred to as K_{sat}. This is what is shown in ***Table 4***.

Table 4: Saturated hydraulic conductivies for soils of the Fontein Street Cemetery.

Borehole ID	K_{sat} high (m/s)
BH1a	2,62E-03
BH1b	2,53E-03
BH2a	2,57E-03
BH3a	7,93E-04

On the one hand, test results show a similarity in saturated hydraulic conductivities of BH1a, BH1b and BH2a which are representative of clay-silty material. On the other hand, BH3a shows a different saturated hydraulic conductivity which is representative of sandy material. This sandy material is only noted near the land surface in BH3a, since the borehole is seen to be composed of clayey material as the borehole gets deeper. However, it should be noted though that the tests conducted do not provide the true measure of soil permeability or transmissivity. The K-value of a soil profile can be highly variable from place to place, and will also vary at different depths (spatial variability). Not only can different soil layers have different hydraulic conductivities, but, even within a soil layer, the hydraulic conductivity can vary.

3.2.5. Groundwater quality

Groundwater sampling was conducted on drilled boreholes within the cemetery and on some boreholes at a delineated radius of 1 km around the cemetery through a hydrocensus. A hydrocensus was conducted in the community around the cemetery to compare water quality results to those of the cemetery boreholes. Samples were collected for analyses of general water quality parameters.

The groundwater sampling programme was conducted as follows:

Liaison with the analytical laboratory personnel to discuss the aims of the project and the lab requirements in terms of sample quantities, preservation techniques and time & date of submission of samples for analyses. Google Earth map was used for locating the sampling site and GPS was used to map the coordinates of the exact positions of boreholes on site. Water levels and borehole depths were measured using a dip meter. A tape-measure was used for measuring the collar of the borehole. Water samples were collected using a transparent plastic bailer. Purging of boreholes was also employed and this was done using a 25 *l* bucket and a small pump. Groundwater samples were collected in 1 *l* transparent plastic bottles. Samples were kept in a cooler box during transportation to keep them cool. Samples were then stored in a fridge before they were sent to the lab for analyses.

3.2.6. Surface water quality

There is a stream that runs adjacent to the cemetery which forms part of the study area where samples were also collected for comparison of water quality results. The stream occurs 231 metres from the north-western corner of the cemetery and flows in a north-easterly direction. The stream was sampled at three locations (as illustrated in ***Figure 14***). The first point (A) was placed above any likely drainage. The second point (B) was placed closest to the cemetery in a downgradient direction. The last point (C) was placed downstream of the cemetery.

Figure 14: Google Earth © satellite imagery indicating stream sampling points A, B & C and the Fontein Street Cemetery (red polygon).

3.2.7. Analytical methods

Various analyses were performed on water and soil samples from Fontein Street Cemetery. These were done to determine the mineralogical composition, chemical composition, trace element composition and general water quality parameters. The methods employed are explained below.

3.2.7.1. *X-Ray Fluorescence Spectroscopy*

X-Ray Fluorescence analyses were performed on 38 soil samples at the Stoneman Laboratory at the University of Pretoria. These analyses were conducted in order to determine the chemical composition of the Fontein Street Cemetery soils in terms of oxides. Each oxide then represents a weight percentage of the sample being analysed. From these analyses, it can be determined which contaminants are possibly concentrated in the cemetery soils as metals or other contaminants.

The samples were milled in a tungsten-carbide milling pot to achieve particle sizes <75 micron. The samples were then dried at 100 ℃ and roasted at 1000 ℃ to determine Loss On Ignition (LOI) values. 1g sample was mixed with 6g of Lithium-Tetraborate flux and fused at 1050 ℃ to make a stable fused glass bead. For trace element analyses, samples were mixed with PVA binder and pressed in an aluminium cup at 10 tons.

3.2.7.2. *X-Ray Diffraction*

XRD analyses were also performed at the Stoneman Laboratory at the University of Pretoria on 38 soil samples. X-Ray Diffraction gives the composition of soil samples in terms of minerals present.

The samples were first prepared according to the Standardized Panalytical Backloading System which provides nearly random distribution of the particles. The samples were then analyzed using a PANalytical X'Pert Pro powder diffractometer in θ–θ configuration with an X'Celerator detector and variable divergence- and fixed receiving slits with Fe filtered Co-Kα radiation (λ=1.789Å). The phases were identified using X'Pert Highscore Plus software.

3.2.7.3. *Inductively Coupled Plasma Mass Spectrometry*

Inductively Coupled Plasma Mass Spectrometry (ICP-MS) is a type of mass spectrometry which can detect metals and several non-metals at concentrations as low as one part in 10^{15} (part per quadrillion, ppq) on non-interfered low-background isotopes. This is achieved by ionizing the sample with an inductively coupled plasma and then using a mass spectrometer to separate and quantify those ions. The ICP-MS scan was used to analyse the water samples for

heavy metal and trace element concentrations. These analyses were used to detect contaminants present in the water samples from the Fontein Street Cemetery.

3.2.8. Geochemical Modelling

The Geochemist's Workbench 11.0.6 (GWB) software was used to model and interpret the geochemical data. As paraphrased from the GWB essential guide, the Geochemist's Workbench is a set of software tools for manipulating chemical reactions, calculating stability diagrams and the equilibrium states of natural waters, tracing reaction processes, modelling reactive transport, plotting the results of these calculations (as shown in ***Figure 15***), and storing the related data. Hydrogeologists use the Geochemist's workbench to construct fate and transport models accounting for dual porosity media, bioattenuation, contamination sorption, precipitation, and co-precipitation.

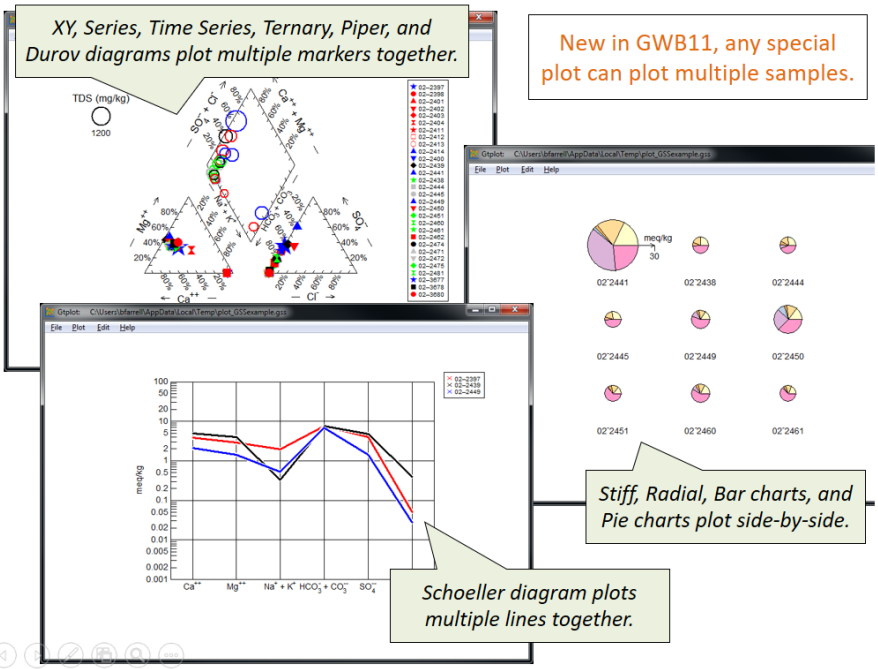

Figure 15: Diagrams which can be plotted using the Geochemist's workbench.

4. RESULTS

4.1. X-Ray Diffraction

X-ray diffraction analyses were performed at Stoneman laboratory at the University of Pretoria. Analysis results are attached under appendix 1. ***Table 5*** gives a summary of the mineral phases present on samples from the Fontein street cemetery.

Table 5: Mineral phases present on site (Fontein Street Cemetery).

Mineral Phase	Chemical Formula
Goethite	$Fe_{3.6}\,Co_{0.4}O_8$
Haematite	Fe_2O_3
Kaolinite	$Al_2Si_2O_5\,(OH)_4$
Quartz	SiO_2
Muscovite	$KAl_3Si_3O_{10}\,(OH)_2$
Anatase	TiO_2
Plagioclase	$NaAlSi_3O_8$ (Albite), $CaAl_2Si_2O_8$ (Anorthite)
Dolomite	$Ca\,Mg\,(CO_3)_2$
Epidote	$Ca_2\,(Al, Fe)_2\,(SiO_4)_3\,(OH)$
Chlorite	$(Mg, Fe)_3\,(Si, Al)_4O_{10}\,(OH)\,(Mg, Fe)_3\,(OH)_6$
Microcline	$KAlSi_3O_8$

Figures 16-18, illustrate the variations in mineral content as weighted percentages for each sample against depth. These graphs display the variations as weighted totals with each colour representing a different mineral phase, as well as the mineral abundances relative to each other for each assemblage at each sample depth. Material that falls outside of the 1% error margin for accuracy may be present in the form of colloidal phases as XRD analysis only detects crystalline phases or analytical value rounding. Also, excess weight percentages may be due to analytical value rounding.

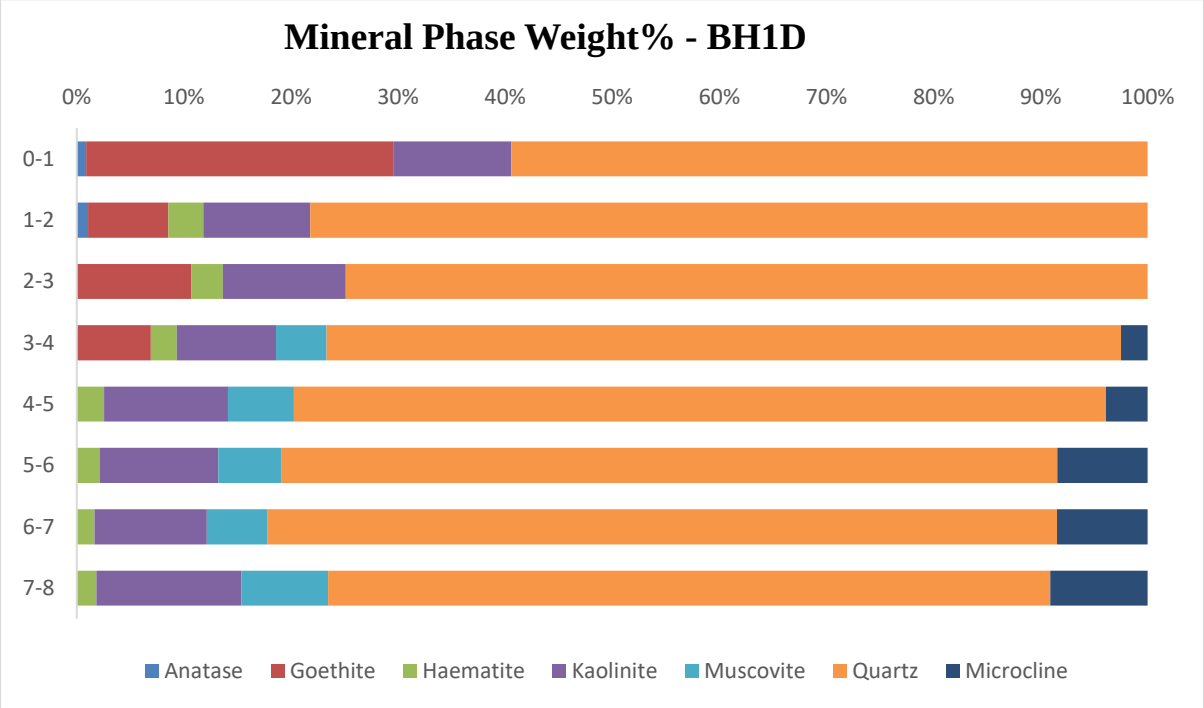

Figure 16: Mineral phase abundances with depth at BH1D.

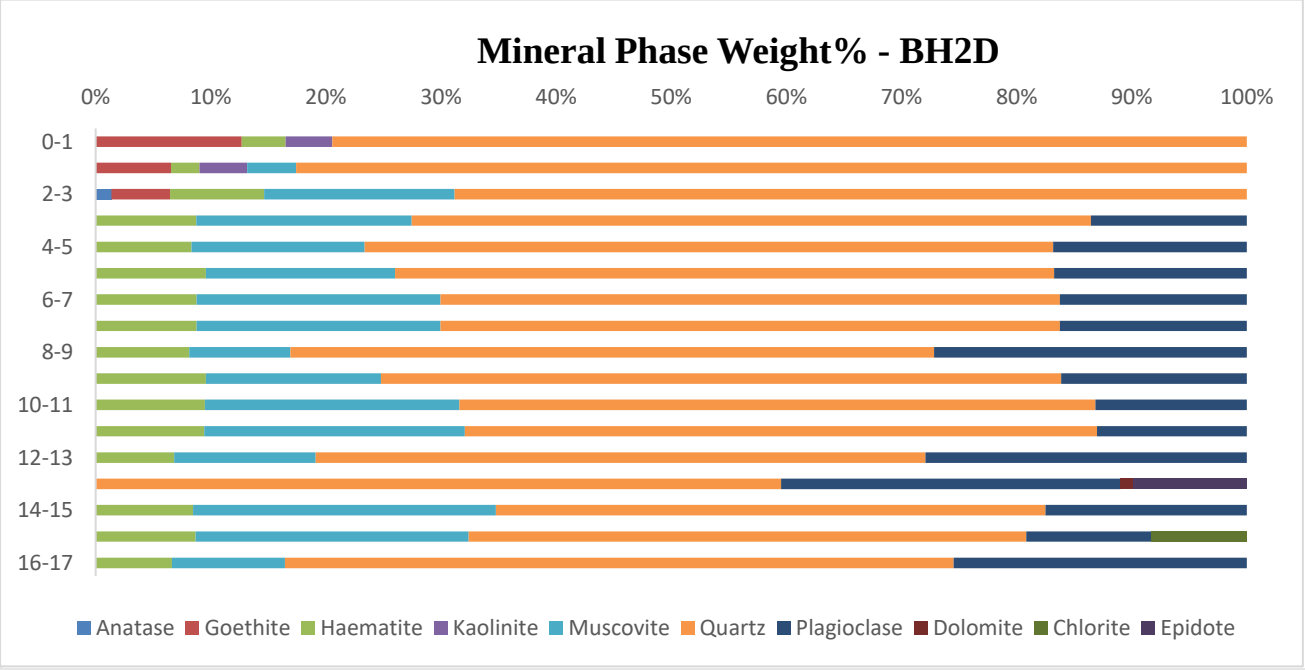

Figure 17: Mineral phase abundances with depth at BH2D.

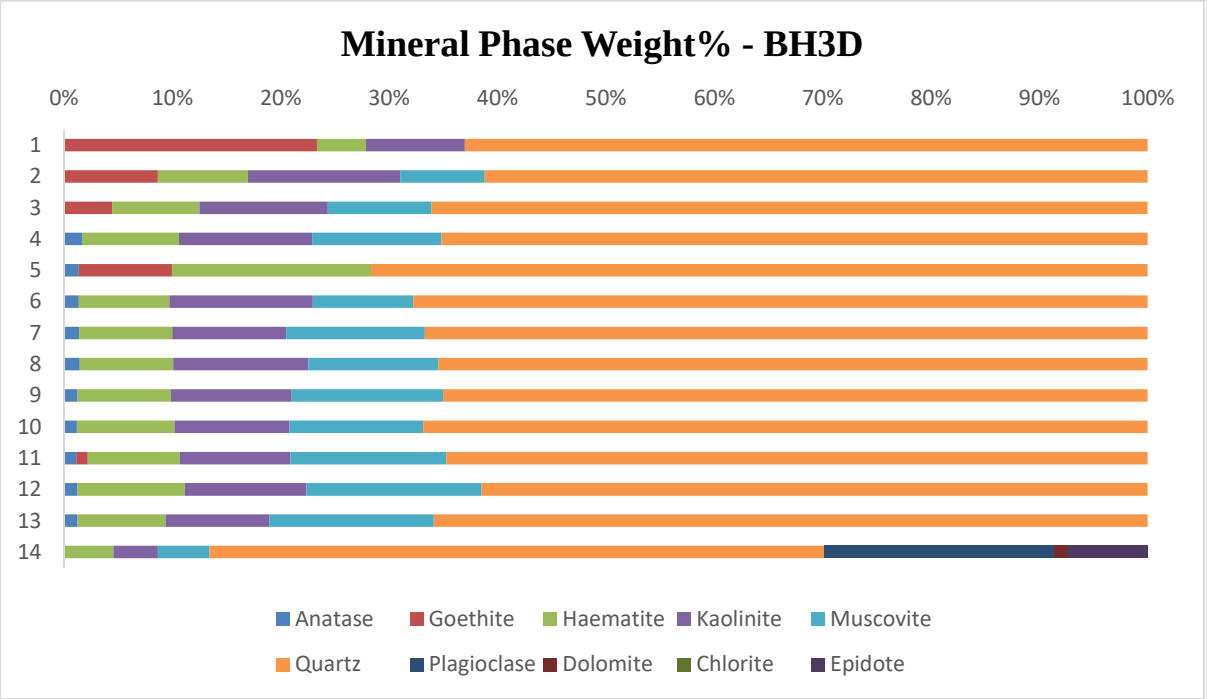

Figure 18: Mineral phase abundances with depth at BH3D.

All diagrams representing the mineral phases show an abundance of Quartz in all the three boreholes. Muscovite, Kaolinite, Plagioclase and Haematite are also seen to be the common existing minerals present.

4.2. X-Ray Fluorescence

X-Ray Fluorescence analyses were performed at Stoneman laboratory at the University of Pretoria. Major elements were detected and expressed as weight percentages in terms of oxides as shown in ***Table 6***. Trace elements were also detected and are shown in ***Table 7***. Analyses results are attached under appendix B.

Table 6: Major Element Oxides as detected by XRF.

Major Element Oxides as detected by XRF				
SiO_2	**Fe_2O_3**	**Al_2O_3**	**LOI**	**Other**

Variations of major element oxides are graphically illustrated for each borehole with depth as weight percentages in ***Figures 19-21***. These graphs display stacked totals with each colour representing a different element oxide, as well as the elemental abundances relative to each other for each assemblage at each borehole depth.

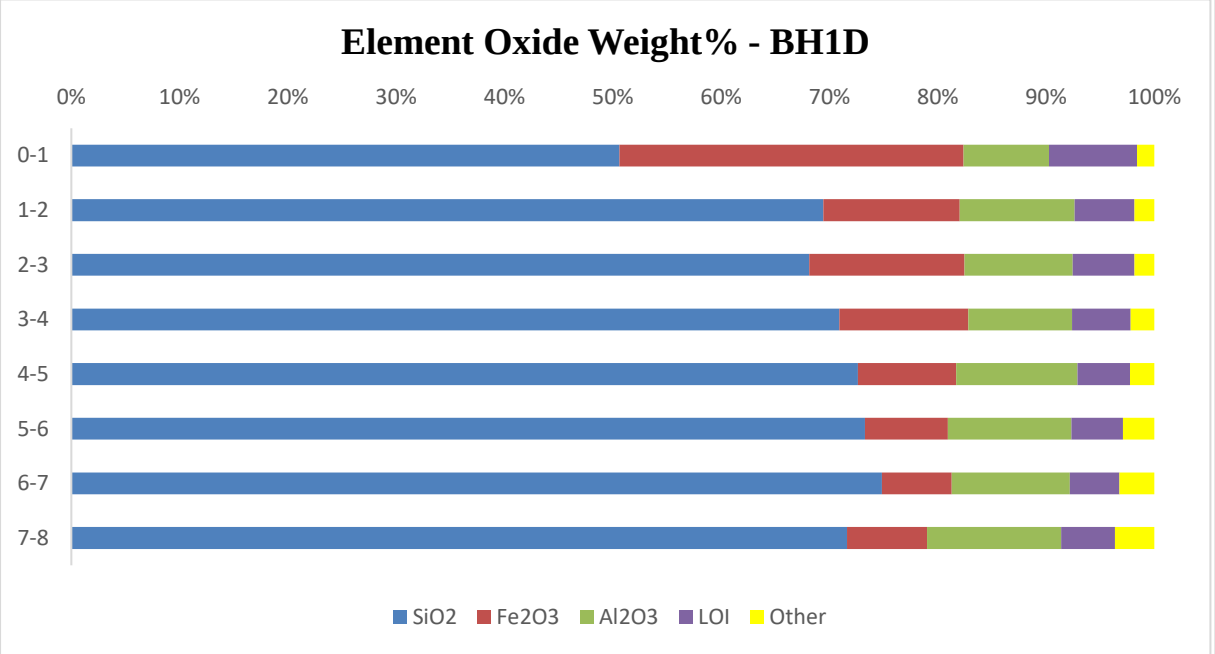

Figure 19: Element Oxide abundances with depth at BH1D.

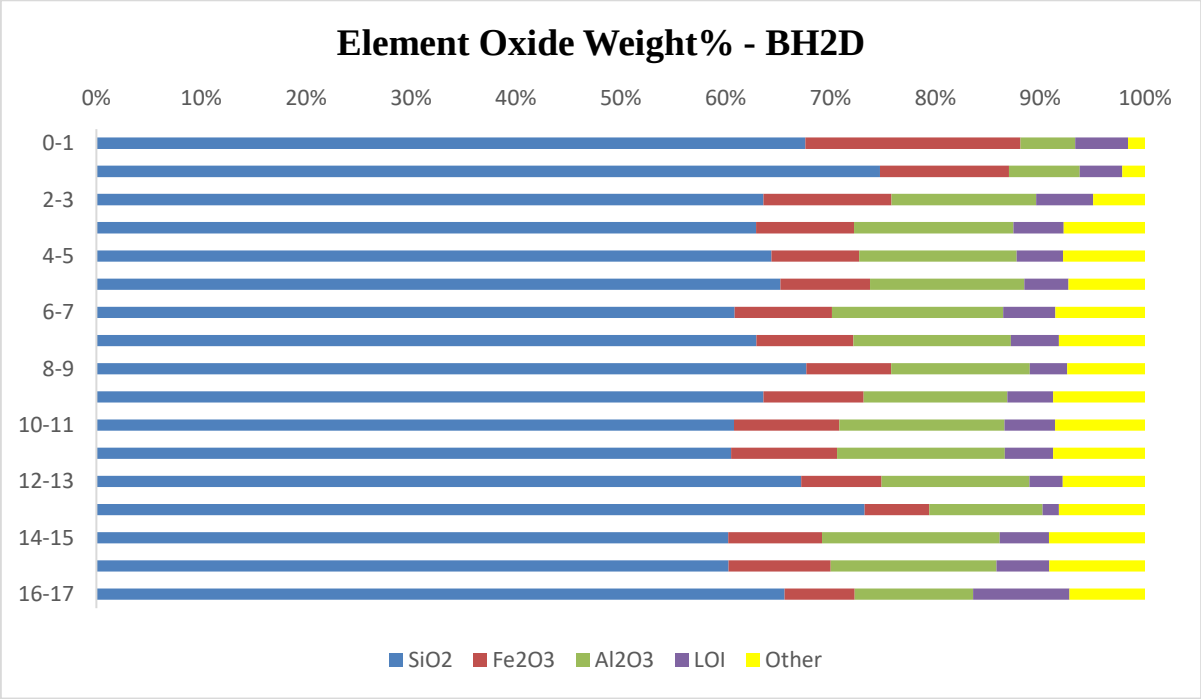

Figure 20: Element Oxide abundances with depth at BH2D.

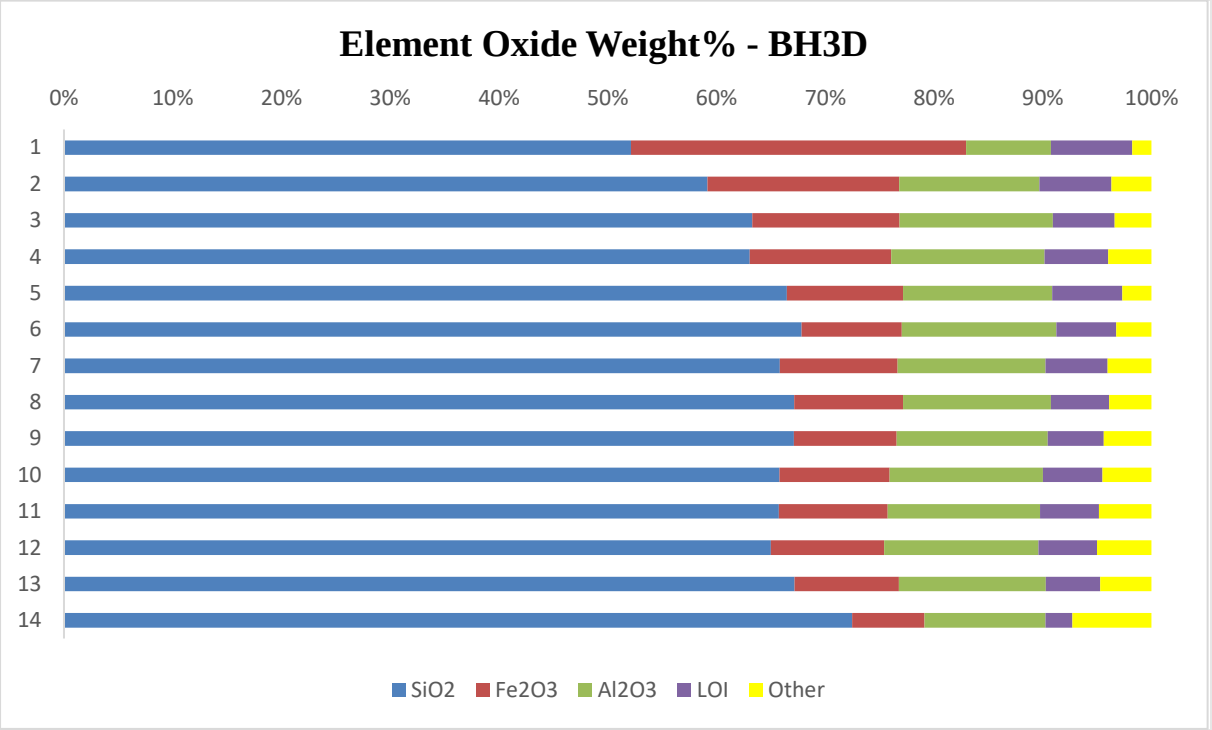

Figure 21: Element Oxide abundances with depth at BH3D.

An abundance of Si is noted to be existing in all the three boreholes. Fe and Al are also noted to be present. Loss on Ignition values are also included in the diagrams together with other minor element oxides.

Table 7: Trace Elements as detected by XRF.

Trace Elements as detected by XRF				
As	Mo	Rb	U	Zn
Cu	Nb	Sr	W*	Zr
Ga	Pb	Th	Y	Ni

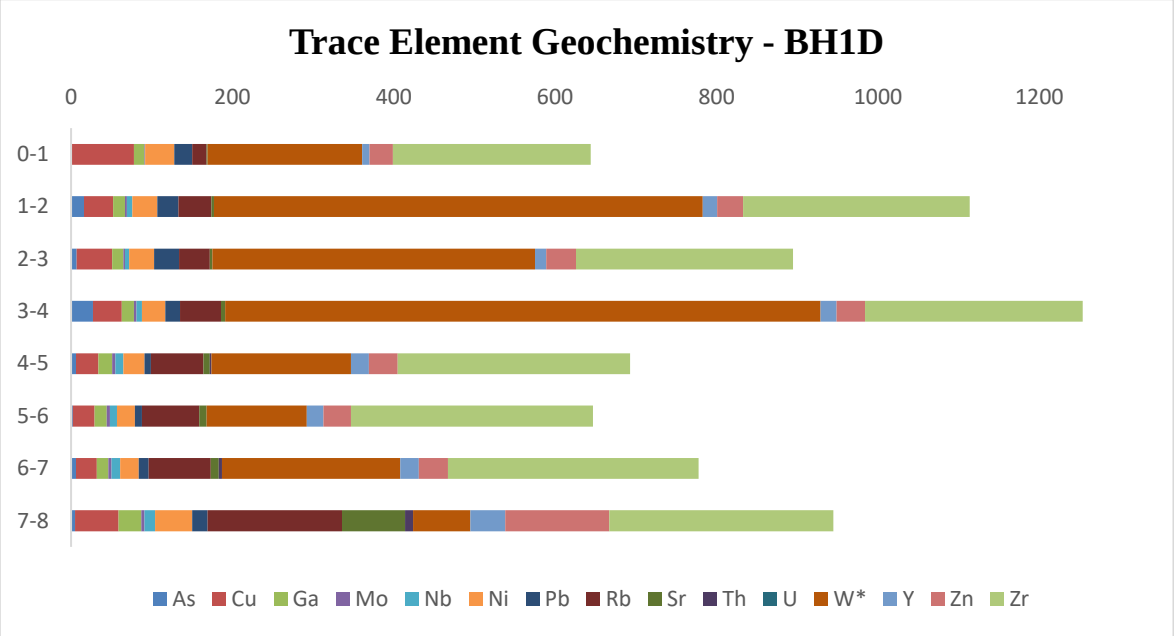

Figure 22: Trace element abundances in ppm with depth at BH1D.

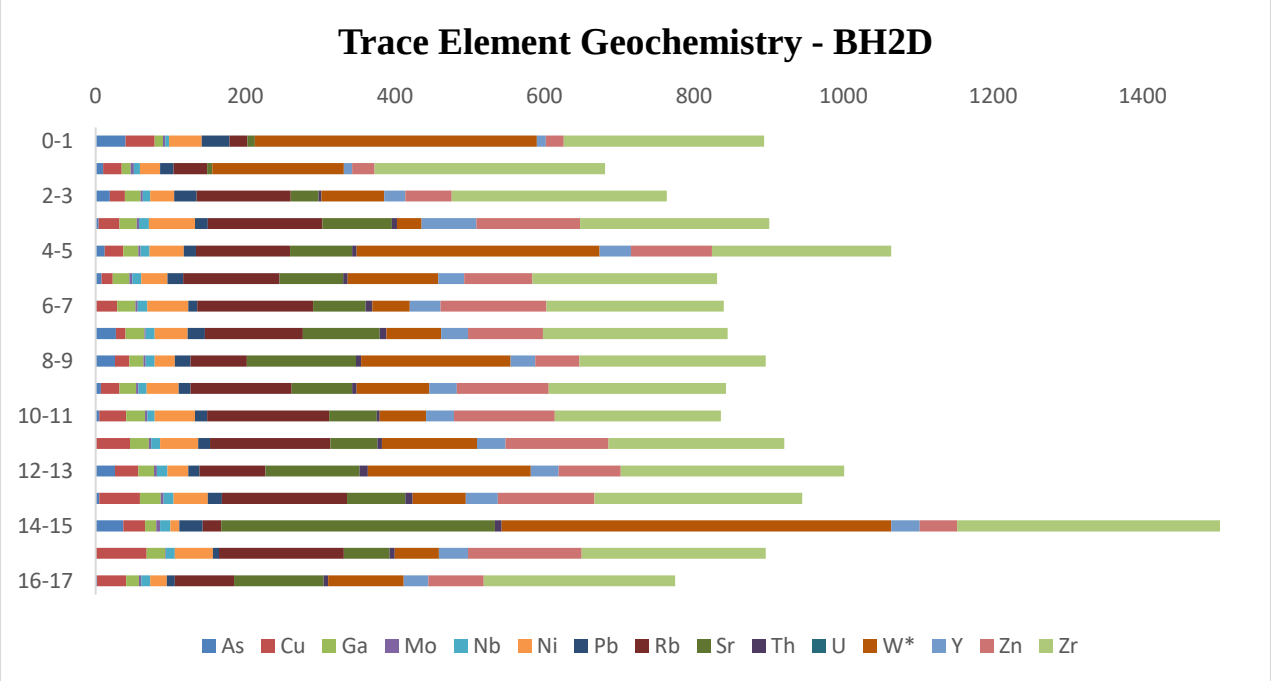

Figure 23: Trace element abundances in ppm with depth at BH2D.

Figures 22 & 23 show concentrations of trace elements present in boreholes BH1D and BH2D against depth. The trace element concentrations are presented in parts per million against depth which is presented in intervals, each interval is equivalent to 0.3 m.

Table 8: Mean mineral concentrations for boreholes BH1D and BH2D.

Metal	Mean mineral concentrations for borehole BH1D (ppm)	Mean mineral concentrations for borehole BH2D (ppm)	Approximate ratio of means for BH1D:BH2D
As	9	13	1:2
Cu	39	32	1:1
Ga	15	21	1:2
Mo	3	3	1:1
Nb	7	11	1:2
Ni	28	40	1:2
Pb	18	19	1:1
Rb	52	115	1:2
Sr	6	94	1:15
Th	1	6	1:6
U	0	0	-
W*	351	159	2:1
Y	18	36	1:2
Zn	34	96	1:3
Zr	281	263	1:1

Table 8 presents a comparison of mean mineral concentrations between boreholes BH1D and BH2D. This was done to note the difference in mineral concentrations between soils below the grave area and soils off-site. This helped in determining whether graves have an impact on the underlying groundwater.

Figure 24 is a graphical illustration of BH3D which represents trace element concentrations. The concentrations are given in parts per million and are plotted against depth intervals.

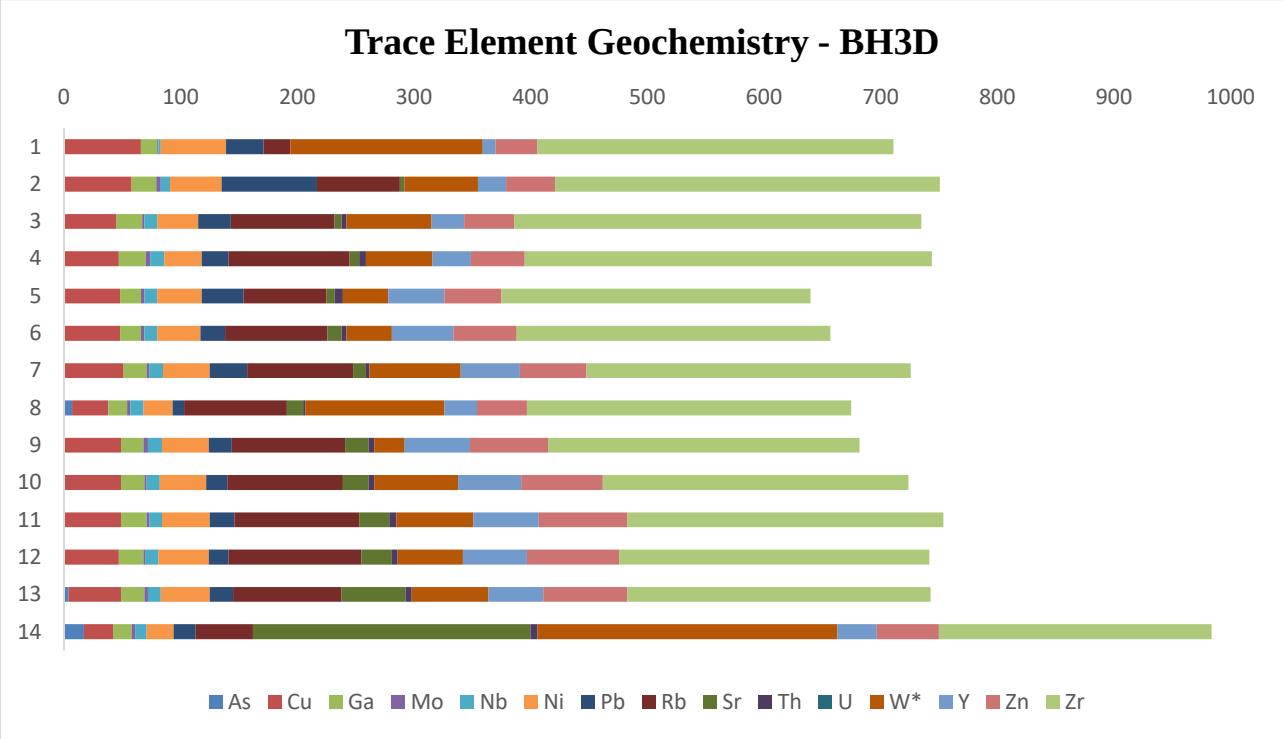

Figure 24: Trace element abundances in ppm with depth at BH3D.

4.3. Inductively Coupled Plasma Mass Spectrometry

Physical and chemical parameters of both surface water and groundwater play an important role in the classification and assessment of the water quality. Presentation of chemical analysis in graphical form makes understanding of complex water system simpler and quicker. Methods of representing the chemistry of water such as stacked bar chart, piper diagram and schoeller diagram were used, in this case, to show the proportion of ionic concentrations in individual samples.

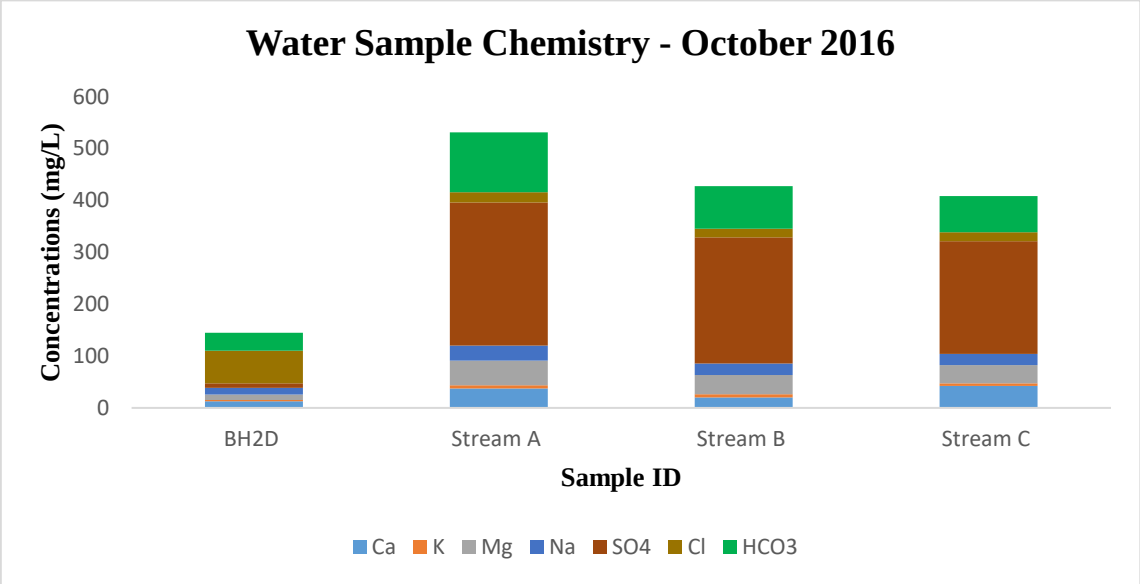

Figure 25: Analysis results for water samples collected in October 2016.

Figure 25 shows a stacked bar chart representing the water chemistry for samples that were collected during the month of October in 2016. The results presented in this diagram are for BH2D and the stream (at points A, B & C). The results show concentrations in mg/L of cations (Ca^{2+}, K^{+}, Mg^{2+}, Na^{+}) and anions (SO_4^{2-}, Cl^{-}, HCO_3^{-}) present in the sampled water.

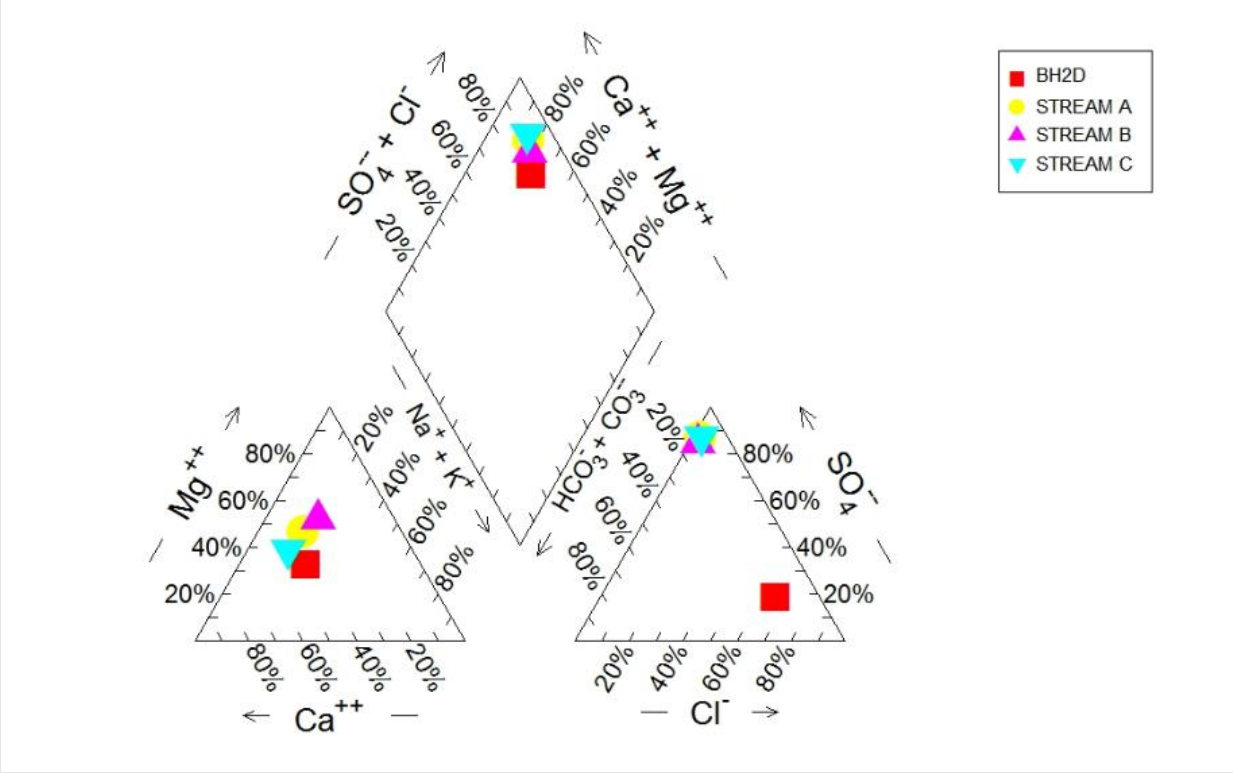

Figure 26: Piper diagram showing the geochemistry of water samples collected in October 2016.

Figure 26 is a piper plot representing the October 2016 water results. Piper plots are used to determine the different water types and interprete their origins. These plots include two triangles, one for plotting cations and the other for plotting anions. The cation and anion fields, from which inference is drawn on the basis of hydro-geochemical facies concept. These tri-linear diagrams are useful in bringing out chemical relationships among groundwater samples in more definite terms rather than with other possible plotting methods. The samples are represented in different colours in order to easily distinguish between one another on the diagram.

The Schoeller diagram in ***Figure 27*** is a logarithmic diagram of major ion analyses in meq/L. It demonstrates different water types on the same diagram. The data represented here were collected from borehole BH2D and the stream in October 2016.

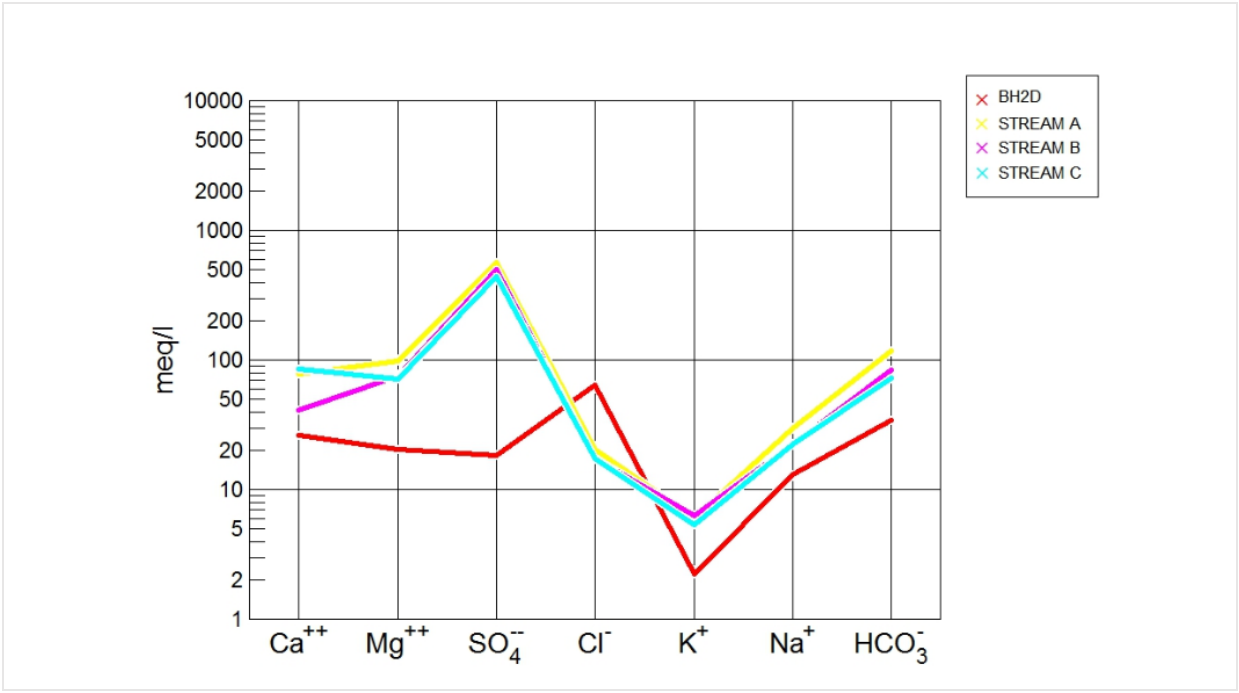

Figure 27: Schoeller diagram showing the geochemistry of water samples collected in October 2016.

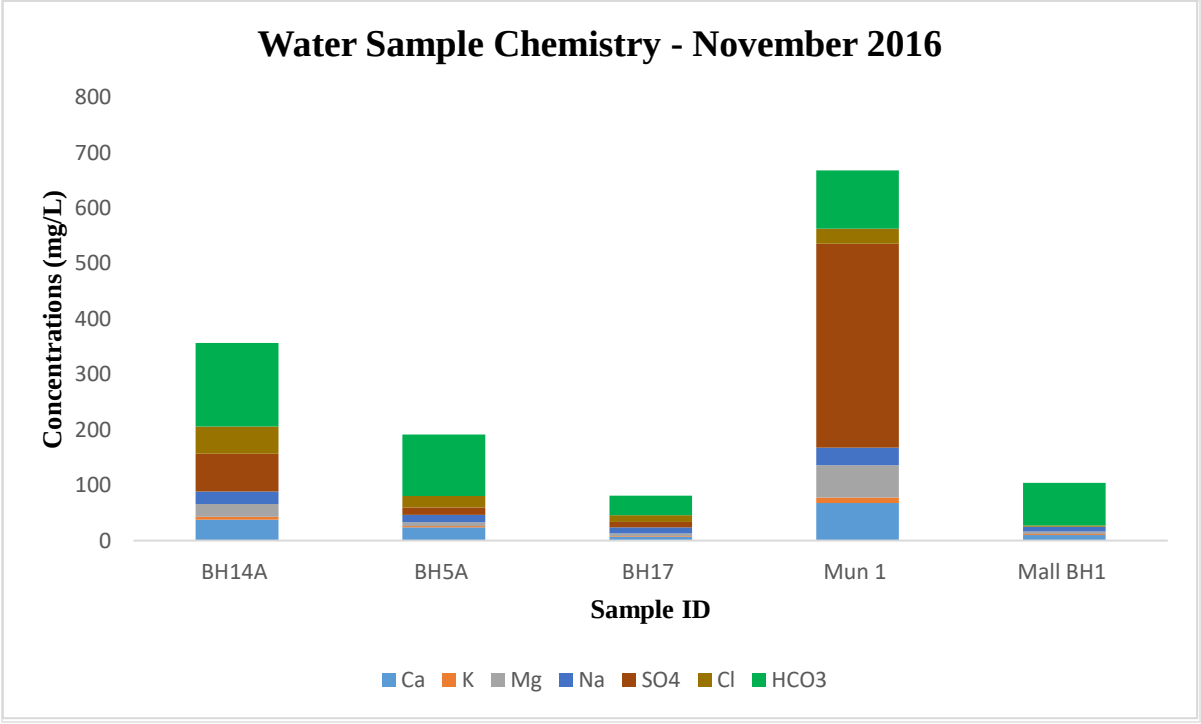

Figure 28: Analysis results for water samples collected in November 2016.

November 2016 water results are represented in ***Figure 28***. These are the hydrocensus results of samples that were collected from boreholes in the surrounding community, the municipal water and the mall borehole. The results show concentrations in mg/L of ions present in the samples collected.

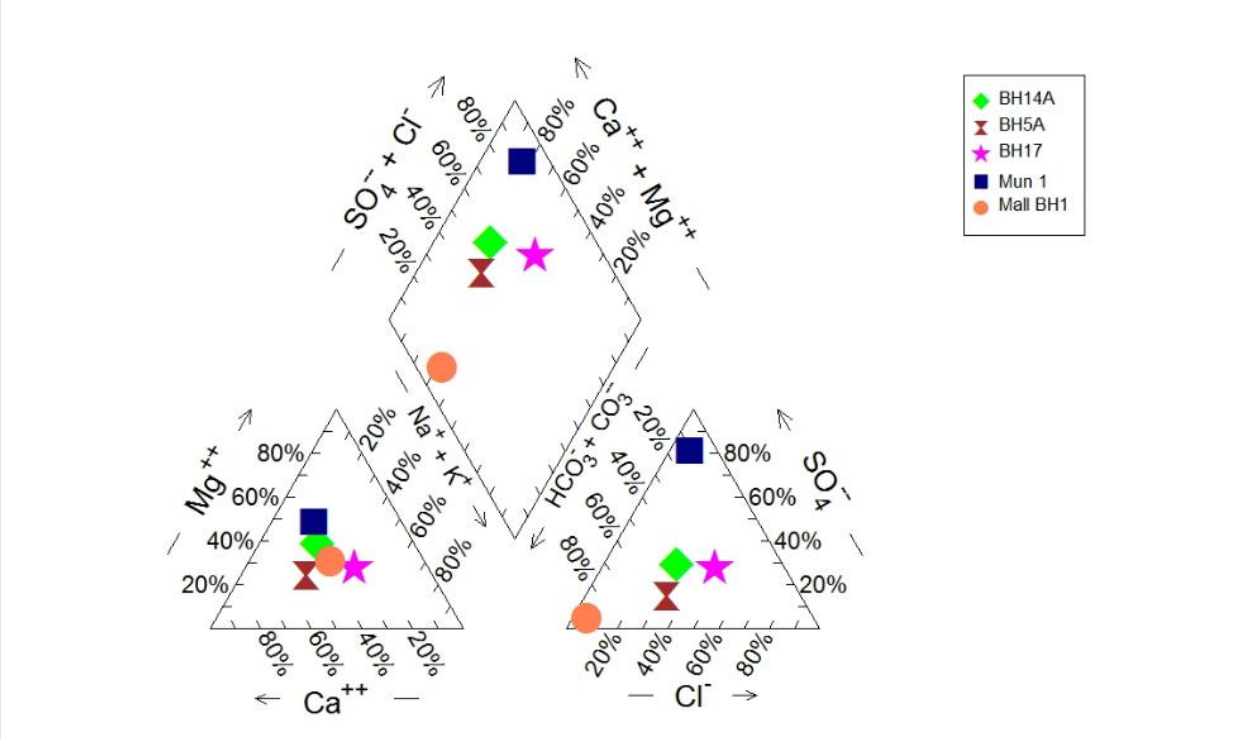

Figure 29: Piper diagram showing the geochemistry of water samples collected in November 2016.

Figure 29 is a piper plot representing the water results for November 2016. Each sample is represented with a different symbol and colour on the diagram in order to distinguish each one of them from the others. Piper plots are used to classify water types and can also be used to identify the mixing of waters.

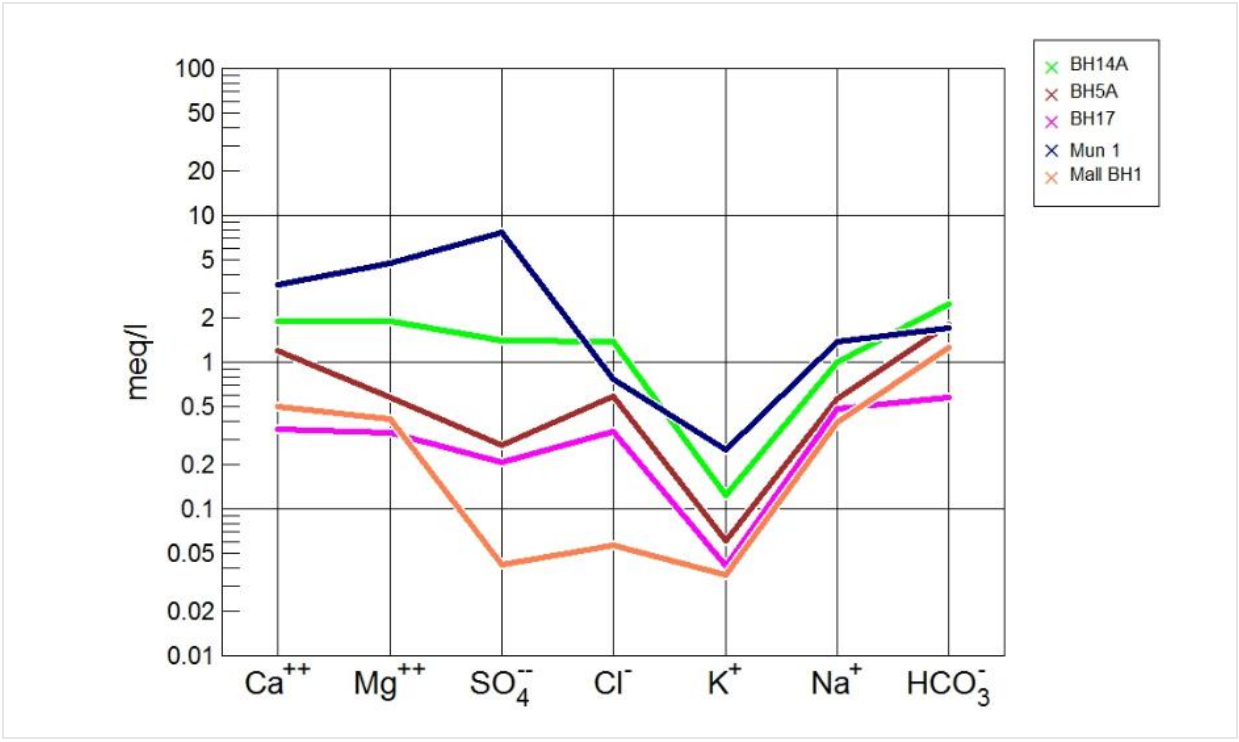

Figure 30: **Schoeller diagram showing the geochemistry of water samples collected in November 2016.**

The schoeller diagram in ***Figure 30*** is a representation of water results from the hydrocensus boreholes, the municipal water and the mall borehole. The diagram shows concentrations of major ions in meq/L. Different water types are demonstrated on the same diagram and can easily be distinguished.

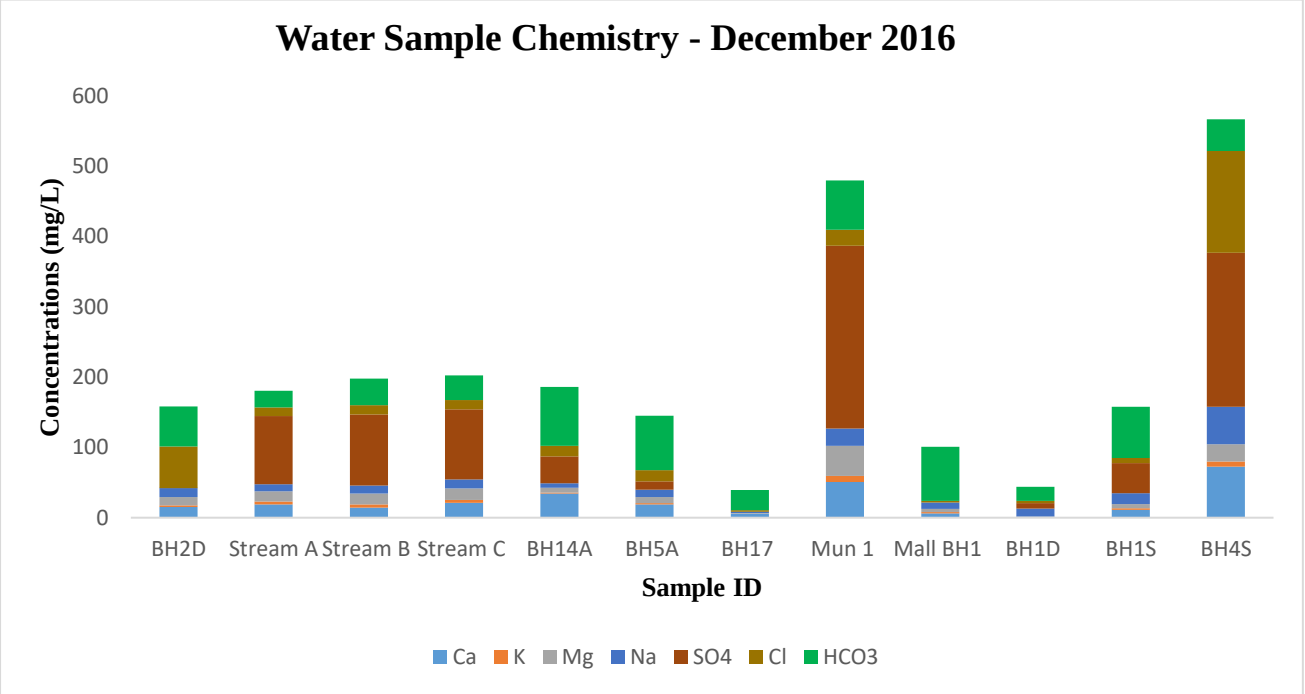

Figure 31: Analysis results for water samples collected in December 2016.

In December 2016, twelve water samples were collected, and their results are shown in ***Figure 31***. The diagram shows concentrations of ions in mg/L for each sample. The results shown in this diagram help in determining how waters from different boreholes differ and in identifying the contaminants in them. The source of contamination is also identified by studying the concentrations of ions in the samples.

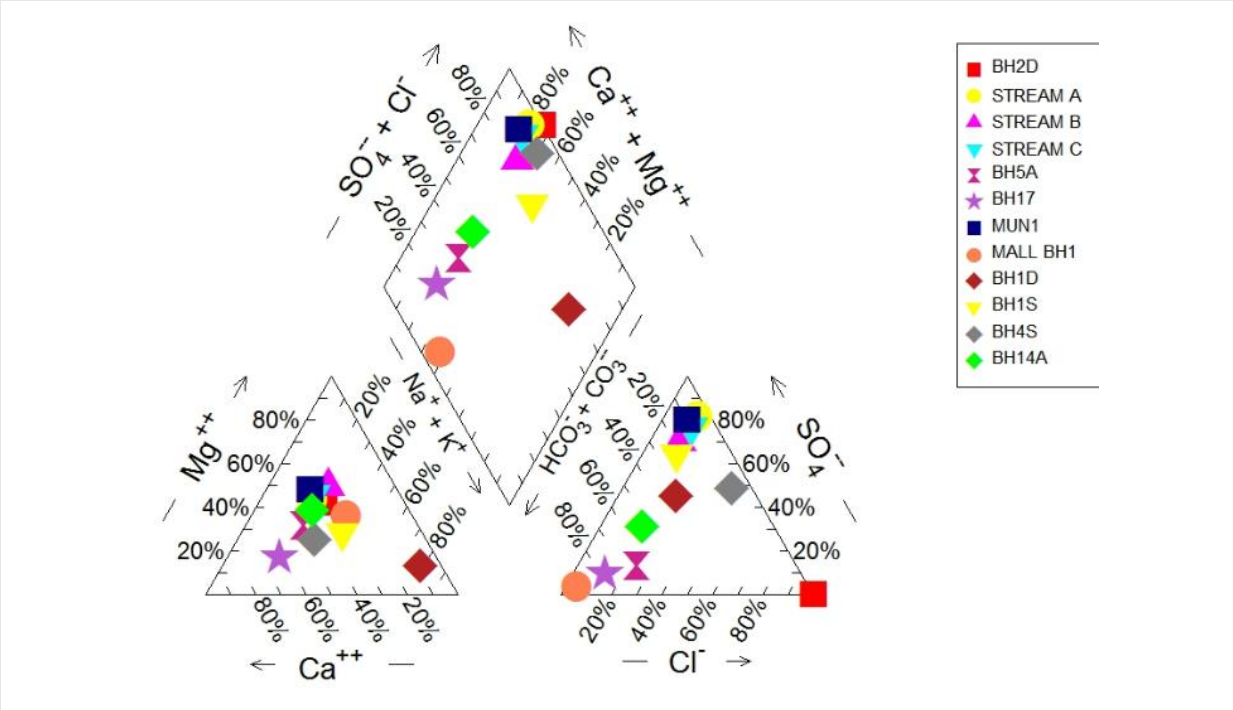

Figure 32: Piper plot showing the geochemistry of water samples collected in December 2016.

Figure 32 shows a piper diagram of water results for December 2016. Twelve water results are shown on the same diagram. The diagram helps determine the different water types based on the concentrations of ions present in each sample. Samples which fall under the same quadrant represent the same water type. Samples are represented in different symbols and colours to easily distinguish them. The concentrations of samples are represented in a form of a percentage.

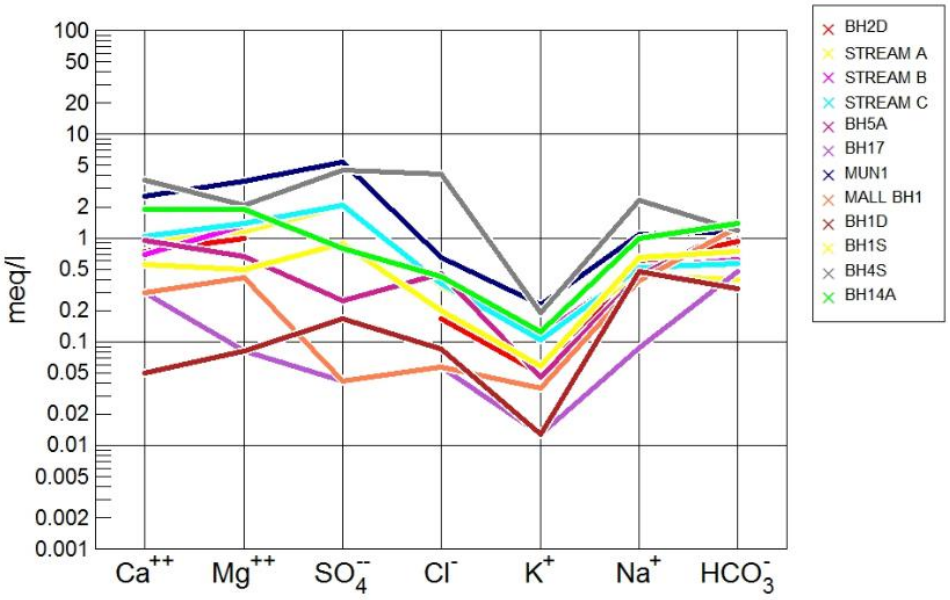

Figure 33: Schoeller diagram showing the geochemistry of water samples collected in December 2016.

December 2016 water results were also presented on a schoeller diagram shown in ***Figure 33***. The diagram shows different trends of water types from different boreholes. The concentrations of ions are shown in meq/L on a logarithmic diagram. This diagram clearly shows different water types and therefore makes it easy to analyse and interprete the water results. Different colours and symbols were used for the presentation of different samples.

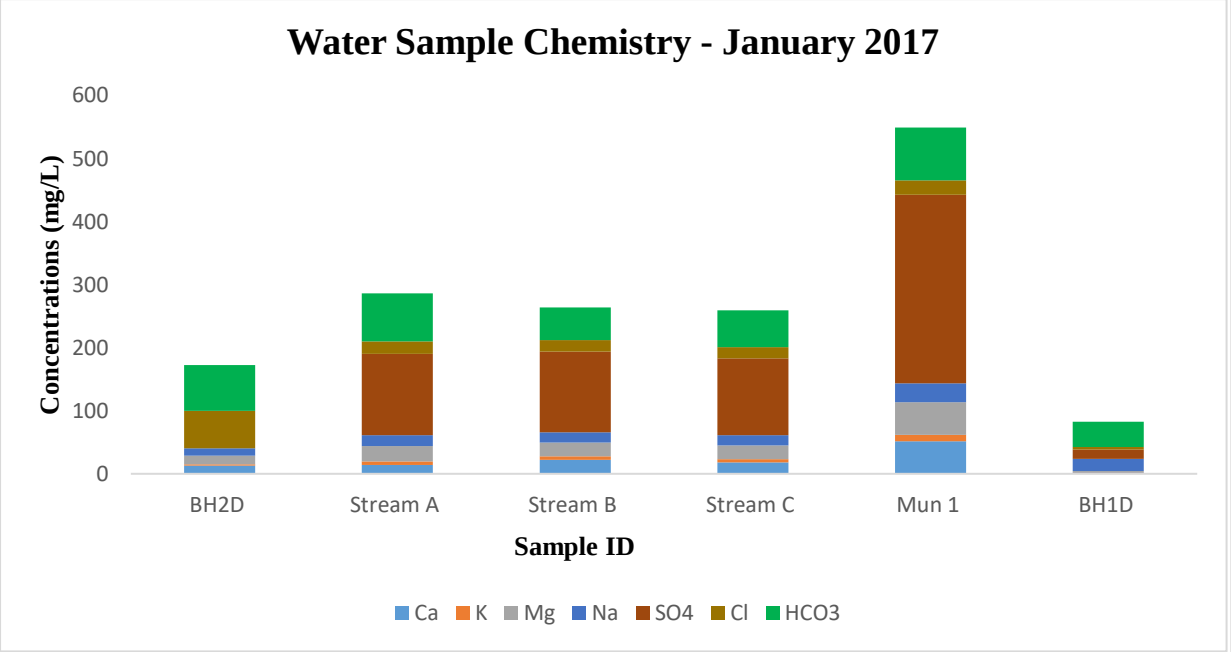

Figure 34: Analysis results for water samples collected in January 2017.

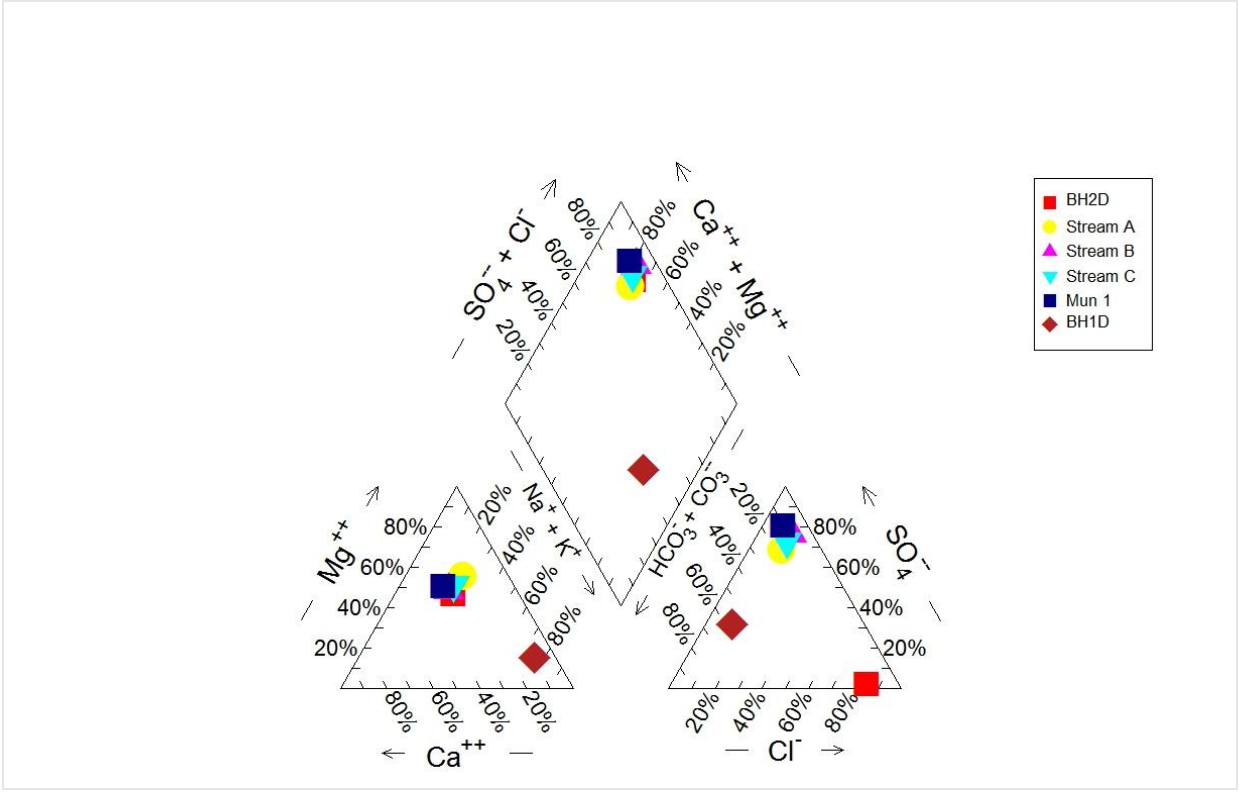

Figure 35: Piper diagram showing the geochemistry of water samples collected in January 2017.

Six samples were collected in January 2017, ***Figure 34*** is a graphical illustration of the results of these samples. Their concentrations are presented in milligrams per litre. These results are attached under Appendix C. The samples were collected to give a direct indication of the fluids permeating the cemetery soils and how they are related to the stream and the municipal water.

A piper diagram of January 2017 water results is illustrated in ***Figure 35***. This was done in order to determine the different water types and interprete their origins. The samples were collected from boreholes which had enough water for sampling, the stream, municipal water and athlone dam. These results are attached under Appendix C.

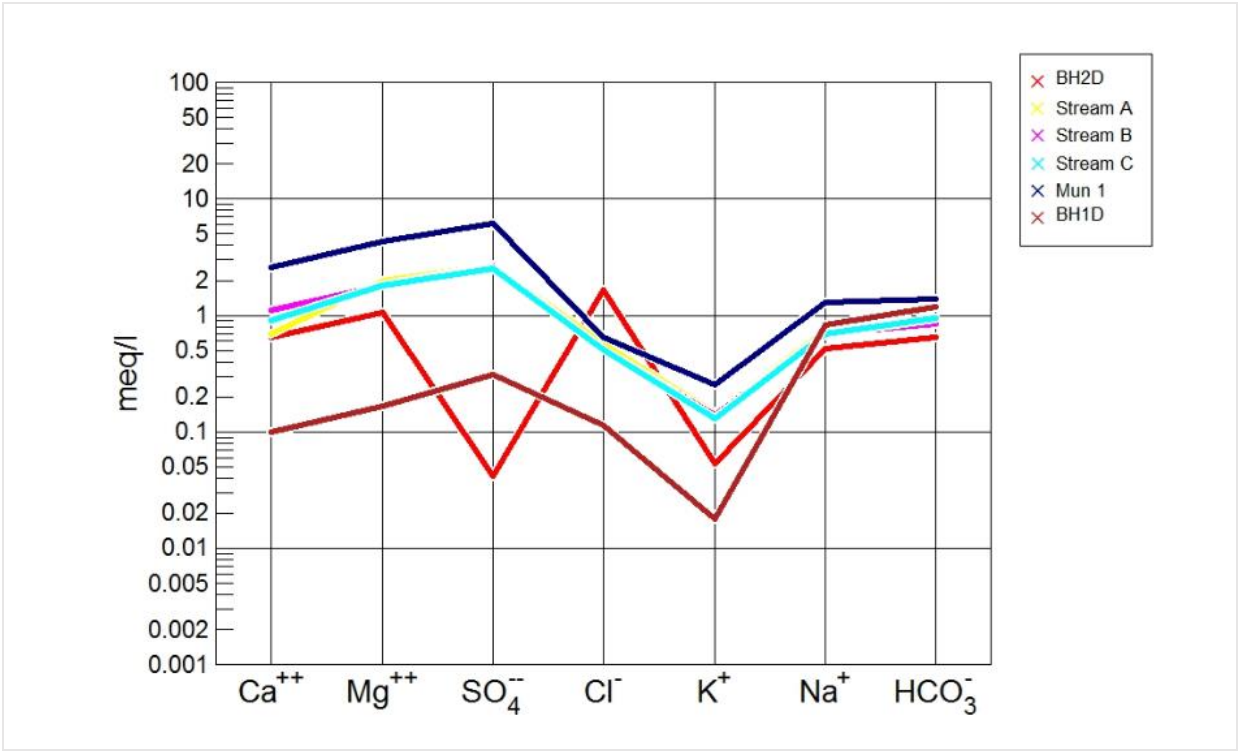

Figure 36: Schoeller diagram showing the geochemistry of water samples collected in January 2017.

Figure 36 *is* a schoeller diagram illustrating the geochemistry of water samples that were collected in January 2017. The diagram shows different water types from different origins. The trends are illustrated in different colours in order to clearly indicate the difference between them.

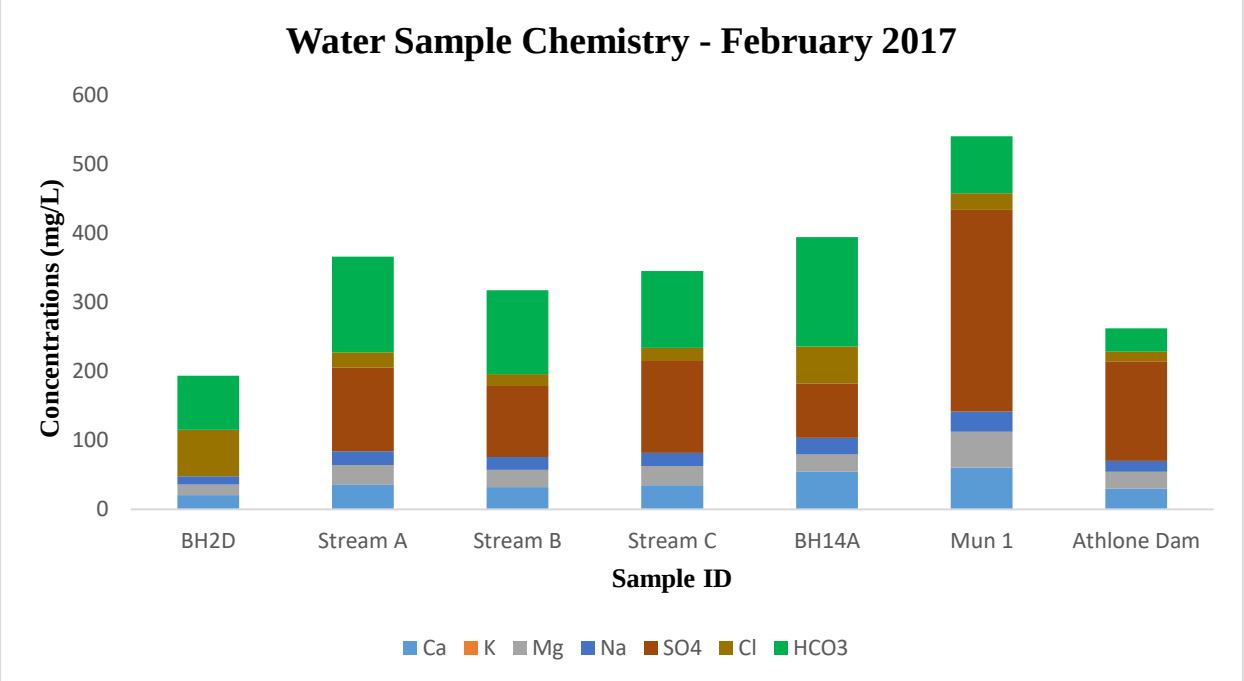

Figure 37: Analysis results for water samples collected in February 2017.

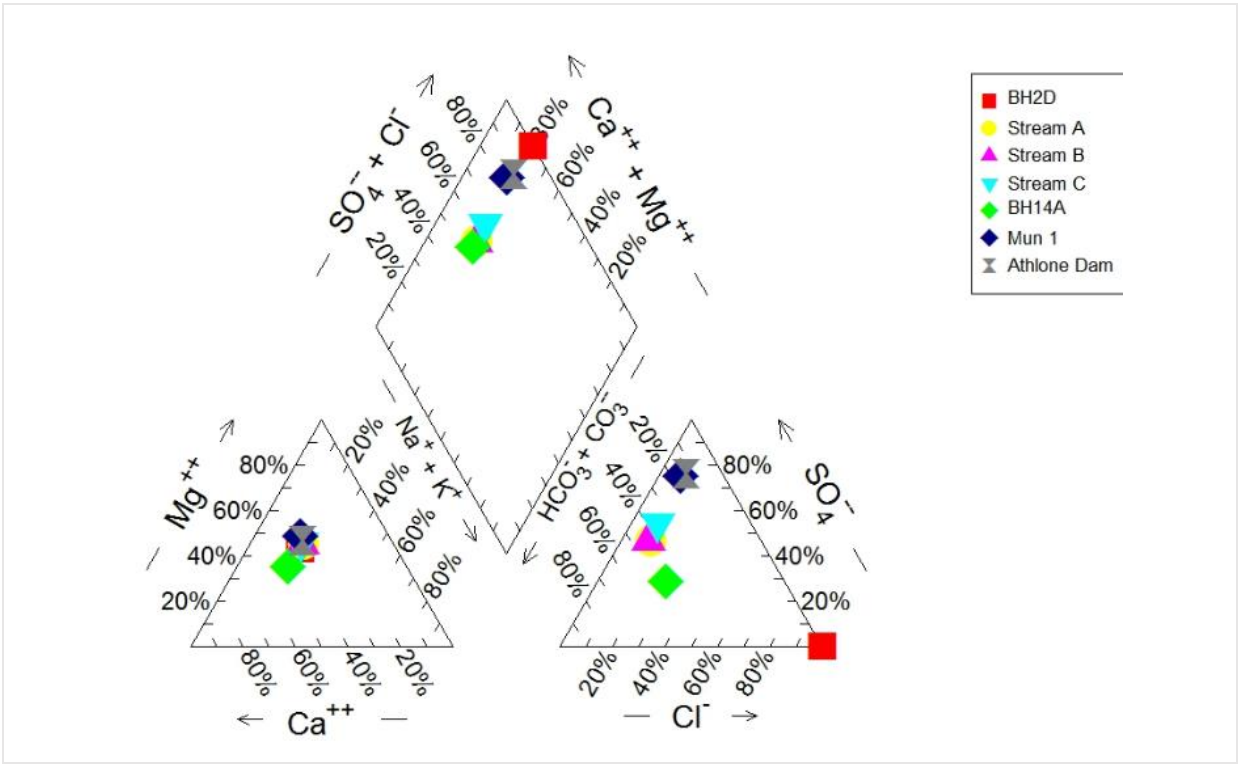

Figure 38: Piper diagram showing the geochemistry of water samples collected in February 2017.

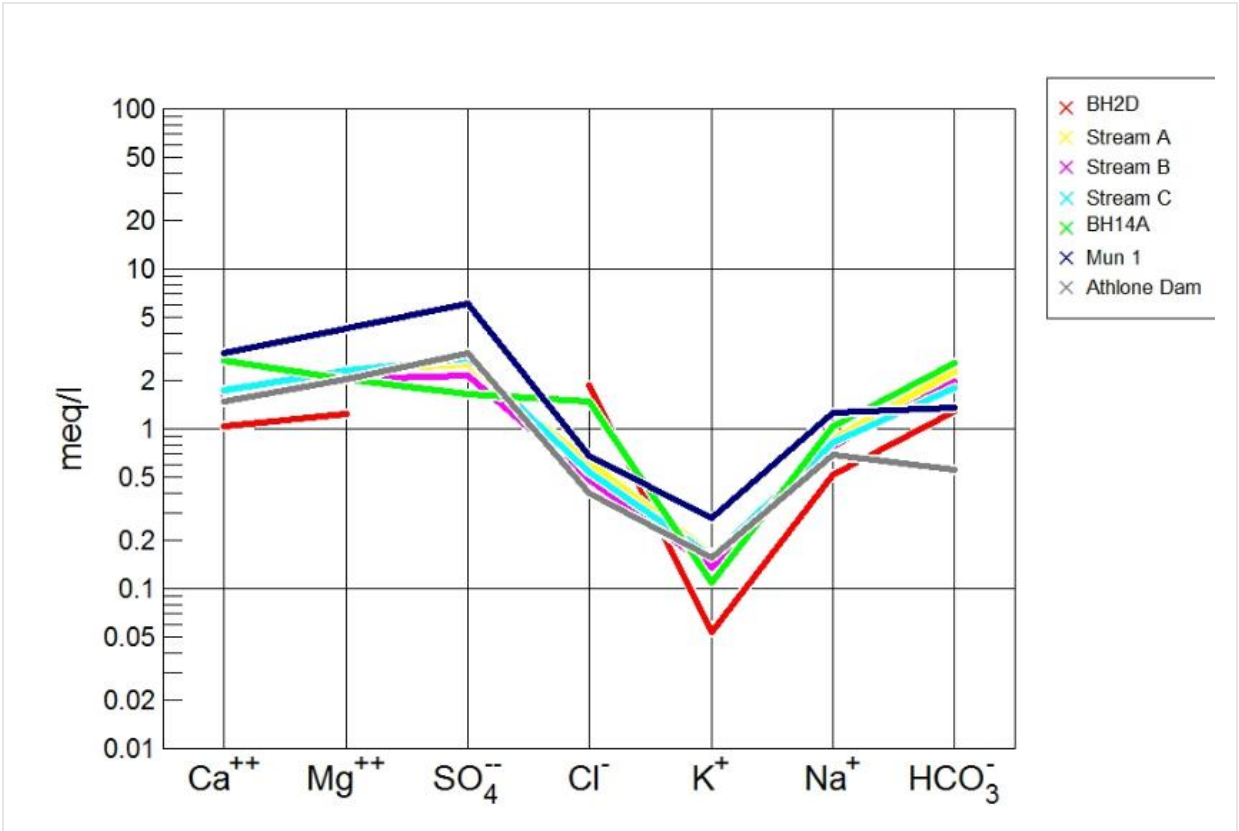

Figure 39: Schoeller diagram showing the geochemistry of water samples collected in February 2017.

The February 2017 site visit included sampling of borehole BH2D, the stream, municipal water, BH14A and Athlone dam. Graphical illustrations of their results are shown in ***Figures 37-39***. The graphs were used for the analyses and interpretations of results.

The last site visit took place in March 2017 where nine samples were collected from the four monitoring boreholes (BH1D, BH2D, BH1S and BH4S), the three points of the stream, the municipal water and Athlone dam. The results are presented in terms of a stacked bar chart, piper plot and a schoeller diagram.

Figure 40 is a stacked bar chart which displays stacked totals with each colour representing a different ion. These major and minor ion values are presented in terms of concentrations in milligram per litre for each sample. The piper diagram of major ion analyses for March water results is shown in ***Figure 41***. The individual cation and anion concentration values are expressed as percentages of the total cations and total anions and then plotted within the two triangular fields at the lower left and lower right of the diagram. The two points representing each sample are then projected to the central diamond field and the point of intersection found.

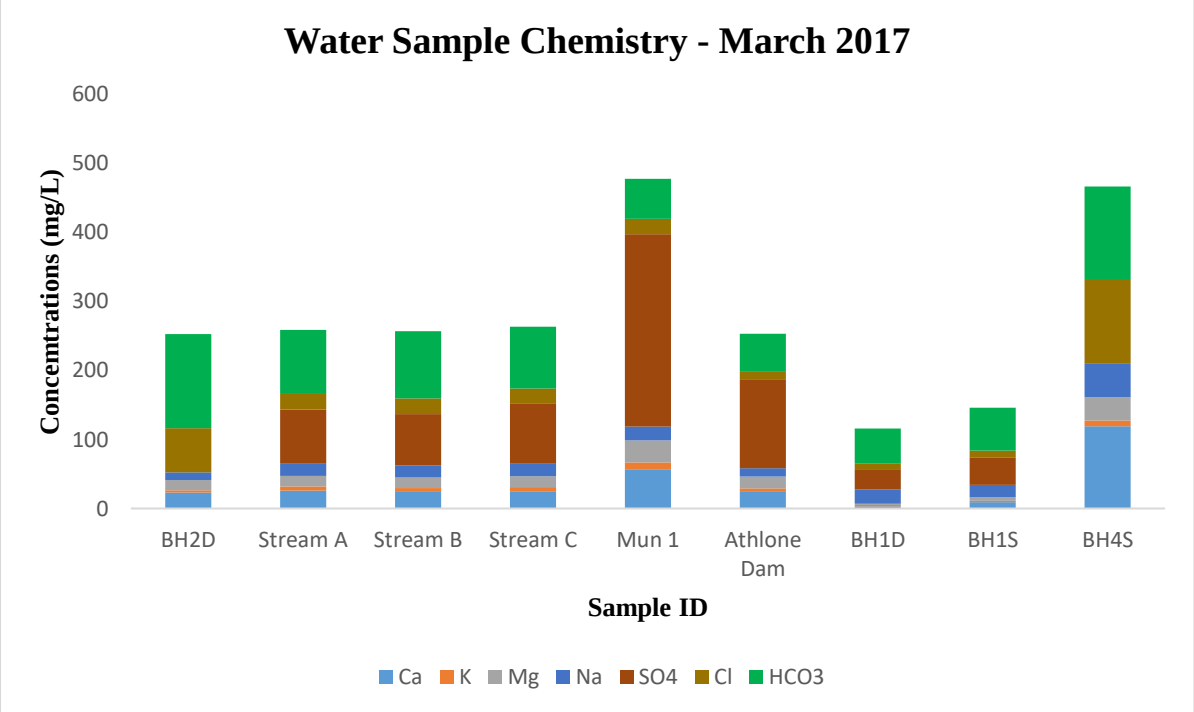

Figure 40: Analysis results for water samples collected in March 2017.

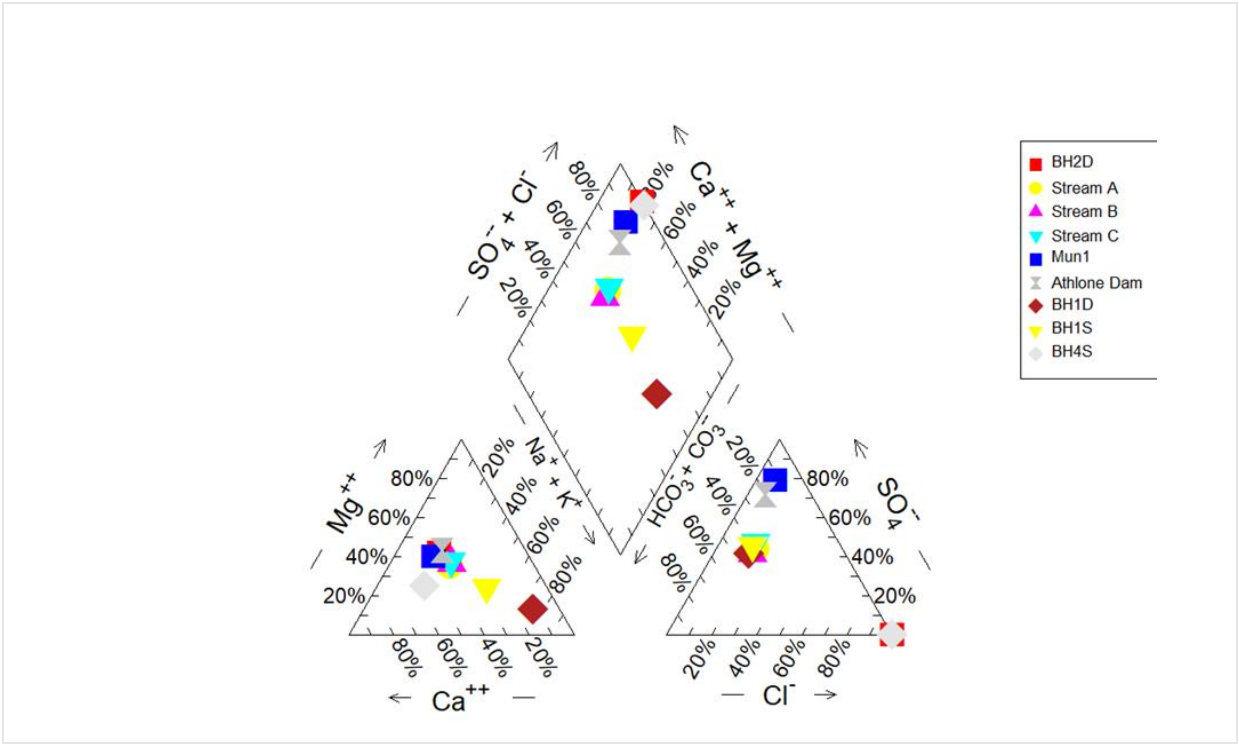

Figure 41: Piper diagram showing the geochemistry of water samples collected in March 2017.

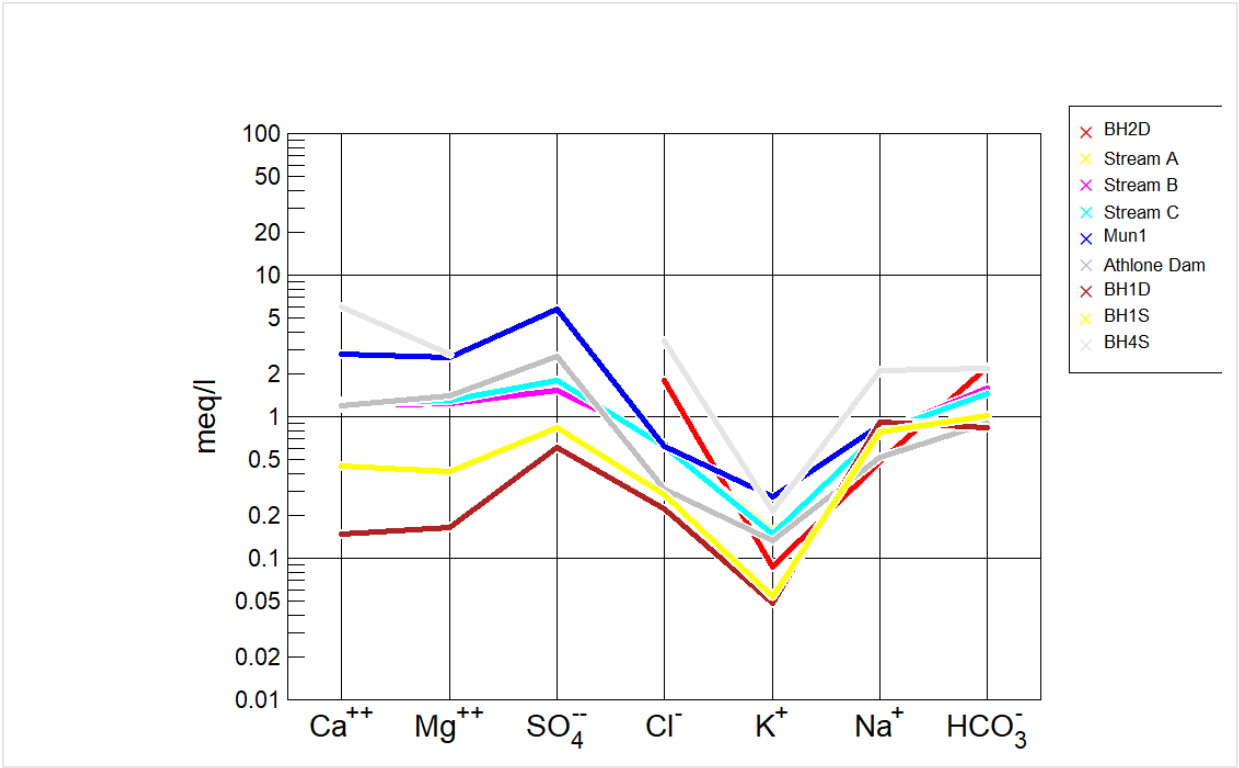

Figure 42: Schoeller diagram showing the geochemistry of water samples collected in March 2017.

4.4. Conceptual Model

A conceptual site model was developed based on the literature review performed and the data obtained from the site, to provide a conceptual understanding of the hydrogeological, geochemical and geological characteristics in the study area. Contaminants are introduced into the soil through graves and the landfill southward to the cemetery. The study is interested in finding out whether these contaminants mobilize and reach the watertable. In doing so, the study focuses on investigating the source of contamination between anthropogenic and geological/pedological sources. Some contaminants get absorbed by the roots while others leach down to the underlying watertable depending on their concentrations and mobility.

The movement of contaminants that reach the watertable is influenced by the direction of groundwater flow. Areas upslope are less contaminated than areas downslope. The boreholes in the study area were placed strategically up and downslope to the cemetery where they were expected to intersect the same aquifer. High concentrations of contaminants are expected to be noted at the borehole downslope to the cemetery. Water samples were also collected from hydrocensus boreholes downslope and the stream that runs downslope to the study site where contaminants were expected to be carried to through the flowing groundwater.

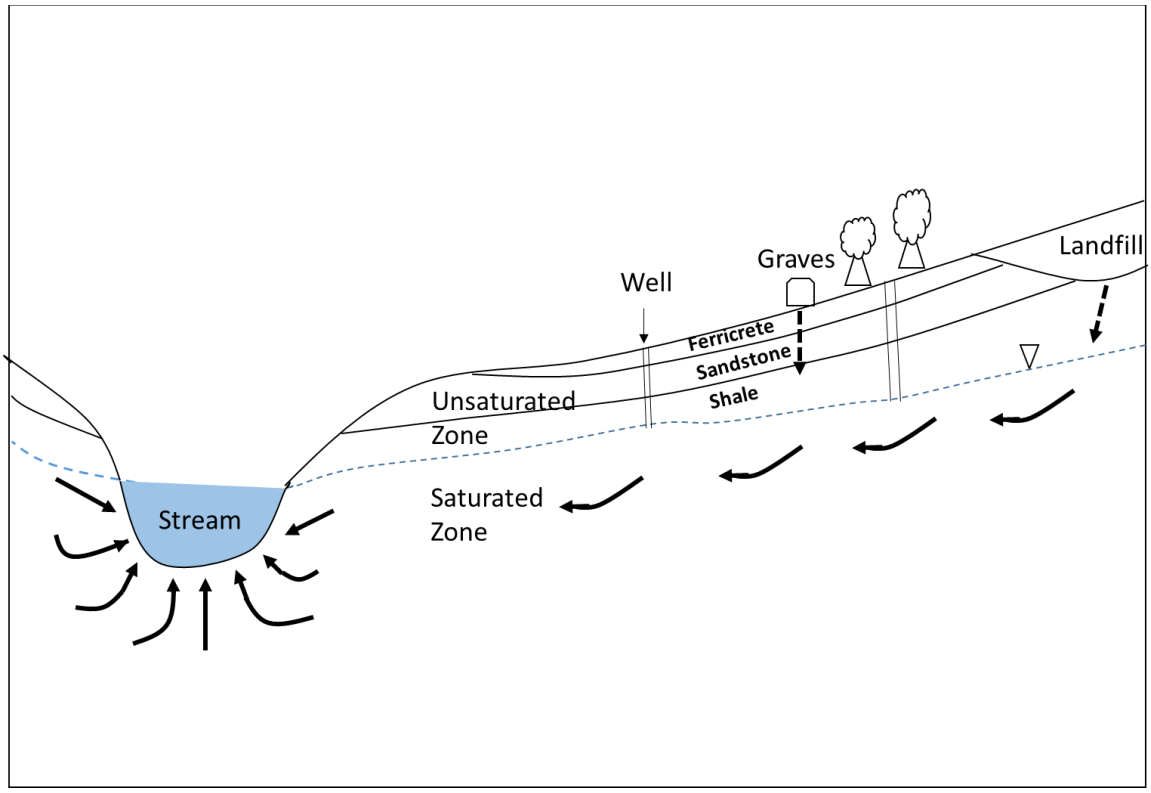

Figure 43: Hydrogeological Conceptual Model of the study site.

5. DISCUSSION

Mineral Phases

Quartz (displayed in orange) is noted as the most abundant mineral phase in BH1D and this is mainly because the study site is underlain by the Loskop Formation Sandstone. Among other reasons for its abundance are; its stability in a wide pressure and temperature range, its chemical and physical resistance to weathering. The abundance of Quartz stays relatively constant throughout the entire borehole. Furthermore and related to the aforesaid, Anatase is only present in small amounts near the land surface, up to 0.6 m. The abundance of Goethite decreases with depth, its abundance near the land surface might be due the presence of ferricrete in the area. At approximately 1.2 m, Goethite gets completely replaced by Haematite. However, Haematite concentrations decrease with the borehole depth. Kaolinite is a clay mineral which is composed within the Dwyka Group Shale that underlies the study site, hence its abundance. Kaolinite also gets replaced by muscovite. Microcline is also noted to be introduced into the profile at 1.2 m. Other mineral phases are present in minor amounts and can be ignored in this case.

The abundance of Quartz continues to be noted in BH2D, however, this time its quantity decreases with depth. Quartz is chemically more stable than most other minerals under conditions at or near the land surface, hence its abundance at the Fontein Street Cemetery soils. Muscovite and Plagioclase mineral phases are also noted in the same borehole, with Quartz appearing as the most abundant mineral phase. Haematite was also observed to replace Goethite in this borehole as well. Anatase is only present in minor amounts. Traces of Dolomite and Epidote are introduced at the watertable level (4.2 m), as noted in Appendix 4. Epidote is a product of hydrothermal alteration of micas, hence it's existence at the watertable level where it completely replaces muscovite. Traces of Dolomite and Epidote then disappear with the borehole depth. Chlorite gets introduced into the profile at 4.8 m, it also then disappears with the borehole depth. The abundance of Quartz is due to weathering of Sandstone. The presence of Goethite could be associated with the presence of ferricrete at the land surface of the cemetery.

BH3D shows greater amounts of Quartz. Abundances of clay minerals such as Muscovite, Goethite, Haematite and Kaolinite are also noted. The presence of these clay minerals might

be due to weathering of shale, since the study site is underlain by the Dwyka Group Shales. New mineral phases such as Epidote, Chlorite and Dolomite are noticed as the borehole depth increases but only present in minor amounts.

The three boreholes were drilled in the same area (Fontein Street Cemetery) but differ slightly in mineral phases. BH3D is seen to be consisting of a few clay minerals even with Quartz being the most abundant mineral phase. This could be due to the fact that BH3D is placed in a location which is mostly clayey and hence the dryness of the borehole. Similarly, BH1D and BH3D are recorded to possess higher amounts of Kaolinite as compared to BH2D. BH2D and BH1D consist mostly of sandy material near the land surface, this allows water to infiltrate and penetrate through, hence the presence of water in the two boreholes. Water gets held up by the clay material in BH2D as the borehole depth increases. The watertable was intersected at 4.06 m in BH2D and at 1.96 m in BH1D, see Appendix 4. The difference in watertable levels is due to the topography of the study area. Borehole BH2D was drilled at a location upslope to the location of BH1D, this explains why the watertable is deeper at BH2D.

95% of all sedimentary rocks consist of sandstones, mudrocks & shales (made up of silt and clay sized fragments) and carbonate rocks (made up of mostly calcite, aragonite, or dolomite). Because of their detrital nature, any mineral can occur in a sedimentary rock. Clay minerals are the most dominant minerals produced by chemical weathering of rocks. Quartz because it is stable under conditions present at the surface of the Earth is the most abundant mineral in Sandstones and the second most abundant mineral in mudrocks & shales. The Fontein Street Cemetery is underlain by sedimentary rocks hence the presence of the afore-mentioned minerals within the study area.

Major Ions

The three boreholes (BH1D, BH2D & BH3D) show variations of Si, Fe and Al which are the abundant major elements in the profile with Si being the most abundant. These major elements Si, Fe and Al correlate with the abundances of Quartz, Haematite and Kaolinite, respectively. BH1D shows a decrease of Fe with depth, this is because Fe is mostly composed within ferricretes found at or near the land surface. Si on the other hand increases with depth, whereas Al content stays relatively constant. BH2D and BH3D show variations of Si, Fe and Al. Si appears as the most abundant major ion. Al content in BH2D and BH3D increases with depth,

this might be due to weathering of the Dwyka Group Shales which underlies the Loskop Formation Sandstones in the study site.

Trace Elements

An abundance of Zirconium is noted in BH1D due to its resistance to weathering. Zirconium is only slightly mobile in the environment and unlikely presents a hazard to the environment. Zinc concentrations increase with depth. This may be due to its mobile character. Zinc contaminants in cemeteries result from handles and hinges of coffins, but then again Zinc is naturally present in soils. Zinc concentrations in this borehole are below the detection limit, so this basically means that the Zinc present in the soils of borehole BH1D are naturally occurring and of geological/pedological origin. Copper is only present in minor amounts. Soils below BH1D do not show any high concentrations of metals which could be considered as potential sources of contamination. It must be noted that results indicated with an asterisk (*) should be considered semi-quantitative.

Borehole BH2D is located in the centre of the cemetery below graves, whereas BH1D is located a few metres from the graves but still within the same cemetery yard. For the purpose of this discussion, BH1D will be referred to as off-site borehole and BH2D as on-site borehole. ***Table 8*** presents approximate ratios of mineral mean concentrations for boreholes BH1D and BH2D. The table indicates that the mean metal concentrations of off-site borehole are less than the on-site borehole mean metal concentrations. This could mean that offsite borehole metal concentrations are of geological/pedological origin whereas those of onsite borehole are of anthropogenic origin associated with burial practices.

Mean metal concentrations of Zn, Sr and Rb (highlighted in red) in BH2D are noted to be even more elevated than those of other metals. High concentrations of Zn could be resulting from hinges and handles of coffins. Rb is a lithophile metallic element that does not form any minerals on its own, but it is present in several common minerals in which it substitutes for potassium. Compared to K and Na, Rb is relatively rare, it substitutes for K in mica such as muscovite and to a lesser extent in K-feldspar such as microcline and orthoclase. High concentrations of Rb could be resulting from its substitution for K in muscovite or microcline present in the soils of the Fontein Street Cemetery.

Strontium is also a lithophile metallic element which may substitute for Ca in dolomite or Ca-plagioclase (Anorthite). Sr high concentrations in this case indicate its substitution for Ca in dolomite. The results in this study indicate that burial practices do indeed influence the concentration of metals in cemetery soils. The Fontein Street Cemetery soils are mostly sandy around the land surface and a few metres deep, they then get clayey with depth. This explains why metals are more concentrated at larger depths, clayey soil retains high amount of metals when compared to sandy soil. Metal concentrations of borehole BH2D, follows the same trend as those of borehole BH1D except that they are more elevated. This indicates that burial practices do have an influence on cemetery soil mineral concentrations.

BH3D also shows abundances of Zr, Zn, Rb and Sr. Other trace elements are only present in minor amounts. The presence of Zr is due to its resistance to weathering. Zn concentrations are below the detection limit, therefore would be of natural existence. The diagram shows an increase in Sr with depth, Sr high concentrations indicate its substitution for Ca in dolomite. High concentrations of Rb could be resulting from its substitution for K in mica or microcline present in the soils of the Fontein Street Cemetery.

Water Quality

Major ions (Ca^{2+}, Mg^{2+}, Na^{+}, K^{+}, Cl^{-}, SO_4^{2-}, HCO_3^{-}) are naturally variable in surface and groundwaters due to local geological, climatic and geographical conditions. This is the case with the water quality results of the Fontein Street Cemetery and the surrounding areas where the data was collected. Interpretations and analysis of water results were done based on the data presented in stacked charts, piper plots and schoeller diagrams. The boreholes at the Fontein Street Cemetery, the stream, Athlone dam and the Hydrocensus boreholes were monitored for a period of 6 months, from October 2016 to March 2017, in order to trace any changes of water quality which might have resulted due to metal contamination from graves.

The October 2016 stream samples are noted to be plotting in the quadrant representing Ca-SO_4 waters as shown on the piper plot. This indicates that the stream has higher concentrations of sulphate which might have resulted from contamination of surface water by acid mine drainage from the surrounding mines in the area. The area falls within the B12D quaternary catchment of the Upper Olifant's water management area, the water quality of this catchment is under a

lot of threat by coal mines. BH2D samples on the other hand plot in the quadrant representing Ca-Cl waters which are representative of deep ancient waters. This is clearly shown on the schoeller plot. There is no correlation between the stream and BH2D water qualities, and this means they were sourced from different origins.

The conceptual model of the study assumes the watertable intersected by borehole BH2D to flow into and recharge into the stream since the cemetery is upgradient with reference to the stream, however, the water results have proven otherwise. Therefore, contaminants from the cemetery would not have had any impact on the stream water quality, in this case. BH2D water is representative of Ca-Cl waters and this suggests that there are no potential contaminants from the grave that might have leached into the groundwater intersected by BH2D. This means that the watertable intersected by borehole BH2D at 4.06 m, contains only naturally occurring ions with concentrations that fall within the acceptable limits of the South African National Standards of drinking water.

The Hydrocensus data show that the municipal water (Mun 1) plots in the quadrant that represents Ca-SO_4 waters. High concentrations of SO_4 in the municipal water samples, indicate that the water is impacted by the acid mine drainage. However, those high concentrations still fall within the acceptable limits of SANS of drinking water. Therefore, this means the water is potable/drinkable and allowed to be used by the community.

The mall borehole (Mall BH1) plots in the Na-HCO_3 water type which is representative of unpolluted groundwater. There is no correlation between Mall BH1 water quality and those of other boreholes. This makes sense since Mall BH1 falls outside the delineated 1 km radius of the hydrocensus. The three private/hydrocensus (BH14A, BH5A & BH17) boreholes show a slight correlation, they all plot in the quadrant that is representative of the Ca-HCO_3 waters. Ca-HCO_3 water type represents shallow fresh groundwater which has recently been recharged.

December 2017 water qualities of the stream, BH1D, BH1S, BH4S and Mun 1 plot in the same quadrant, the Na-Ca-SO_4 water type quadrant. Their water qualities show high concentrations of sulphate which might have resulted from the acid mine drainage, since there are a lot of mining activities taking place around the Middelburg area. The three boreholes are shallow and

December is a rainy month. The water that was encountered in these shallow boreholes might have been recharged from the dams as they discharged.

BH1S and BH4S are shallow boreholes and their water quality indicates that the shallow aquifer is also affected by the acid mine drainage. BH2D plots in the Ca-Cl waters which are representative of deep ancient waters. BH2D intersects the water table at 4.06 m, it therefore represents a deep aquifer in this case. The shallow aquifer water quality is represented by those of BH1S and BH4S. This indicates that the water quality of the shallow aquifer in study area is different from that of the deep aquifer. The difference between the two aquifers is that the shallow aquifer is contaminated by acid mine drainage whereas the deep aquifer is only contaminated by naturally occurring metals. The concentrations of these metals are, however, detected below SANS limits.

The depth of BH1D is somewhat shallow even though it is regarded as a deep borehole in this study, this supports its similarity of water quality results to those of BH1S and BH4S. Borehole BH2D water quality stays the same as the October one, Ca-Cl water type. This proves that no new contaminants were introduced into the deep aquifer.

Hydrocensus boreholes (BH14A, BH5A & BH17) and Mall BH1 water qualities remain the same as those of the month of November. Hydrocensus boreholes plot in the Ca-HCO_3 quadrant which represents shallow fresh groundwater, whilst Mall BH1 still plots in the Na-HCO_3 quadrant which represents unpolluted groundwater.

The January and February water results stay the same as those of the previous months. Athlone dam was sampled in February and its water quality results have similarities to those of the stream, shallow onsite boreholes and the municipal water. This proves that the dam was also affected by acid mine drainage. It is of no surprise that the water quality of Athlone dam has similarities to that of the stream since Athlone dam discharges into the stream when full.

In March 2017, the stream water quality remained the same, representing Ca-SO_4 waters due to contamination resulting from acid mine drainage. This applies to Athlone dam and the municipal water as well. They both also represent Ca-SO_4 waters. Boreholes BH1D and BH1S plot on the Na-HCO_3 quadrant which represents unpolluted groundwater. The two boreholes

are located close to one another and their depths are also almost similar. This explains the similarity in their groundwater qualities. BH2D plots in the Ca-HCO_3 which is representative of shallow fresh groundwater which has recently been recharged. BH4S plots on the Ca-Cl quadrant which is representative of deep ancient water, which does not make sense since BH4S is a shallow borehole.

Water qualities of onsite boreholes, the stream, Athlone dam, municipal and those of private/hydrocensus boreholes seem to be following the same pattern/trend even after having been monitored for a period of 6 months. They all contain the most common ions found in water, which include Mg^{2+}, Ca^{2+}, Na^{+}, K^{+}, Cl^{-} and $SO4^{2-}$. This suggests that no metals from the grave area have impacted the study site, however elevated metal concentrations below the grave area do prove that burial practices influence cemetery soils metal concentrations. It was noted from the results that the study area (B12D Quaternary Catchment) is heavily impacted by the acid mine drainage (elevated sulphate concentrations) since the mine water in the Olifant's river catchment amounts to 4.6% of the total water usage and contributes 78% of the sulphate load (Van Zyl et al., 2001).

6. CONCLUSIONS

The following conclusions were made based on the data collected, analyses performed, tests performed, assumptions and interpretations made.

1. The chemical composition of the Fontein Street Cemetery Soils is dominated by major elements Si, Fe and Al. The dominant trace elements contributing to the cemetery soils are Zr, Zn, Sr and Rb. The high concentrations of Zirconium may be due to its resistance to weathering and its slight mobility in the environment. Elevated concentrations of Zinc were noted in the borehole located in the centre of the cemetery, where burial has taken place. These concentrations of Zinc are higher than those of the borehole metres away from the graves. This proves that burial practices do indeed influence metal concentrations in cemetery soils. Zinc contaminants below the interment level result from handles and hinges of coffins and are of anthropogenic origin. However, Zinc concentrations at the borehole located a few metres away from graves are lower and may be naturally occurring. The presence of Sr in the soils of the Fontein Street Cemetery may be due to its substitution for Ca in dolomite. The presence of Rb in the study area may also be due its substitution for K in Mica such as Muscovite or in K-Feldspar.

2. The mineralogical composition of the study site consists of the following clay and sandy minerals.
    - Goethite $Fe_{3.6}\,Co_{0.4}O_8$
    - Haematite Fe_2O_3
    - Kaolinite $Al_2Si_2O_5\,(OH)_4$
    - Quartz SiO_2
    - Muscovite $KAl_3Si_3O_{10}\,(OH)_2$
    - Anatase TiO_2
    - Plagioclase $NaAlSi_3O_8$ (Albite), $CaAl_2Si_2O_8$ (Anorthite)
    - Dolomite $Ca\,Mg\,(CO_3)_2$
    - Epidote $Ca_2\,(Al, Fe)_2\,(SiO_4)_3\,(OH)$
    - Chlorite $(Mg, Fe)_3\,(Si, Al)_4O_{10}\,(OH)\,(Mg, Fe)_3\,(OH)_6$
    - Microcline $KAlSi_3O_8$

The dominant mineral phases are Quartz, Haematite and Kaolinite which correlate with the abundaces of Si, Fe and Al, respectively. Quartz forms part of the Loskop Formation Sandstones which underlie the area. The Loskop Formation Sandstones are inturn underlain by the Dwyka Group Shales which compose clay minerals.

3. Percolation test results show a similarity in saturated hydraulic conductivities of some of the augered boreholes which are representative of clay-silty material. On the other hand, there was another augered borehole that showed a different saturated hydraulic conductivity which is representative of sandy material. This sandy material is only noted near the land surface, since the borehole is seen to be composed of clayey material as the borehole depth increases.

4. The groundwater quality of the Fontein Street cemetery is dominated by Ca, Mg, Cl and Na metals. BH2D water samples plot in the quadrant representing Ca-Cl waters which is representative of deep ancient groundwater which contains naturally occurring ions. Whereas the stream samples plot in the quadrant representing Ca-SO_4 waters which is representative of gypsum groundwater and mine drainage. This indicates high concentrations of SO_4 in the stream which might have resulted from contamination of surface water by acid mine drainage from the surrounding mines. There was no relationship noted between the stream and BH2D water qualities as the study had predicted, since the cemetery is upgradient to the stream.

5. The Municipal water quality falls in the same quadrant as the stream, this indicates a correlation between the two. The municipal water quality also shows high concentrations of SO_4, this suggests the acid mine drainage impact. The high concentrations of SO_4 in the municipal water are, however, below detection limits of the South African National Standards of drinking water. Therefore, the municipal water is still drinkable/potable. Hydrocensus boreholes (BH14A, BH5A & BH17) water qualities are representative of Ca-HCO_3 waters. These waters are shallow fresh groundwaters which have recently been recharged, they do not have any foreign contaminants in them. Shallow onsite boreholes also show high concentrations of SO_4. This indicates that the cemetery soils near the land surface (the unsaturated zone) have also been impacted by acid mine drainage. Athlone dam is also representative of Ca-

SO_4 waters. The mall BH1 water quality does not show a correlation with any of the above-mentioned water qualities, this makes sense since the mall borehole falls outside the 1 km delineated radius of the hydrocensus conducted. The only relationship noted in the study is that of the stream, the shallow on-site boreholes (BH1S & BH4S) and the Athlone dam water qualities, and that relationship proves they were all impacted by the acid mine drainage.

6. The soils below BH2D have noticeable concentrations of Zinc metals, but that is not the case with the groundwater underneath them. This suggests that contaminants from graves might have not reached the watertable of the Fontein Street Cemetery. This also proves that clay-sand mix of low porosity prevents contaminants from leaching into the groundwater, since these contaminants get retained by clay. This holds true for soils of the Fontein Street Cemetery. Burial practices do indeed influence cemetery soils metal concentrations, though it takes longer for them to reach deeper levels and eventually leach into the groundwater.

7. REFERENCES

1. Anderson, M. P. (1984). Movement of contaminants in groundwater: Groundwater transport-advection and dispersion: Groundwater Contamination. Washington, D. C., National Academy Press, 37-45.
2. Alloway, B.J. (1995). Heavy metals in soils. (2nd Ed.). Blackie, London.
3. Aydinalp, C. and Marinova, S. (2003). Distribution and forms of heavy metals in some agricultural soils. Polish Journal of Environmental Studies, 12 (5): 629 - 633.
4. Bang, J. and D. Hesterberg. (2004). Dissolution of trace element contaminants from two coastal plain soils as affected by pH. J. Environ. Qual. 33, 891-901.
5. Barnard, R.O. (2000). Carbon sequestration in South African soils. ARC-ISCW Report No GW/A/2000/48. (ARC-Institute for Soil, Climate and Water: Pretoria).
6. Basta, N.T., Ryan, J.A. and R. L. Chaney. (2005). Trace element chemistry in residual – treated soil: Key concepts in metal bioavailability. J. Environ. Qual. 34: 49-63.
7. Bethke, C. M. (2008). Geochemical and Biogeochemical Reaction Modeling. 2nd edition. Cambridge, New York. 303pp
8. Boulding, J.R and Ginn, J.S. (2004). Soil, Vadose Zone, and Ground-water Contamination Assessment, Prevention and Remediation. 2nd edition. Lewis Publishers, London. 50pp.
9. Borch, T., Kretzschmar, R., Kappler, A., Van Cappellen, P., Ginder-Vogel, M.,Voegelin, A., and K. Campbell. (2010). Biogeochemical redox processes and their impact on contaminant dynamics. Environ. Sci. Technol. 44:15-23.
10. Brusseau, Ml. and Wilson, L.G. (1995). Estimating the transport and fate of contaminants in the vadose zone based on physical and chemical properties of the vadose zone and chemicals of interest. In L.J. Wilson, L.G. Everett & S.J. Cullen (eds), Handbook of vadoze zone characterization & monitoring. Geraghty & Miller environmental science and engineering series:203-215. Lewis Publishers.
11. Brady, N. C. and R. R. Weil. (2002). The Nature and Properties of Soils. (13th Ed.) Springer Netherlands.
12. Campbell, K.M. and D. K. Nordstrom. (2014). Arsenic speciation and sorption in natural environments. Rev. Mineral. Geochem. 79:185-216.

13. Chuan, M. C., Shu, G. Y. and J. C. Liu. (1995). Solubility of heavy metals in a contaminated soil: Effects of redox potential and pH. Water, Air and Soil pollution, 90:543-556.
14. Coyne, M.S. and J. A. Thompson. (2006). In: Fundamental soil science, Thomson Delmar learning, Clifton Park, New York.
15. Dippenaar, M. A., Van Rooy, J. L., Breedt, N., Muravha, S. E., Mahlangu, S. and J. A. Mulders. (2014). Vadose Zone Hydrology: Concepts and Techniques. WRC Report No. TT 584/13. Water Research Commission. Pretoria. 174pp.
16. Department of Mines, Geological Survey. (1973). 1:250 000-scale Geological Map Series 2528 Pretoria. Government Printer, Pretoria.
17. Dresel, P. E., Wellman, D. M., Cantrell, K. J. and M. J. Truex. (2011). Technical and Policy Challenges in Deep Vadose Zone Remediation of Metals and Radionuclides. Environmental Science and Technology, 45 (10): 4207 - 4216
18. Elzahabi, M. and R. N. Yong. (2001). pH influence on sorption characteristics of heavy metal in the vadose zone. Engineering Geology, 60:61-68.
19. Engelbrecht, J. F. P. (1993). An assessment of health aspect on the impact of domestic and industrial waste disposal activities on groundwater resources. WRC Report no. 371/1/93. Pretoria.
20. Engelbrecht, J. F. P. (1998). Groundwater pollution from cemeteries. Biennial Conference and Exhibition. Proceedings of the Water Institute of South Africa (WISA), Cape Town, 4 – 7 May 1998, volume 1: session 1C-3 1, pp. 1-8.
21. Engelbrecht, J. F. P. (2000). Groundwater pollution from cemeteries, CSIR Report. Groundwater Group, Cape Water Programme CSIR, PO Box 320. Steilenbosch 7599 pp. 1-8. http:www.ewisa.co.za/literature/files/1998%20-%2017.pdf, cited 4.02.2012.
22. Environment Agency. (2004). Mobilising Nature's Armoury: Monitored Natural Attenuation- Dealing With Pollution Using Natural Processes. Booklet SCHO0104BHTD-E-E, Environment Agency.
23. Essington, M.E. (2004). Soil and Water Chemistry: An integrated approach, Florida, CRC Press LLC.
24. Farah, H. and W. F. Pickering. (1977). The sorption of lead and cadmium species by clay minerals. Australian Journal of Chemistry, 30: 1417-1422.
25. Fetter, C. (1994). Applied Hydrogeology (3rd ed.). Prentice-Hall Inc. New Jersey.

26. Fielder, S., Breuer, J., Pusch, C. M., Holley, S., Wahl, J., Ingwersen, J. and M. Graw. (2012). Graveyards- Special landfills. Science of the Total Environment, 419: 90-97.
27. Fischer, G. J. and L. Croukamp. (1993). Ground Water Contamination and its Consequences, Resulting from the Indiscriminate Placing of Cemeteries in the Third World Context. Conference Africa Needs Groundwater. University of the Witwatersrand, Johannesburg, South Africa.
28. Fitts, C. R. (2002). Groundwater Science. Academic Press. London.
29. Freeze, R. A. and J. A. Cherry. (1979). Groundwater. Prentice Hall, Englewood Cliffs, NJ.
30. Ghayoraneh, M. and A. Qishlaqi. (2017). Concentration, distribution and speciation of toxic metals in soils along a transect around a Zn/Pb smelter in the northwest of Iran. Journal of Geochemical Exploration, 180: 1-14.
31. Gräfe, M., Donner, E., Collins, R.N. and E. Lombi. (2014) Speciation of metal(loid)s in environmental samples by X-ray absorption spectroscopy: a critical review. Anal. Chim. Acta 822:1–22.
32. Gray, D. A., Mather, J. D. and J. B. Harrison. (1974). Review of groundwater pollution from waste disposal sites in England and Wales with provisional guidelines for future site selection. The Quarterly Journal of Engineering Geology, 7: 181-196.
33. Hanzlick, R. (1994). Embalming. Body preparation, burial and disinterment. An overview for forensic Pathologists. The American Journal of Forensic Medicine and Pathology, 15: 122-131.
34. Herselman, H. E., Papenfus, M., Steyn, C. de Jager., P. C. and E. H. Tesfamariam. (2013). Evaluation of partitioning coefficients for South African soils to inform the National Framework for the Management of Contaminated Land with emphasis on the protection of water resources. WRC Report No. 2102/1/13.
35. Hiscock, K. M. and V. F. Bense. (2014). Hydrogeology – Principles and Practice. 2nd edition. John Wiley & Sons. https://app.knovel.com/hotlink/toc/id:kpHPPE0033?hydrogeology principles/hydrogeology-principles.
36. Jonker, C and J. Olivier. (2012). Mineral contamination from cemetery soils: case study of Zandfontein Cemetery, South Africa. J. Environ. Res. Public Health, 9:511–520.
37. Kirpichtchikova, A. T, Manceau, A, Spadini, L, Panfili, F, Marcus, M. A. and T. Jacquet. (2006). Speciation and solubility of heavy metals in contaminated soil using

X-ray micro fluorescence, EXAFS spectroscopy, chemical extraction and thermodynamic modeling. Geochimica et Cosmochimica Acta, 70: 2163-2190.

38. Kuo, S. and A. S. Baker. (1980). Sorption of copper, zinc, and cadmium by some acid soils. Soil Sci. Soc. Am. J. 44: 969-974.
39. Latterell, J. J., R. H. Dowdy and W. E. Larson. (1978). Correlation of extractable metals and metal uptake of snap beans grown on soil amended with sewage sludge. J. Environ. Qual. 7: 435-440.
40. McBride, M.B. (1994). Environmental chemistry of soils, Oxford University Press, Oxford.
41. McBride, M. B. and J. J. Blasiak. (1979). Zinc and copper solubility as a function of pH in an acidic soil. Soil Sci. Soc. Am. J. 43: 866-870.
42. McGrath, S. P. and P. J. Loveland. (1992). The Soil Geochemical Atlas of England and Wales. London: Blackie.
43. McLean, J. E. and B. E. Bledsoe. (1992). Behaviour of Metals in Soils. EPA/540/S-92/018.
44. Mehes-Smith, M., Nkongolo, K. K., Narendrula, R. and E. Cholew. (2014). Mobility of Heavy Metals in Plants and Soil: A Case Study From A Mining Region in Canada. American Journal of Environmental Science. 9 (6): 483-493.
45. Mondofacto Ltd. (Compiler). (October 9th, 1997, cited April 24th, 2011). Fick's Law of Diffusion. (Internet). (Place unknown). (Publisher Unknown). (approx. 1p.)http://www.mondofacto.com/facts/dictionary?fick's+law+of+diffusion.
46. Muldoon, M. and J. Payton. (1993). Determining Wellhead Protection Area Boundaries. An introduction. WR313-92, Wisconsin Department of Natural resources.
47. Mulligan, C. N., Yong, R. N. and B. F. Gibbs. (2001). Remediation technologies for metal-contaminated soils and groundwater: an evaluation. Engineering Geology. 60: 193-207.
48. Naidu, R. Sumner, M. E. and R. D. Harter. (1998). Sorption of heavy metals in strongly weathered soils: an overview. Environmental Geochemistry and Health, 20: 5-9.
49. Niagru, J. O. (1990). Global Metal Pollution: Poisoning the Biosphere. Environment: Science and Policy for Sustainable Development, 32 (7): 7-33
50. Nimmo, J. R. (2009). Vadose Water. In: Gene E. Likens, (Editor) Encyclopaedia of Inland Waters. Volume 1, pp. 766-777 Oxford: Elsevier.

51. Pacheco, A., Mendes, J. M. B., Martins, T., Hassuda, S. and A. A. Kimmelmann. (1991). Cemeteries- a potential risk to groundwater. Water Science Technology, 24: 97-101.
52. Palmer, C. M. (1996). Principles of contaminant hydrogeology. 2nd edition. CRC press.
53. Patil, S. B. and H. S. Chore. (2014). Contaminant transport through porous media: An overview of experimental and numerical studies. Advances in Environmental Research, 3(1): 45-69. DOI: http://dx.doi.org/10.12989/aer.2014.3.1.045.
54. Pettry, D. E. and R. E. Switzer. (2001). Arsenic concentrations in selected soils and parent materials in Mississippi. Mafes Bulletin 104. Office of Agricultural Communications, Mississippi State University.
55. Rieuwerts, J. S., Thornton, I., Farago, M. E. and M. R. Ashmore. (1998). Factors influencing metal bioavailability in soils: preliminary investigations for the development of a critical loads approach for metals. Chemical Speciation & Bioavailability, 10:2, 61-75.
56. SABS. (2009). Profiling, and percussion and core borehole logging in Southern Africa for Engineering purposes. SANS 633:2009, Pretoria: South African Bureau of Standards.
57. Santillan-Medrano, J. and J. J. Jurinak. (1975). The chemistry of lead and cadmium in soils: solid phase formation. Soil Sci. Soc. Am. Proc. 29: 851-856.
58. Schraps, W. G. (1972). Die Bedeutung der filtereigenschaften des Bedens fur die Anage von Friedhofen. Mitticilugen Deutsche Bodenkundl. Gesellsschaft 16, 225-229 (As reported in: Bouwer, H., 1978).
59. Sauvé, S., Hendershot, W., and H. E. Allen. (2000). Solid-solution partitioning of metals in contaminated soils: dependence on pH, total metal burden, and organic matter. Environ. Sci. Technol. 34, 1125-1131.
60. Sherene, T. (2010). Mobility and transport of heavy metals in polluted soil environment. Biological Forum- An International Journal, 2(2): 112-121.
61. Sililo, O.T.N. (1997). Migration and attenuation of organic contaminants in the unsaturated zone - Field experiments in the Western Cape, South Africa. In Chilton et al. (Editors): Groundwater in the urban environment. Proc. IAH XXVII Congress, Nottingham, UK: 181-186.

62. Sililo, O. T. N. and I. C. Saayman. (2001). Groundwater Vulnerability to Pollution in Urban Catchments. The Water Programme Division of Water, Environment and Technology CSIR. WRC Project No 1008/1/01.
63. Silviera, D. J. and L. E. Sommers. 1977. Extractability of copper, zinc, cadmium, and lead in soils incubated with sewage sludge. J. Environ. Qual. 6: 47-52.
64. Simunek, J. and M. T. Van Genuchten. (2006). Contaminant Transport in the Unsaturated Zone Theory and Modelling. The Handbook of Groundwater Engineering.
65. Sparks, D. L. (2003). Environmental soil chemistry. (2nd Ed.). Orlando, Florida, Academic Press.
66. Sposito, G. (1989). The chemistry of soils. Oxford University Press. New York.
67. Tood, D. K. and L. W., Mays. (2005). Groundwater Hydrology. (3rd Ed.). John Wiley & Sons. New Jersey.
68. Tredoux, G., Cave, L. and P. Engelbrecht. (2014). Groundwater pollution: Are we monitoring appropriate parameters?. Water SA, 30:5.
69. Trick, J. K., Williams, G. M., Noy, D. J., Moore, Y. and S. Reeder. (1999). Pollution potential of cemeteries: Impact of the 19th century Carter Gate Cemetery, Nottingham. British Geological Survey, Keyworth, Nottingham, United Kingdom (Technical Report WE/994, Environmental Agency Technical Report, NC/99/24) pp. 1-34.
70. Van Allemann, S.T., Olivier, J. and M. A. Dippenaar. (2018). A laboratory study of the pollution of formaldehyde in cemeteries (South Africa). Environmental Earth Science. https://doi.org/10.1007/s12665-017-7219-z.
71. Van Dressel, P. E., Wellman, D. M., Cantrell, K. J. and M. J. Truex. (2011). Review: Technical and Policy challenges in Deep Vadose Zone Remediation of Metals and Radionuclides. Environmental Science and Technology, 45:4207-4216.
72. Van Haaren, F. W. J. (1951). Cemeteries as sources of groundwater contamination. American institute of Chemical Engineering. Water, 35(16): 167-172.
73. Vangheluwe, M., Van Sprang, P., Verdonck, F., Heijerick, D., Versonnen, B., Vandenbroele M. and A. Van Hyfte. (2005). Metals Environmental Risk Assessment Guidance. UK Government – Department for Environment Food and Rural Affairs (Defra).
74. Van Schalkwyk, A. and Vermaak, J.J.G. (2000). The Relationship between Geotechnical and Hydrogeological Properties of Residual Soils and Rocks in the

Vadose Zone, Water Research Commission (South Africa), Report NO.701/1/11/,1-261pp.

75. Van Zyl, H. C., Maree, J. P., Van Niekerk, A. M, Van Tonder, G. J. and C. Naidoo. (2000). Collection, treatment and re-use of mine water in the Olifant's River Catchment. The journal of the South African Institute of mining and Metallurgy. SAIMM Conference, Coal.
76. Verral, D. P., Read, W. W. and K. A. Narayan. (2008). Predicting salt advection in groundwater from saline aquaculture ponds. Journal of Hydrology, 364: 201-206.
77. Wang, C., Xiao-Chen, L., Hai-Tao, M., Jin, Q. and Z. Jin-Bo. (2006). Distribution of extractable fractions of heavy metals in sludge during the wastewater treatment process. J. Hazard. Mater. 137, 1277-1283.
78. Wu, C. F., Luo, Y.M., Deng S.P., Teng, Y. and J. Song. (2014). Spatial characteristics of cadmium in topsoils in a typical e-waste recycling area in southeast China and its potential threat to shallow groundwater. Sci. Total Environ. 472: 556–561.
79. Webb, J. S., Thornson, I., Thompson, M., Howarth, R. and P. Lowenstein. (1978). The Wolfson Geochemical Atlas of England and Wales. GeoJournal library.
80. WHO, Regional Office for Europe. (1998). The impact of cemeteries on the environment and public health- an introduction briefing. World Health Organisation. EUR/ ICP/ EHNA 01 04 01 (A): 1-11.
81. Yong, R. N., Galvez-Cloutier, R. and Y. Phadungchewit. (1993). Selective sequential extraction analysis of heavy metal retention in soil. Canadian Geological Journal, 30: 834-847.
82. Young, C. P., Blackmore, K. M., Leavens, A. and P. J. Reynolds. (1999). Pollution potential of cemeteries. Draft guidance. Environmental Agency R & D Dissemination Centre, United Kingdom (R & D Technical Report P223).
83. Zhao, K.L., Lui, X.M., Xu, J.M. and H. M. Selim. (2010). Heavy metal contaminations in a soilrice system: identification of spatial dependence in relation to soil properties of paddy fields. J. Hazard. Mater. 181, 778-787.
84. Zychowski, J. (2010). Geological aspects of decomposition of corpses in mass graves from WW1 and 2, located in SE Poland. Environmental Earth Sciences. Doi:10.1007/s12665-010-0867-x.
85. Żychowski, J., Lach, J., Kolber, M. (2000b), Przestrzenna zmienność chemizmu wód

podziemnych w otoczeniu nekropolii w Polscepołudniowej [Physico-chemical features of ground waters on cemeteries of south-eastern Poland], in Burchard, J. (ed.), Stan i antropogeniczne zmiany jakości wód w Polsce [State and anthropogenic changes of water quality in Poland], Vol. 1, Wydawnictwo Uniwersytetu Łódzkiego, Łódź, 261–269.

86. Żychowski, J., Lach, J., Kolber, M. (2002), Zróżnicowanie zawartości lizyny i kwasu glutaminowego w wodach podziemnychna wybranych cmentarzach w Polsce południowo-wschodniej [The differentiation of lysine and glutamic acid contents in the ground water in cemeteries of south-eastern Poland], in Burchard, J. (ed.), Stan i antropogeniczne zmiany jakości wód w Polsce [State and anthropogenic changes of water quality in Poland], Vol. 2, Wydawnictwo Uniwersytetu Łódzkiego, Łódź, 241–251.
87. Żychowski, J., Lach, J., Kolber, M. (2005), Zróżnicowanie zawartości glicyny, leucyny i izoleucyny w wodach podziemnych na cmentarzach zlokalizowanych w różnych podłożach
    [The differentation of glycine, leucine and isoleucine contents in the ground water in cemeteries located on different bedrock], in Burchard, J. (ed.), Stan i antropogeniczne zmianyjakości wód w Polsce [State and anthropogenic changes of water quality in Poland], Vol.3, Wydawnictwo Uniwersytetu Łódzkiego, Łódź, 281–290.
88. Żychowski, J. (2007), Wpływ masowego grobu nazawartość wybranych związków organicznychw wodzie gruntowej [The effect of mass grave on the content of selected organic compounds in groundwater], in Ziułkiewicz, M. (ed.), Stan i antropogeniczne zmiany jakości wódw Polsce [State and anthropogenic changes of water quality in Poland], Vol.5, Wydawnictwo Uniwersytetu Łódzkiego, Łódź, 359–366.

89. Zychowski, J. and B. Tomasz (2014). Impact of cemeteries on groundwater chemistry: A review. Journal of Water and Health, 93: 29-37.

APPENDICES

APPENDIX 1: X-RAY DIFFRACTION ANALYSES RESULTS

The samples were prepared according to the standardized Panalytical backloading system, which provides nearly random distribution of the particles.
The samples were analyzed using a PANalytical X'Pert Pro powder diffractometer in θ–θ configuration with an X'Celerator detector and variable divergence- and fixed receiving slits with Fe filtered Co-Kα radiation (λ=1.789Å). The phases were identified using X'Pert Highscore plus software. Graphical representations of the qualitative results follow below.

The relative phase amounts (weight%) were estimated using the Rietveld method (Autoquan Program). Errors are on the 3-sigma level in the column to the right of the amount.

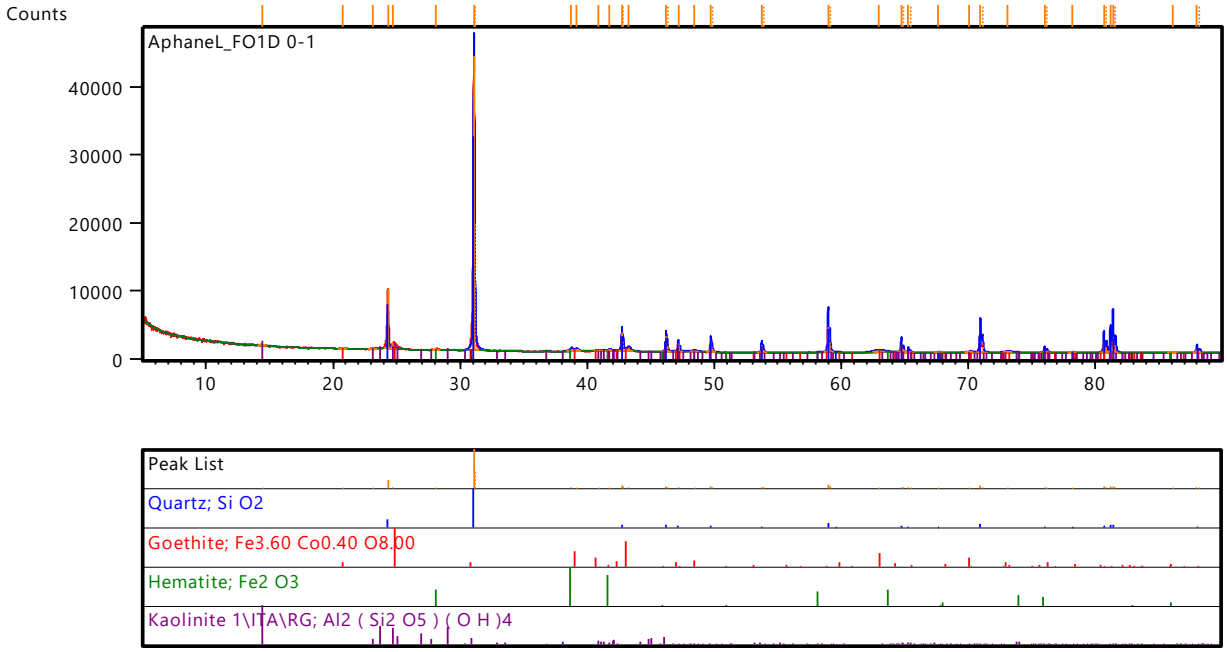

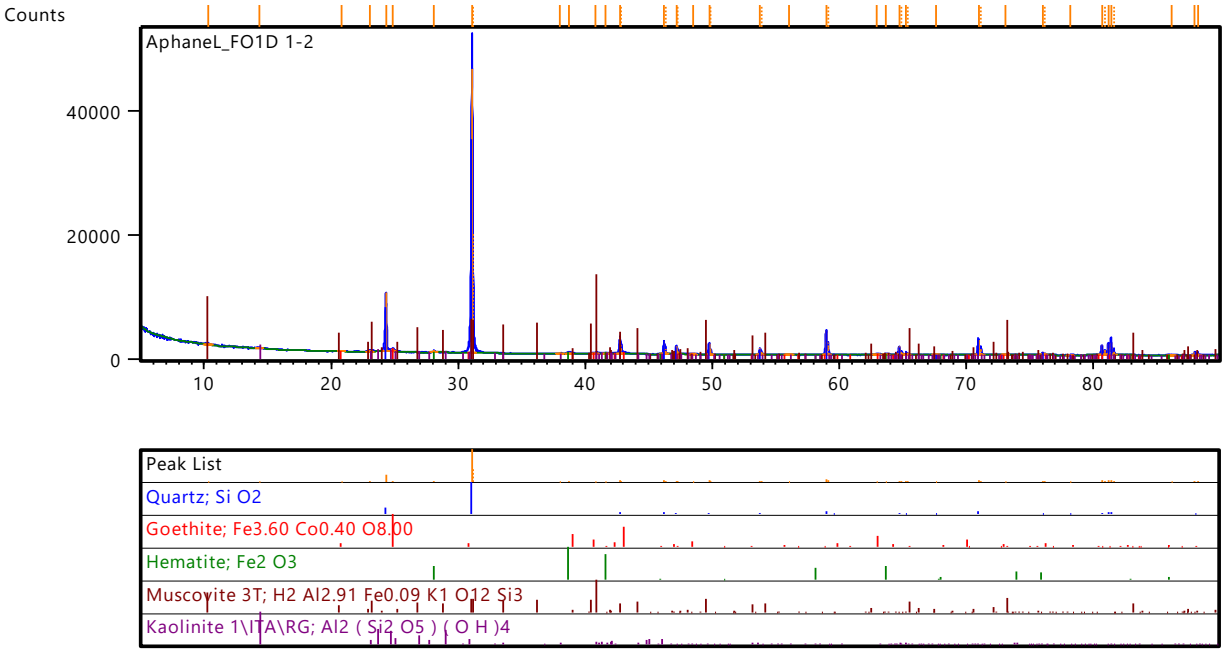
Counts
AphaneL_FO1D 1-2
40000
20000
0
10
20
30
40
50
60
70
80
Peak List
Quartz; Si O2
Goethite; Fe3.60 Co0.40 O8.00
Hematite; Fe2 O3
Muscovite 3T; H2 Al2.91 Fe0.09 K1 O12 Si3
Kaolinite 1\ITA\RG; Al2 (Si2 O5) (O H)4

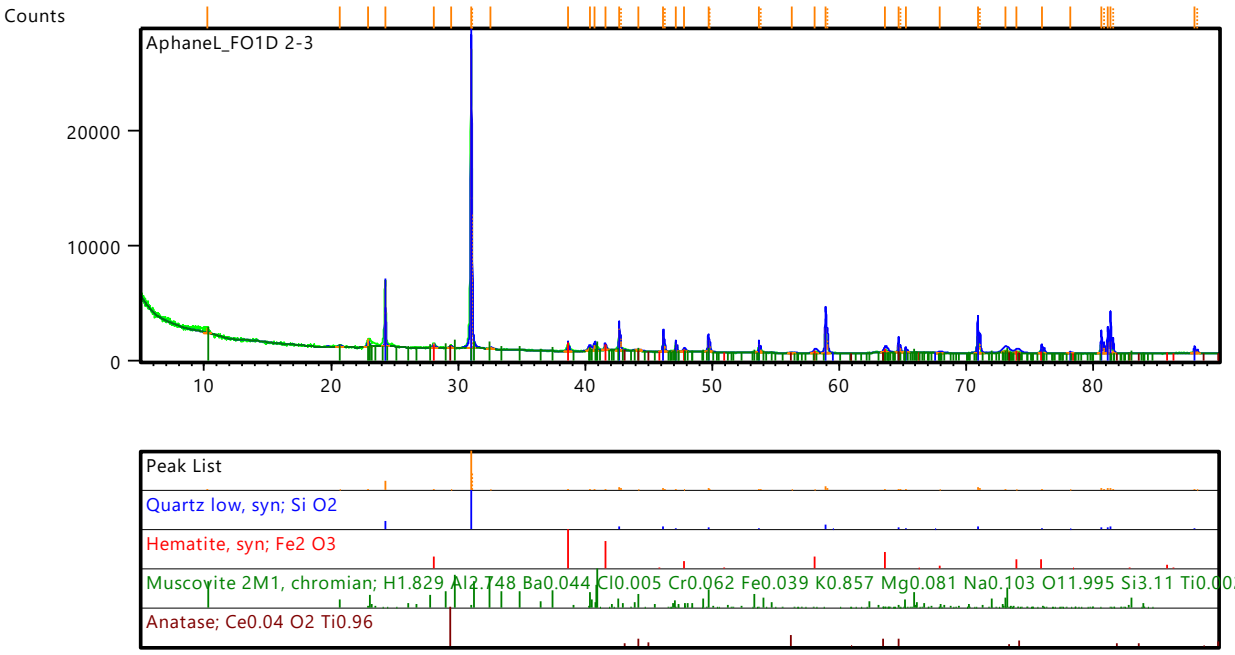
Counts
AphaneL_FO1D 2-3
20000
10000
0
10
20
30
40
50
60
70
80
Peak List
Quartz low, syn; Si O2
Hematite, syn; Fe2 O3
Muscovite 2M1, chromian; H1.829 Al2.748 Ba0.044 Cl0.005 Cr0.062 Fe0.039 K0.857 Mg0.081 Na0.103 O11.995 Si3.11 Ti0.02
Anatase; Ce0.04 O2 Ti0.96

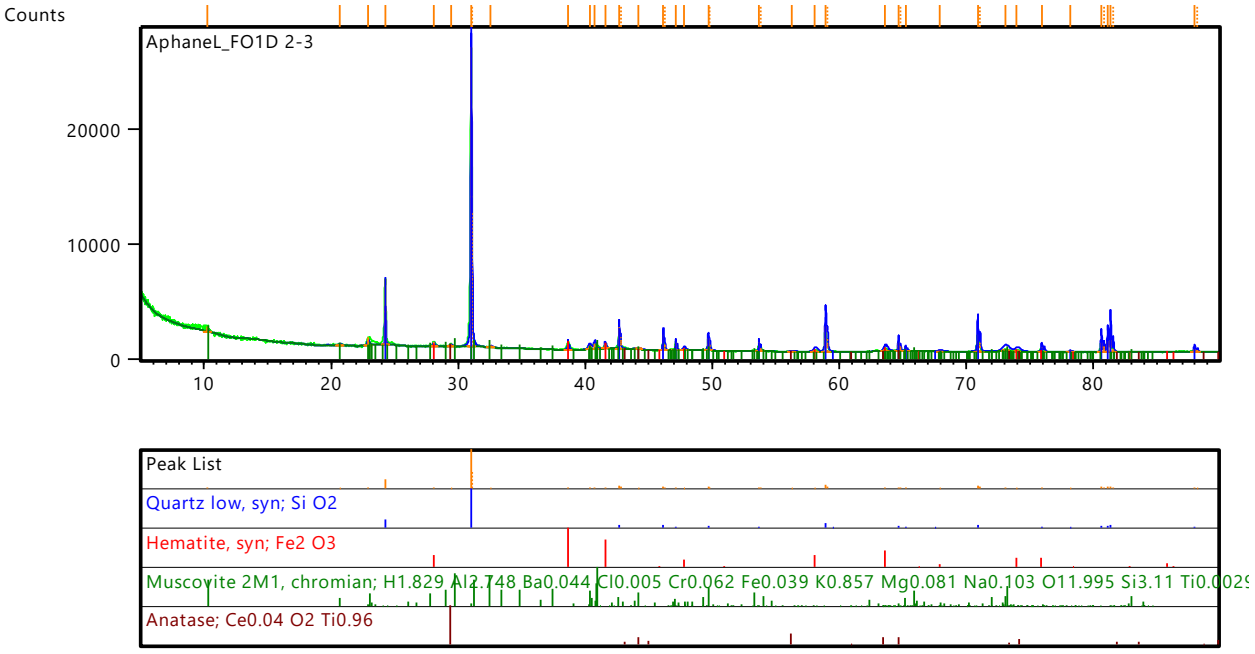
Counts
AphaneL_FO1D 2-3
20000
10000
0
10
20
30
40
50
60
70
80
Peak List
Quartz low, syn; Si O2
Hematite, syn; Fe2 O3
Muscovite 2M1, chromian; H1.829 Al2.748 Ba0.044 Cl0.005 Cr0.062 Fe0.039 K0.857 Mg0.081 Na0.103 O11.995 Si3.11 Ti0.02
Anatase; Ce0.04 O2 Ti0.96

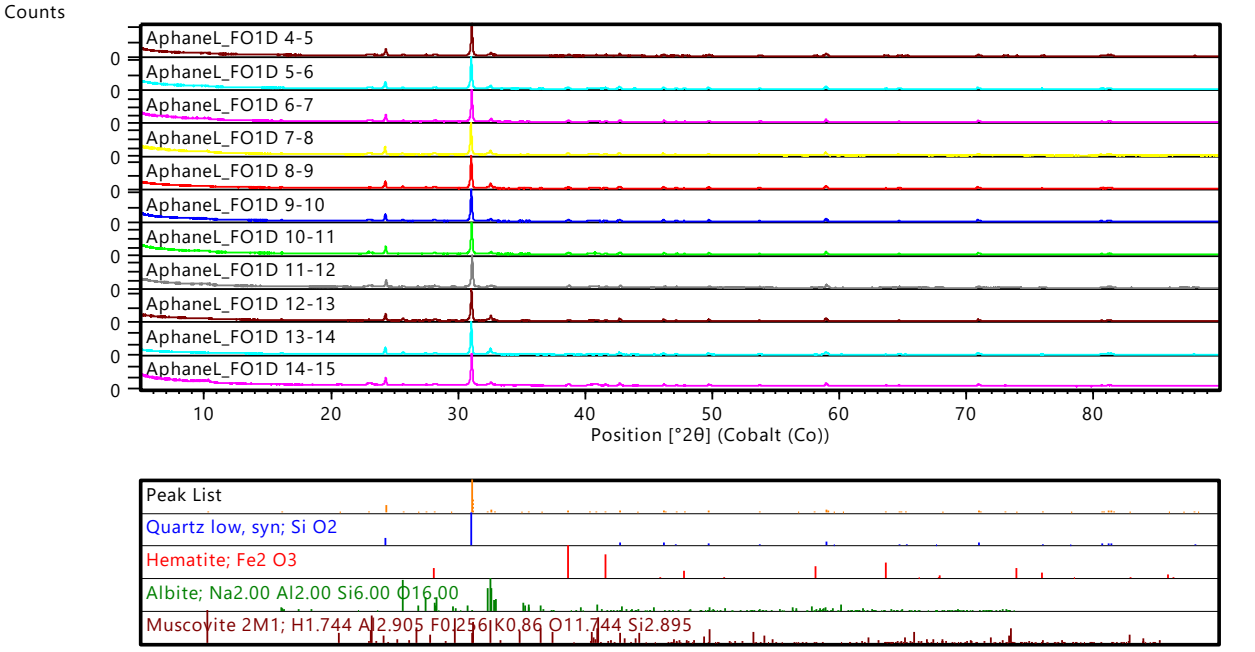
Counts
AphaneL_FO1D 4-5
AphaneL_FO1D 5-6
AphaneL_FO1D 6-7
AphaneL_FO1D 7-8
AphaneL_FO1D 8-9
AphaneL_FO1D 9-10
AphaneL_FO1D 10-11
AphaneL_FO1D 11-12
AphaneL_FO1D 12-13
AphaneL_FO1D 13-14
AphaneL_FO1D 14-15
0
10
20
30
40
50
60
70
80
Position [°2θ] (Cobalt (Co))
Peak List
Quartz low, syn; Si O2
Hematite; Fe2 O3
Albite; Na2.00 Al2.00 Si6.00 O16.00
Muscovite 2M1; H1.744 Al2.905 F0.256 K0.86 O11.744 Si2.895

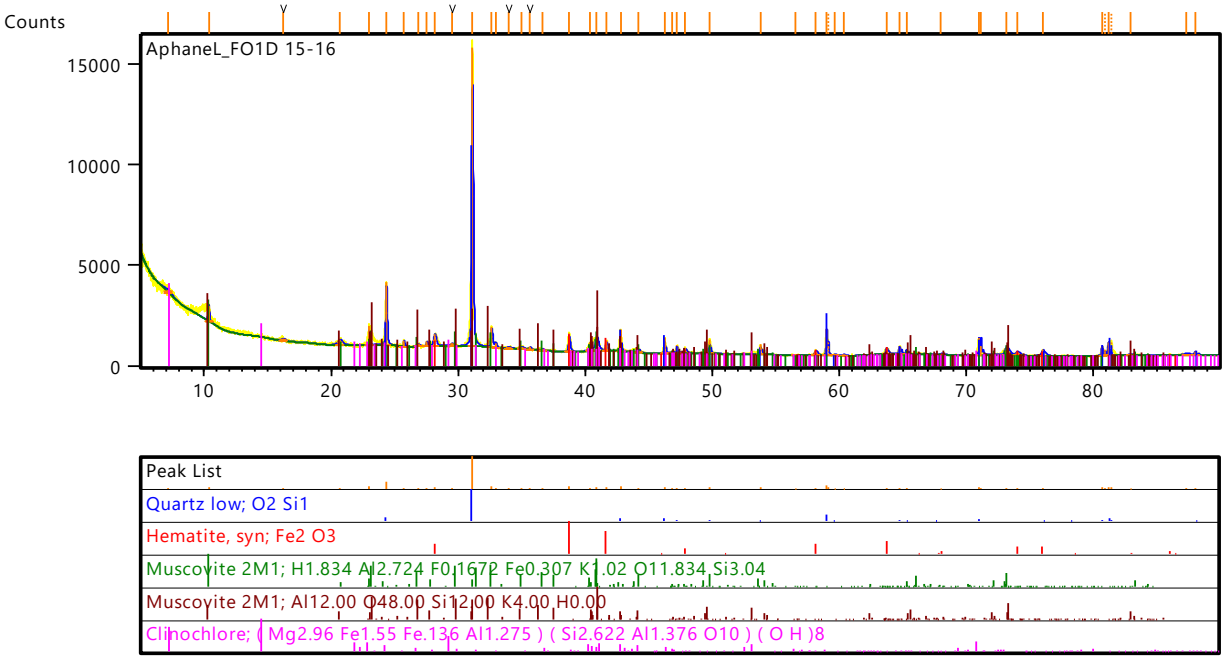
Counts
AphaneL_FO1D 15-16
15000
10000
5000
0
10
20
30
40
50
60
70
80
Peak List
Quartz low; O2 Si1
Hematite, syn; Fe2 O3
Muscovite 2M1; H1.834 Al2.724 F0.1672 Fe0.307 K1.02 O11.834 Si3.04
Muscovite 2M1; Al12.00 O48.00 Si12.00 K4.00 H0.00
Clinochlore; (Mg2.96 Fe1.55 Fe.136 Al1.275) (Si2.622 Al1.376 O10) (O H)8

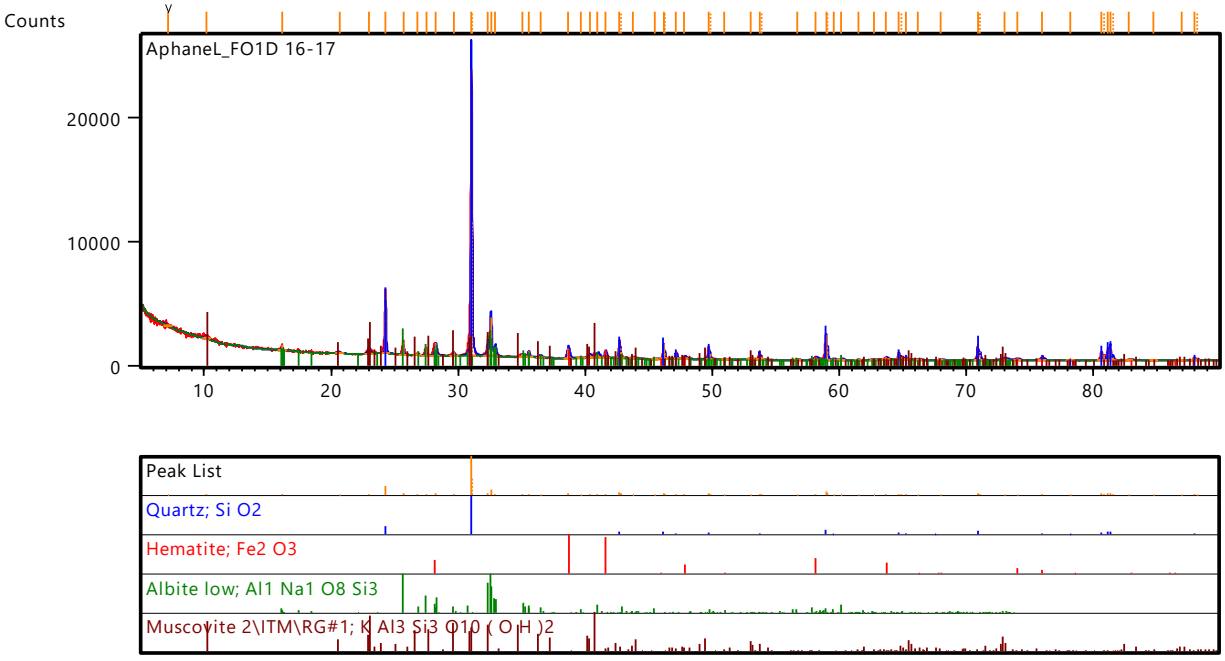
Counts
AphaneL_FO1D 16-17
20000
10000
0
10
20
30
40
50
60
70
80
Peak List
Quartz; Si O2
Hematite; Fe2 O3
Albite low; Al1 Na1 O8 Si3
Muscovite 2\ITM\RG#1; K Al3 Si3 O10 (O H)2

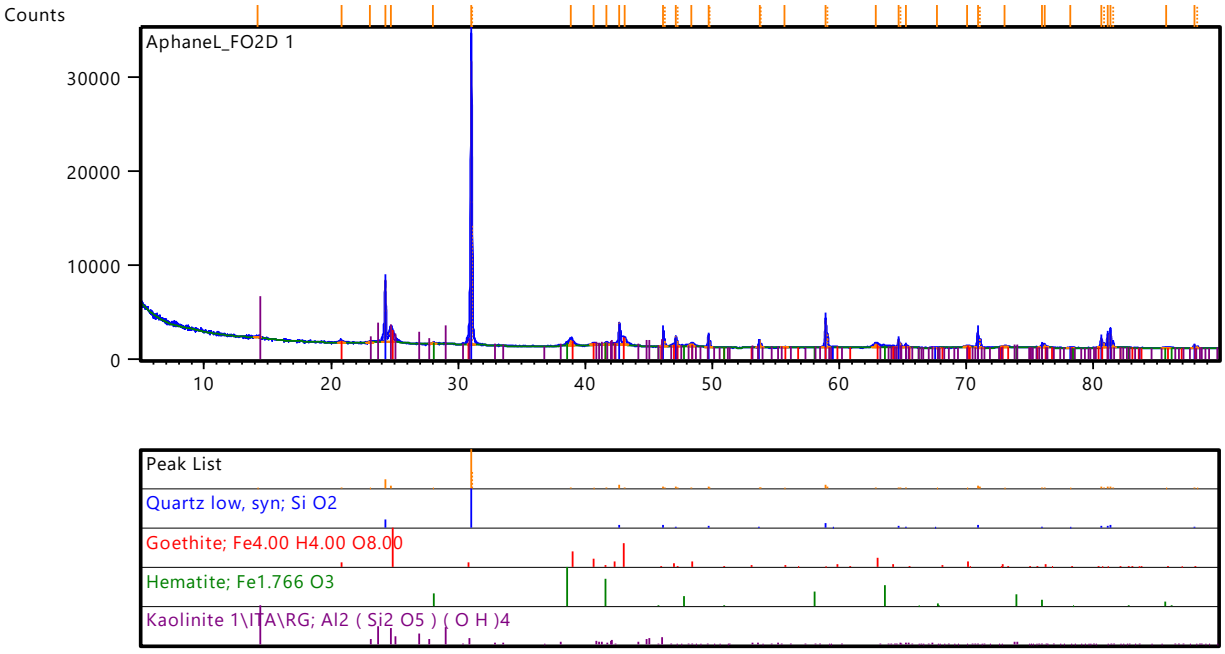
Counts
AphaneL_FO2D 1
30000
20000
10000
0
10
20
30
40
50
60
70
80
Peak List
Quartz low, syn; Si O2
Goethite; Fe4.00 H4.00 O8.00
Hematite; Fe1.766 O3
Kaolinite 1\ITA\RG; Al2 (Si2 O5) (O H)4

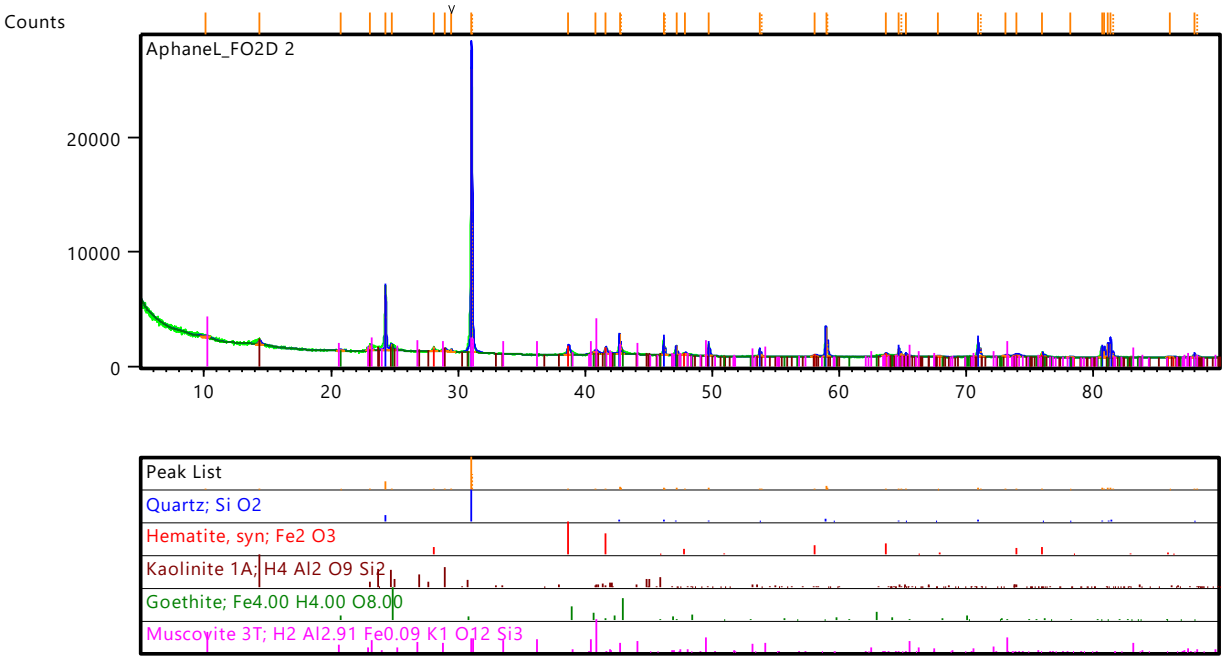
Counts
AphaneL_FO2D 2
20000
10000
0
10
20
30
40
50
60
70
80
Peak List
Quartz; Si O2
Hematite, syn; Fe2 O3
Kaolinite 1A; H4 Al2 O9 Si2
Goethite; Fe4.00 H4.00 O8.00
Muscovite 3T; H2 Al2.91 Fe0.09 K1 O12 Si3

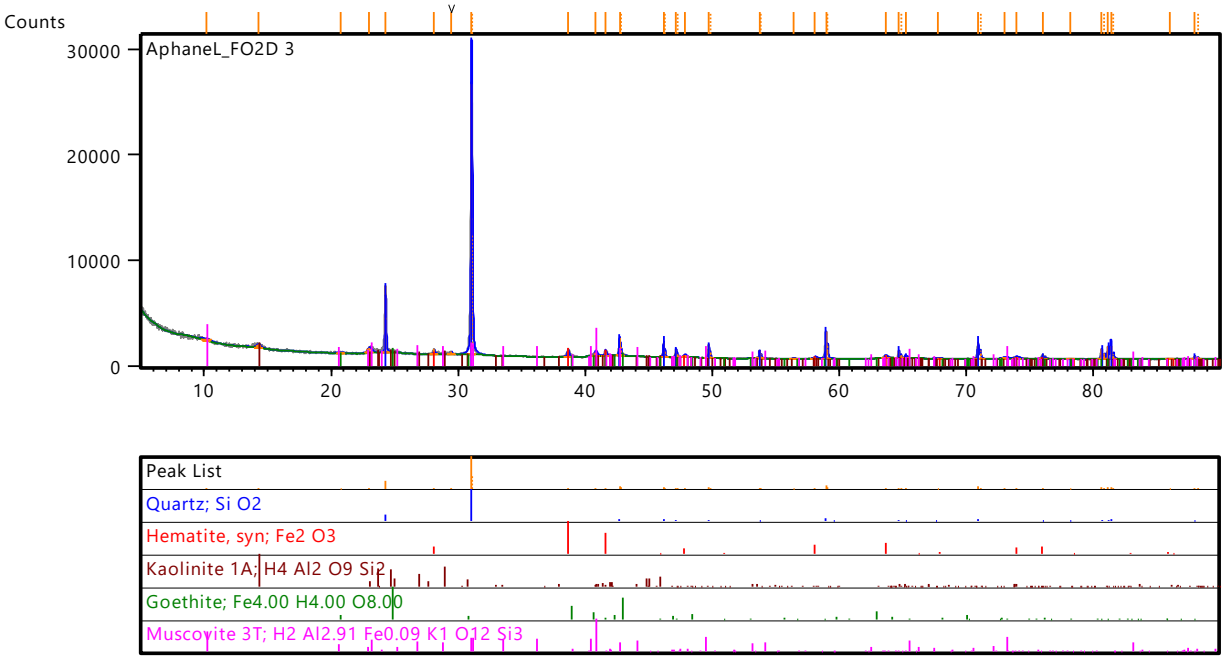
Counts
AphaneL_FO2D 3
30000
20000
10000
0
10
20
30
40
50
60
70
80
Peak List
Quartz; Si O2
Hematite, syn; Fe2 O3
Kaolinite 1A; H4 Al2 O9 Si2
Goethite; Fe4.00 H4.00 O8.00
Muscovite 3T; H2 Al2.91 Fe0.09 K1 O12 Si3

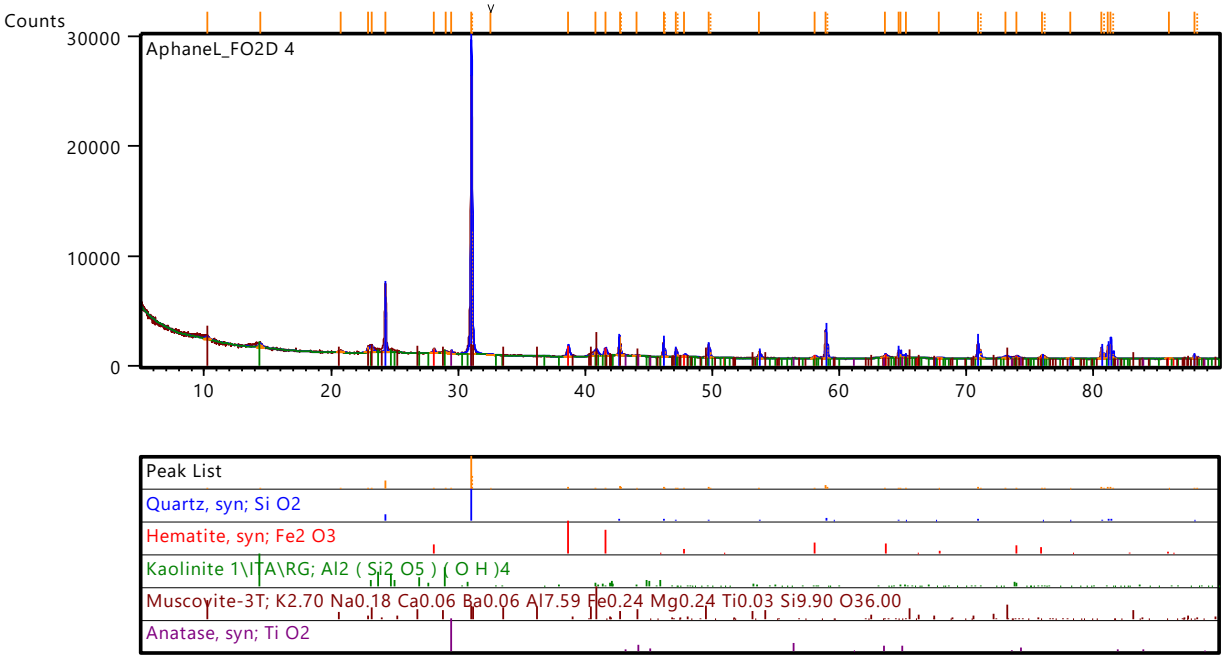
Counts
AphaneL_FO2D 4
30000
20000
10000
0
10
20
30
40
50
60
70
80
Peak List
Quartz, syn; Si O2
Hematite, syn; Fe2 O3
Kaolinite 1\ITA\RG; Al2 (Si2 O5) (O H)4
Muscovite-3T; K2.70 Na0.18 Ca0.06 Ba0.06 Al7.59 Fe0.24 Mg0.24 Ti0.03 Si9.90 O36.00
Anatase, syn; Ti O2

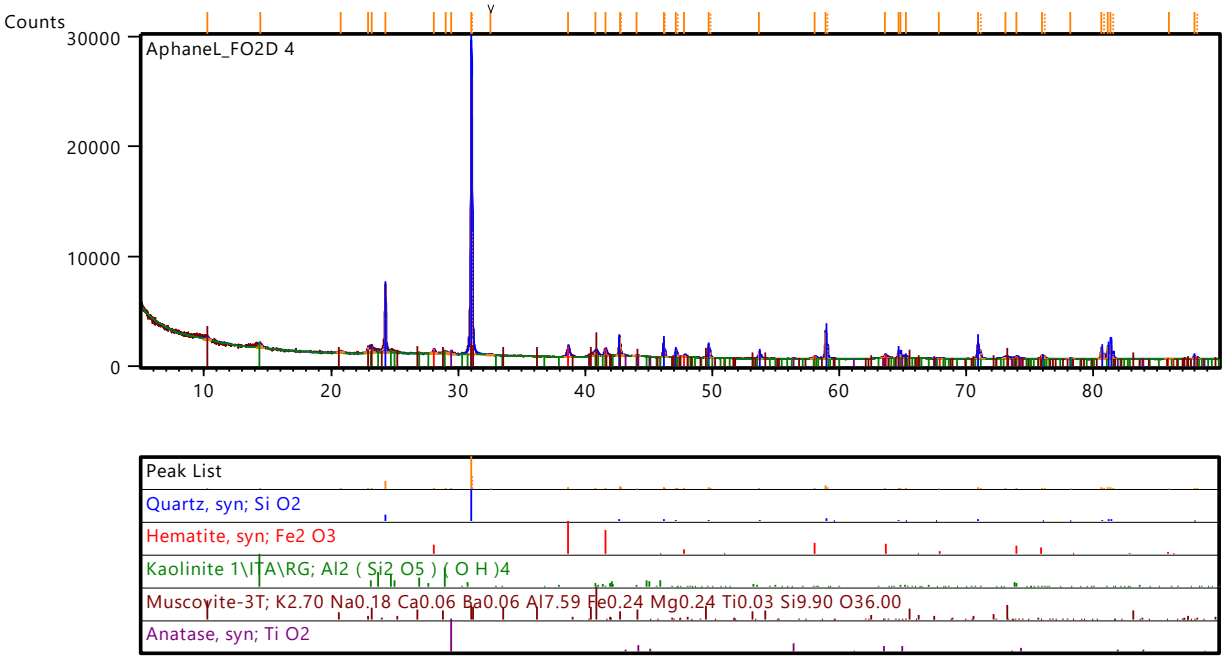
Counts
AphaneL_FO2D 4
30000
20000
10000
0
10
20
30
40
50
60
70
80
Peak List
Quartz, syn; Si O2
Hematite, syn; Fe2 O3
Kaolinite 1\ITA\RG; Al2 (Si2 O5) (O H)4
Muscovite-3T; K2.70 Na0.18 Ca0.06 Ba0.06 Al7.59 Fe0.24 Mg0.24 Ti0.03 Si9.90 O36.00
Anatase, syn; Ti O2

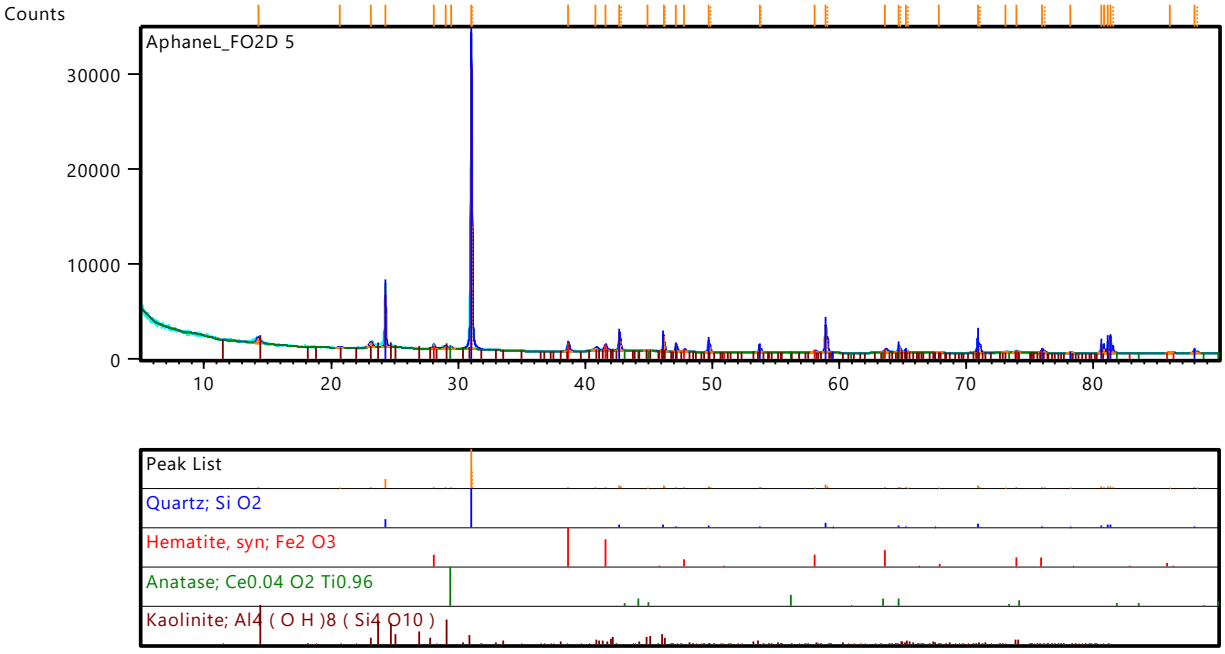
Counts
AphaneL_FO2D 5
30000
20000
10000
0
10
20
30
40
50
60
70
80
Peak List
Quartz; Si O2
Hematite, syn; Fe2 O3
Anatase; Ce0.04 O2 Ti0.96
Kaolinite; Al4 (O H)8 (Si4 O10)

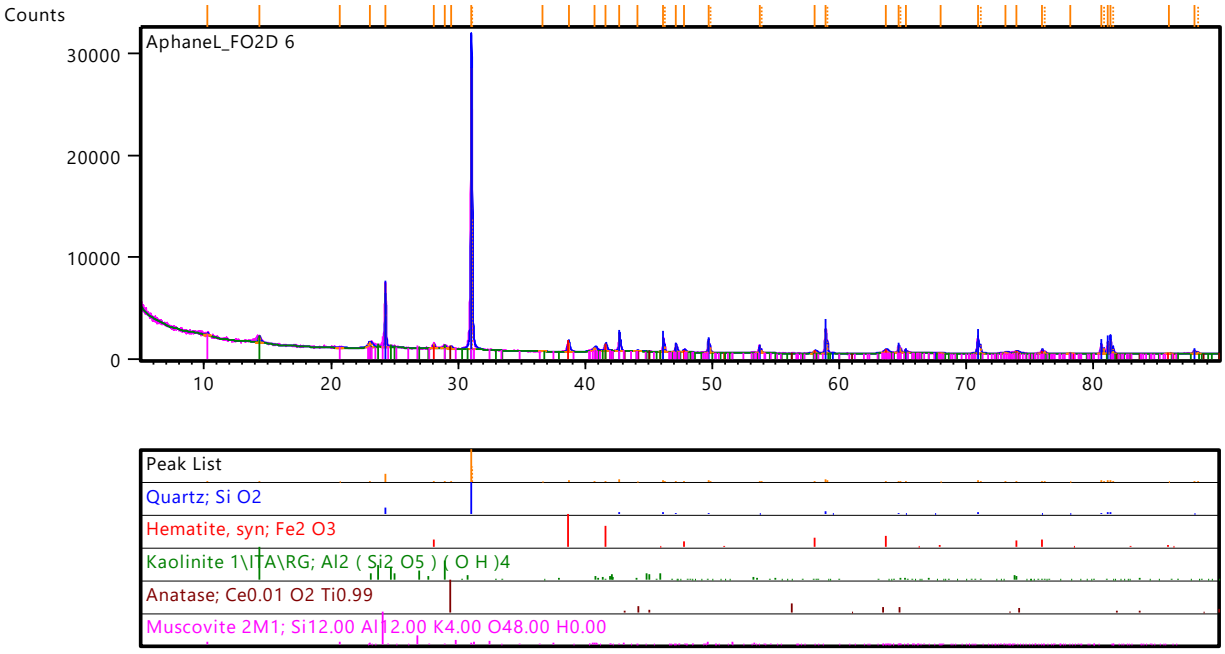
Counts
AphaneL_FO2D 6
30000
20000
10000
0
10
20
30
40
50
60
70
80
Peak List
Quartz; Si O2
Hematite, syn; Fe2 O3
Kaolinite 1\ITA\RG; Al2 (Si2 O5) (O H)4
Anatase; Ce0.01 O2 Ti0.99
Muscovite 2M1; Si12.00 Al12.00 K4.00 O48.00 H0.00

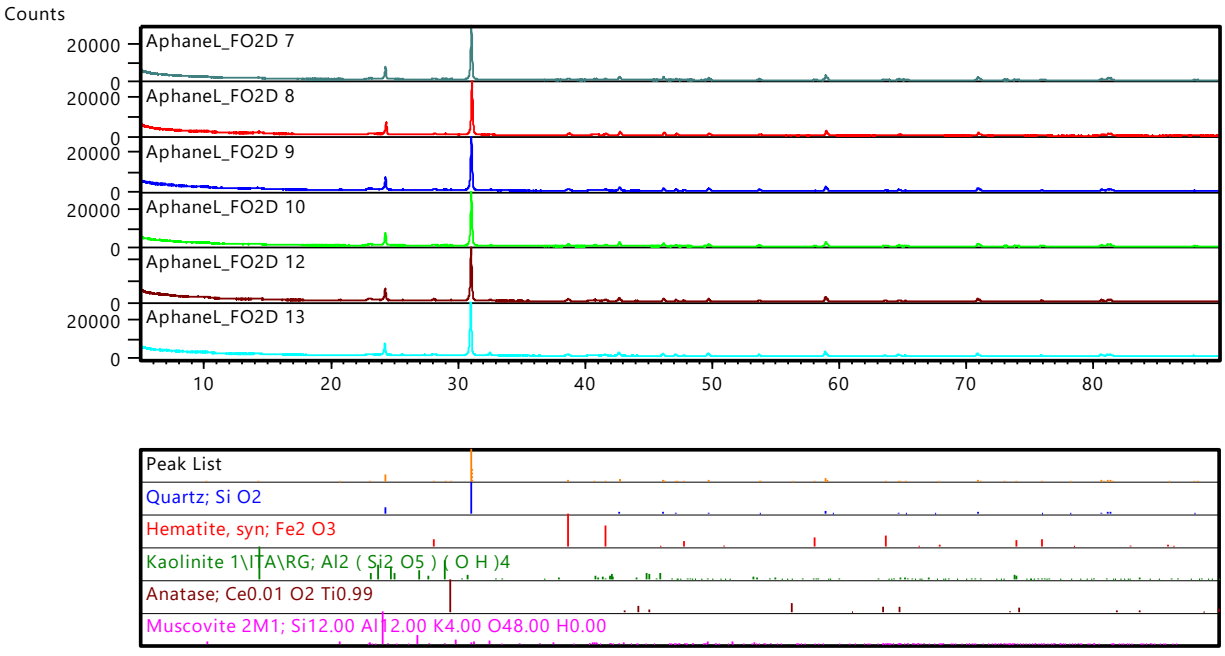
Counts
AphaneL_FO2D 7
AphaneL_FO2D 8
AphaneL_FO2D 9
AphaneL_FO2D 10
AphaneL_FO2D 12
AphaneL_FO2D 13
20000
0
10
20
30
40
50
60
70
80
Peak List
Quartz; Si O2
Hematite, syn; Fe2 O3
Kaolinite 1\ITA\RG; Al2 (Si2 O5) (O H)4
Anatase; Ce0.01 O2 Ti0.99
Muscovite 2M1; Si12.00 Al12.00 K4.00 O48.00 H0.00

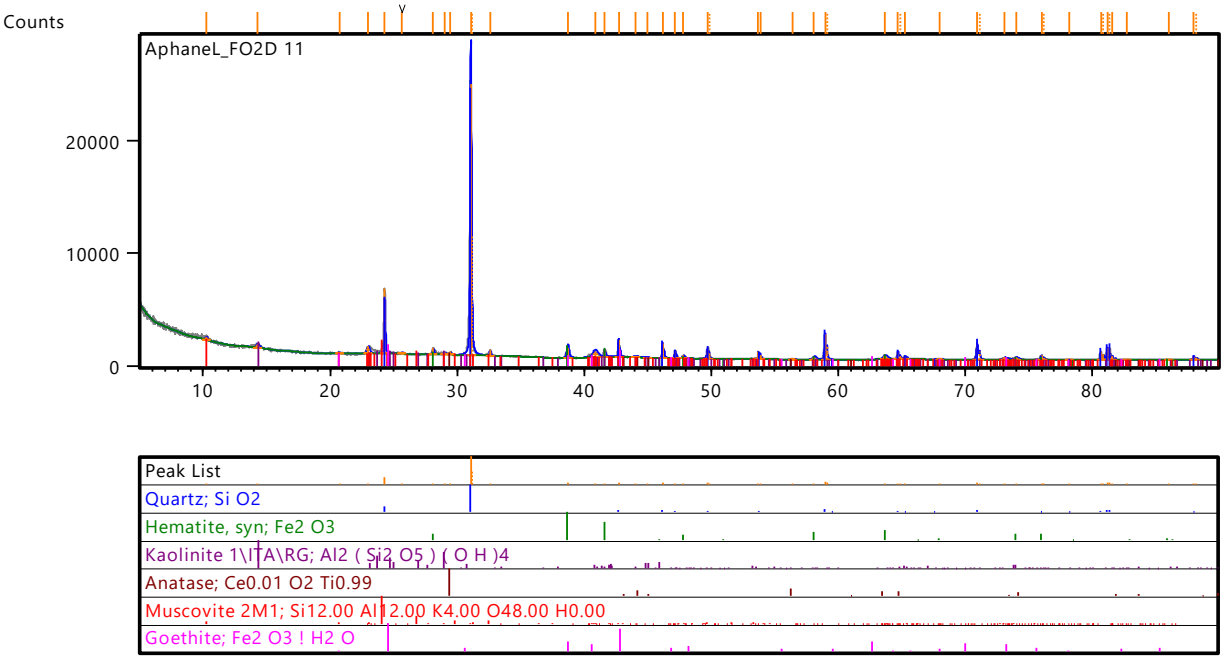
Counts
AphaneL_FO2D 11
20000
10000
0
10
20
30
40
50
60
70
80
Peak List
Quartz; Si O2
Hematite, syn; Fe2 O3
Kaolinite 1\ITA\RG; Al2 (Si2 O5) (O H)4
Anatase; Ce0.01 O2 Ti0.99
Muscovite 2M1; Si12.00 Al12.00 K4.00 O48.00 H0.00
Goethite; Fe2 O3 ! H2 O

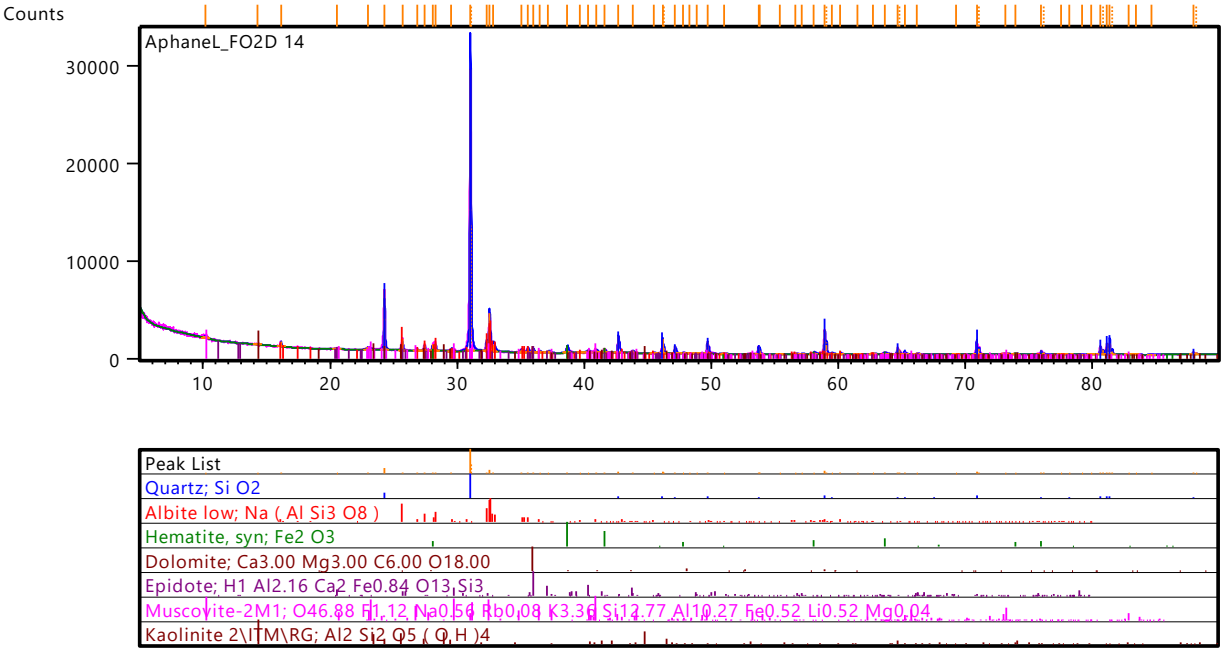
Counts
AphaneL_FO2D 14
30000
20000
10000
0
10
20
30
40
50
60
70
80
Peak List
Quartz; Si O2
Albite low; Na (Al Si3 O8)
Hematite, syn; Fe2 O3
Dolomite; Ca3.00 Mg3.00 C6.00 O18.00
Epidote; H1 Al2.16 Ca2 Fe0.84 O13 Si3
Muscovite-2M1; O46.88 H1.12 Na0.56 Rb0.08 K3.36 Si13.77 Al10.27 Fe0.52 Li0.52 Mg0.04
Kaolinite 2\ITM\RG; Al2 Si2 O5 (O H)4

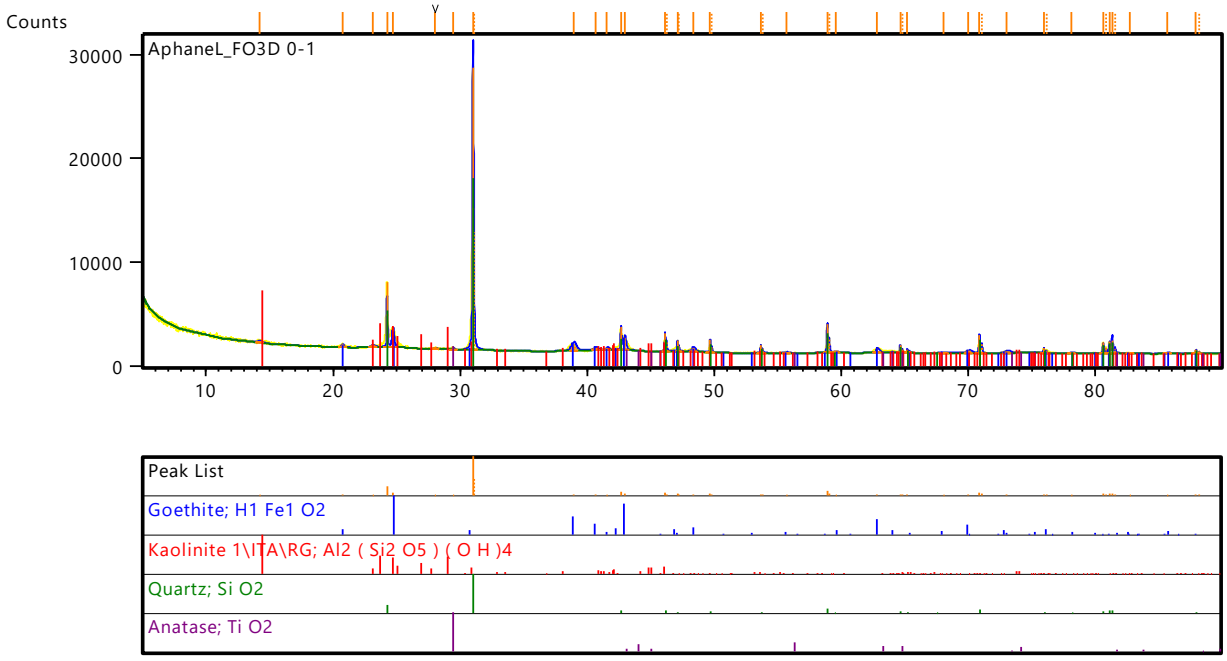
Counts
AphaneL_FO3D 0-1
30000
20000
10000
0
10
20
30
40
50
60
70
80
Peak List
Goethite; H1 Fe1 O2
Kaolinite 1\ITA\RG; Al2 (Si2 O5) (O H)4
Quartz; Si O2
Anatase; Ti O2

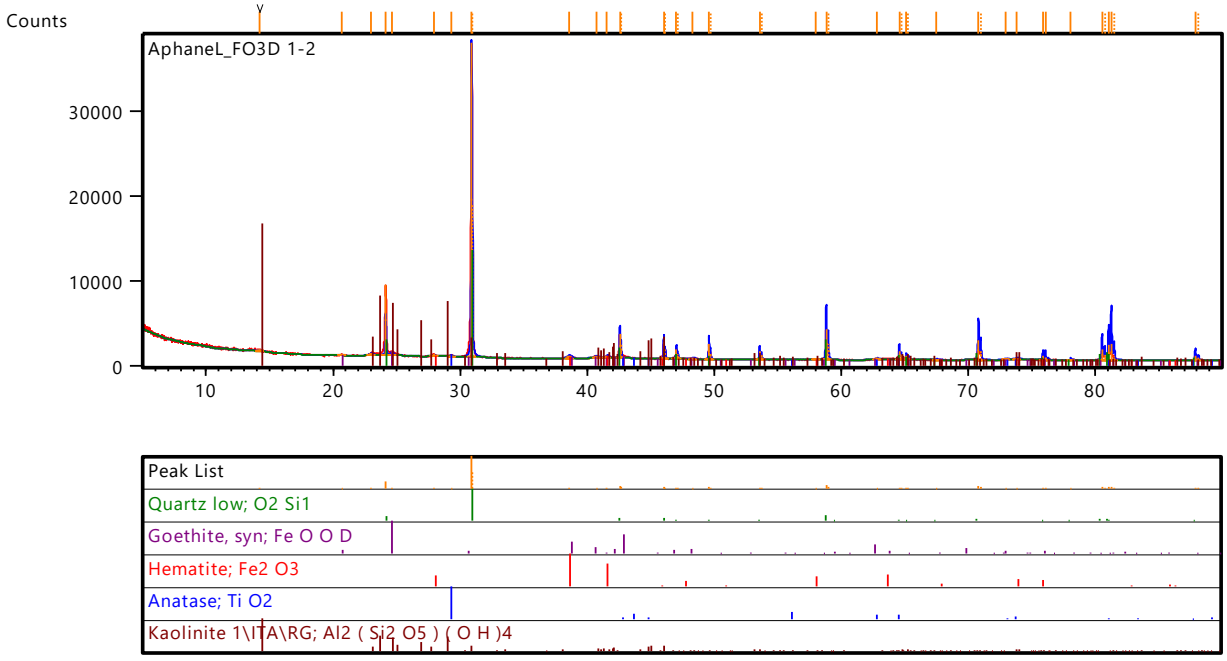
Counts
AphaneL_FO3D 1-2
30000
20000
10000
0
10
20
30
40
50
60
70
80
Peak List
Quartz low; O2 Si1
Goethite, syn; Fe O O D
Hematite; Fe2 O3
Anatase; Ti O2
Kaolinite 1\ITA\RG; Al2 (Si2 O5) (O H)4

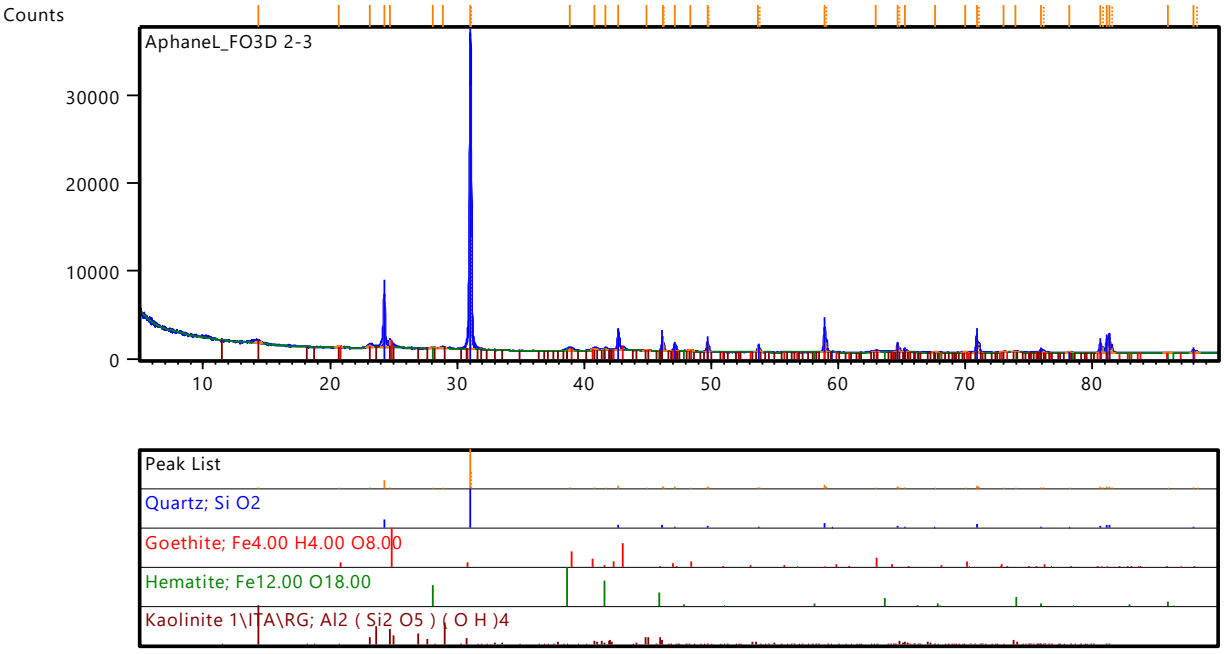
Counts
AphaneL_FO3D 2-3
30000
20000
10000
0
10
20
30
40
50
60
70
80
Peak List
Quartz; Si O2
Goethite; Fe4.00 H4.00 O8.00
Hematite; Fe12.00 O18.00
Kaolinite 1\ITA\RG; Al2 (Si2 O5) (O H)4

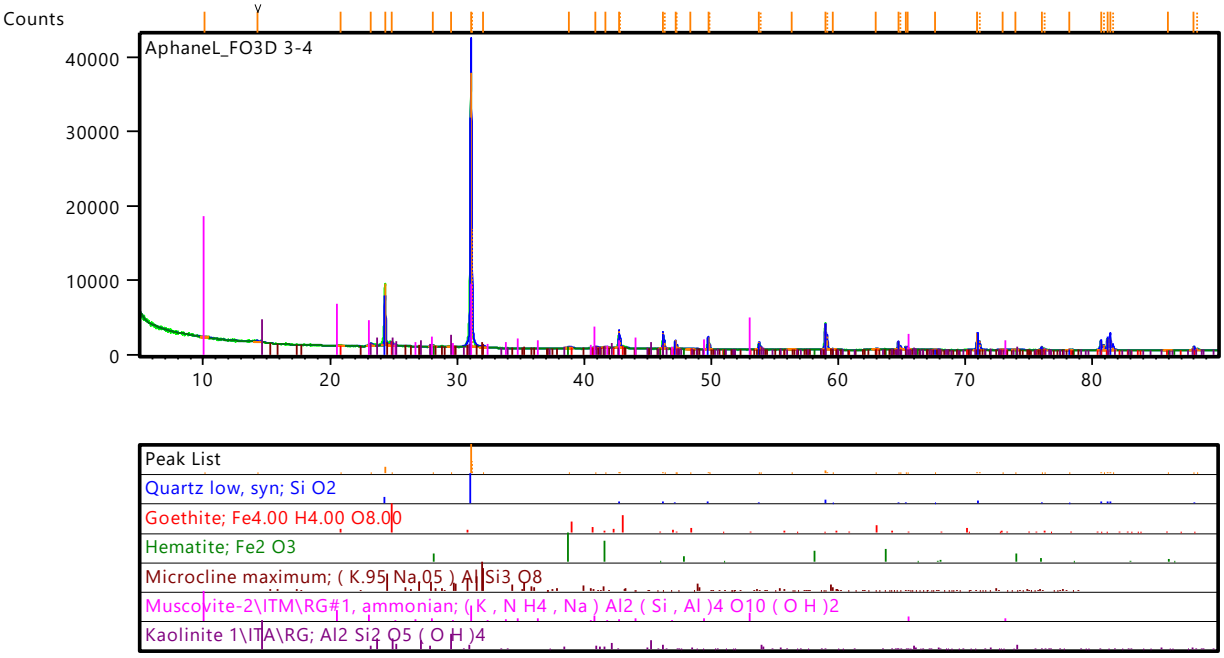
Counts
AphaneL_FO3D 3-4
40000
30000
20000
10000
0
10
20
30
40
50
60
70
80
Peak List
Quartz low, syn; Si O2
Goethite; Fe4.00 H4.00 O8.00
Hematite; Fe2 O3
Microcline maximum; (K.95 Na.05) Al Si3 O8
Muscovite-2\ITM\RG#1, ammonian; (K , N H4 , Na) Al2 (Si , Al)4 O10 (O H)2
Kaolinite 1\ITA\RG; Al2 Si2 O5 (O H)4

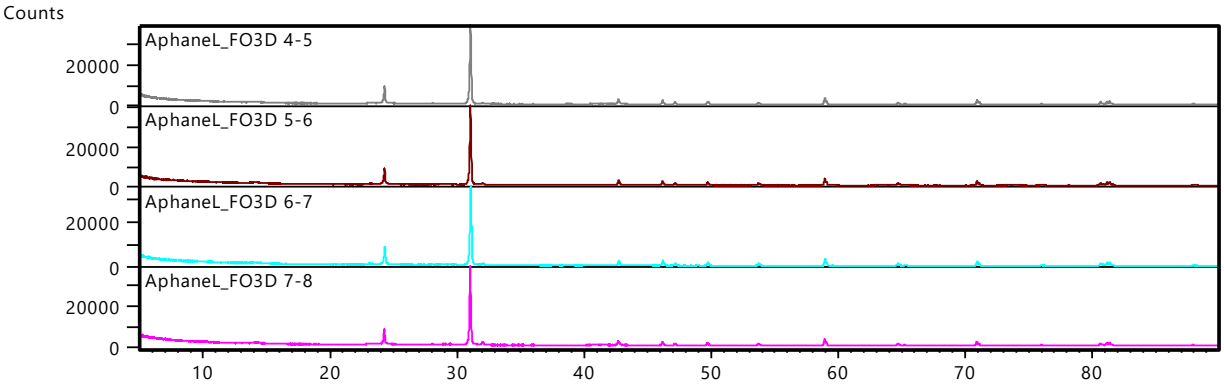

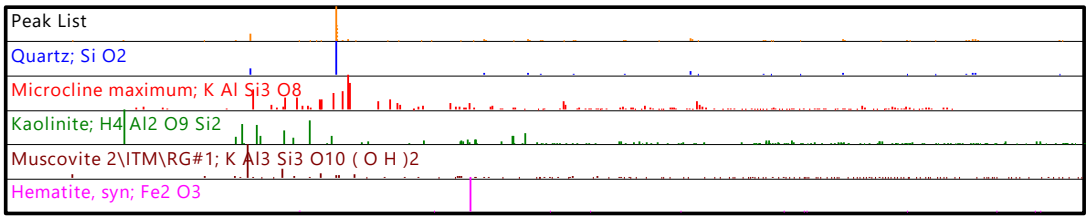

FO1D 0-1			**FO1D 0-2**			**FO1D 2-3**		
	weight %	3 σ error		weight %	3 σ error		weight %	3 σ error
Goethite	12,68	0,45	Goethite	6,53	0,36	Anatase	1,38	0,26
Hematite	3,83	0,26	Hematite	2,49	0,19	Goethite	5,09	0,6
Kaolinite	4,06	0,72	Kaolinite	4,14	0,57	Hematite	8,17	0,51
Quartz	79,42	0,75	Muscovite	4,26	0,57	Muscovite	16,53	0,9
			Quartz	82,58	0,81	Quartz	68,83	0,96
FO1D 3-4			**FO1D 4-5**			**FO1D 5-6**		
	weight %	3 σ error		weight %	3 σ error		weight %	3 σ error
Hematite	8,58	0,45	Hematite	8,33	0,42	Hematite	9,57	0,48
Montmorillonite	1,78	0,48	Muscovite	15,03	0,9	Muscovite	16,45	0,99
Muscovite	18,39	0,96	Plagioclase	16,8	1,41	Plagioclase	16,73	1,47
Plagioclase	13,29	1,02	Quartz	59,85	1,32	Quartz	57,24	1,35
Quartz	57,97	1,17						

FO1D 6-7			**FO1D 7-8**			**FO1D 8-9**		
	weight %	3 σ error		weight %	3 σ error		weight %	3 σ error
Hematite	8,76	0,51	Hematite	8,76	0,51	Hematite	8,12	0,33
Muscovite	21,2	1,08	Muscovite	21,2	1,08	Muscovite	8,79	0,69
Plagioclase	16,24	1,23	Plagioclase	16,24	1,23	Plagioclase	27,15	1,05
Quartz	53,8	1,23	Quartz	53,8	1,23	Quartz	55,94	0,99
FO1D 9-10			**FO1D 10-1**			**FO1D 10-12**		
	weight %	3 σ error		weight %	3 σ error		weight %	3 σ error
Hematite	9,57	0,45	Hematite	9,5	0,51	Hematite	9,43	0,51
Muscovite	15,22	0,93	Muscovite	22,11	1,05	Muscovite	22,63	1,02
Plagioclase	16,13	1,44	Plagioclase	13,13	1,08	Plagioclase	13	0,99
Quartz	59,08	1,32	Quartz	55,26	1,17	Quartz	54,93	1,11
FO1D 12-13			**FO1D 13-14**			**FO1D 14-15**		
	weight %	3 σ error		weight %	3 σ error		weight %	3 σ error
Hematite	6,83	0,33	Dolomite	1,11	0,45	Hematite	8,47	0,57
Muscovite	12,29	0,72	Epidote	9,87	0,84	Muscovite	26,31	1,2
Plagioclase	27,9	1,08	Plagioclase	29,46	1,2	Plagioclase	17,49	1,23
Quartz	52,98	0,96	Quartz	59,56	1,23	Quartz	47,73	1,2
FO1D 15-16			**FO1D 16-17**			**FO2D 1**		
	weight %	3 σ error		weight %	3 σ error		weight %	3 σ error
Chlorite	8,3	0,99	Hematite	6,62	0,33	Goethite	23,34	0,6

Hematite	8,69	0,48	Muscovite	9,83	0,69	Hematite	4,52	0,36
Muscovite	23,72	1,05	Plagioclase	25,46	1,05	Kaolinite	9,13	0,9
Plagioclase	10,84	1,05	Quartz	58,09	0,99	Quartz	63,01	0,81
Quartz	48,44	1,17						
FO2D 2			**FO2D 3**			**FO2D 4**		
	weight %	3 σ error		weight %	3 σ error		weight %	3 σ error
Goethite	8,65	0,51	Goethite	4,43	0,45	Anatase	1,65	0,22
Hematite	8,31	0,3	Hematite	8,06	0,3	Hematite	8,97	0,3
Kaolinite	14,06	0,93	Kaolinite	11,85	0,84	Kaolinite C1, ideal, BISH	12,29	0,87
Muscovite	7,81	0,81	Muscovite	9,58	0,72	Muscovite_2M1	11,93	0,69
Quartz	61,17	0,96	Quartz	66,08	0,9	Quartz	65,16	0,9
FO2D 5			**FO2D 6**			**FO2D 7**		
	weight %	3 σ error		weight %	3 σ error		weight %	3 σ error
Anatase	1,37	0,25	Anatase	1,38	0,2	Anatase	1,39	0,19
Hematite	8,59	0,33	Hematite	8,34	0,36	Hematite	8,61	0,36
Kaolinite	18,38	0,87	Kaolinite	13,25	0,78	Kaolinite	10,52	0,75
Quartz	71,66	0,84	Muscovite	9,25	0,69	Muscovite	12,77	0,72
			Quartz	67,78	0,84	Quartz	66,71	0,84
FO2D 8			**FO2D 9**			**FO2D 10**		
	weight %	3 σ error		weight %	3 σ error		weight %	3 σ error
Anatase	1,45	0,22	Anatase	1,26	0,22	Anatase	1,18	0,21
Hematite	8,64	0,39	Hematite	8,57	0,39	Hematite	9,01	0,39
Kaolinite	12,45	0,87	Kaolinite	11,17	0,87	Kaolinite	10,62	0,84
Muscovite	12	0,72	Muscovite	13,97	0,69	Muscovite	12,33	0,69
Quartz	65,47	0,9	Quartz	65,04	0,87	Quartz	66,86	0,87
FO2D 11			**FO2D 12**			**FO2D 13**		

	weight %	3 σ error		weight %	3 σ error		weight %	3 σ error
Anatase	1,12	0,22	Anatase	1,26	0,24	Anatase	1,25	0,27
Goethite	1,06	0,45	Hematite	9,87	0,42	Hematite	8,11	0,48
Hematite	8,52	0,42	Kaolinite	11,25	0,96	Kaolinite	9,58	1,08
Kaolinite	10,18	0,87	Muscovite	16,14	0,75	Muscovite	15,19	0,78
Muscovite	14,39	0,69	Quartz	61,48	0,93	Quartz	65,87	1,05
Quartz	64,74	0,9						
FO2D 14			**FO3D 0-1**			**FO3D 1-2**		
	weight %	3 σ error		weight %	3 σ error		weight %	3 σ error
Dolomite	1,2	0,34	Anatase	0,87	0,28	Anatase	1,05	0,18
Epidote	7,47	0,57	Goethite	28,73	0,69	Goethite	7,51	0,45
Hematite	4,57	0,24	Kaolinite	10,97	0,99	Hematite	3,25	0,25
Kaolinite C1, ideal, BISH	4,09	0,45	Quartz	59,43	0,93	Kaolinite	9,99	0,63
Muscovite_2M1	4,76	0,51				Quartz	78,19	0,66
Plagioclase Albite	21,14	0,75						
Quartz	56,77	0,81						
FO3D 2-3			**FO3D 3-4**			**FO3D 4-5**		
	weight %	3 σ error		weight %	3 σ error		weight %	3 σ error
Goethite	10,7	0,48	Goethite	6,91	0,39	Hematite	2,55	0,23
Hematite	2,94	0,28	Hematite	2,44	0,22	Kaolinite	11,58	0,84
Kaolinite	11,47	0,69	Kaolinite	9,25	0,78	Microcline	3,89	1,17
Quartz	74,89	0,69	Microcline	2,5	1,17	Muscovite	6,13	0,72
			Muscovite	4,72	0,66	Quartz	75,84	1,32
			Quartz	74,19	1,29			
FO3D 5-6			**FO3D 6-7**			**FO3D 7-8**		

	weight %	3 σ error		weight %	3 σ error		weight %	3 σ error
Hematite	2,16	0,23	Hematite	1,65	0,21	Hematite	1,83	0,25
Kaolinite	11,06	0,78	Kaolinite	10,51	0,81	Kaolinite	13,55	0,9
Microcline	8,45	0,87	Microcline	8,46	0,81	Microcline	9,1	0,9
Muscovite	5,85	0,69	Muscovite	5,65	0,66	Muscovite	8,09	0,72
Quartz	72,48	1,17	Quartz	73,73	1,11	Quartz	67,43	1,17

APPENDIX 2: X-RAY FLUORESCENCE ANALYSES RESULTS

UNIVERSITEIT VAN PRETORIA
UNIVERSITY OF PRETORIA
YUNIBESITHI YA PRETORIA

Faculty of Natural & Agricultural Sciences
XRD & XRF Facility
Department of Geology
Pretoria 0002, South Africa

Direct Telephone: (012) 420-2137
Direct Telefax: (012) 362 5219
E-Mail: jeanette.dykstra@up.ac.za
http://www.up.ac.za/academic/science

CLIENT: Lehlohonolo Aphane
PO NUMBER: A0Y269
DATE: 2016-08-05
ANALYSIS: XRF

ANALYSIS: The samples were milled in a tungsten-carbide milling pot to achieve particle sizes <75micron.
The samples were dried at 100°C and roasted at 1000°C to determine Loss On Ignition (LOI) values.
1g Sample was mixed with 6g Lithiumteraborate flux and fused at 1050°C to make a stable fused glass bead.
Fot trace element analyses the sample was mixed with PVA binder and pressed in an aluminium cup @ 10 tons.
Results indicated with an asterix (*) should be considered semi-quantitative.
The Thermo Fisher ARL Perform'X Sequential XRF instrument with OXSAS software was used for analyses.
Blank and certified reference materials are analysed with each batch of samples and the columns in bold represent one of these.

MAJOR ELEMENT ANALYSES RESULTS:

	SARM49										
%	Certified	Analysed	FO1D 0-1	FO1D 1-2	FO1D 2-3	FO1D 3-4	FO1D 4-5	FO1D 5-6	FO1D 6-7	FO1D 7-8	FO1D 8-9
SiO_2	99,6	99,70	67,60	74,70	63,60	62,90	64,30	65,20	60,80	62,90	67,70
Fe_2O_3	0,05	0,01	20,50	12,30	12,20	9,35	8,36	8,56	9,29	9,27	8,08
Al_2O_3	0,05	0,01	5,23	6,74	13,80	15,20	15,00	14,70	16,30	15,00	13,20
TiO_2	0,01	0,00	0,56	0,61	0,85	0,91	0,91	0,89	0,87	0,96	0,80
K_2O	0,01	0,01	0,36	0,76	2,90	3,87	3,26	3,34	3,95	3,27	1,83
Cr_2O_3	0	0,00	0,08	0,06	0,04	0,04	0,02	0,03	0,02	0,02	0,02
MnO	0,01	0,00	0,23	0,12	0,16	0,18	0,13	0,09	0,14	0,08	0,10
V_2O_5	0	0,00	0,06	0,03	0,03	0,02	0,01	0,02	0,01	0,01	0,02
P_2O_5	0	0,03	0,06	0,00	0,03	0,13	0,06	0,06	0,17	0,15	0,12
ZrO_2	0	0,01	0,06	0,07	0,05	0,02	0,04	0,04	0,04	0,02	0,02
CaO	0,01	0,01	0,04	0,10	0,13	0,34	0,52	0,39	0,66	0,78	0,76
Co3O4	0	0,00	0,02	*<0.01*	*<0.01*	*<0.01*	0,03	*<0.01*	*<0.01*	*<0.01*	*<0.01*
MgO	0,05	0,01	0,11	0,34	0,72	1,34	1,18	1,09	1,51	1,16	0,73
WO3	0	0,00	0,05	0,03	*<0.01*	*<0.01*	0,08	*<0.01*	*<0.01*	*<0.01*	0,03
CuO	0	0,00	0,01	*<0.01*	*<0.01*	*<0.01*	*<0.01*	*<0.01*	*<0.01*	*<0.01*	*<0.01*
SO3	0	0,00	*<0.01*	0,07	*<0.01*	*<0.01*	0,11	*<0.01*	0,02	*<0.01*	*<0.01*
BaO	0	0,00	*<0.01*	*<0.01*	0,04	0,15	*<0.01*	*<0.01*	0,13	0,10	*<0.01*
Na_2O	0,05	0,02	*<0.01*	*<0.01*	*<0.01*	0,66	1,44	1,29	0,98	1,61	2,98
ZnO	0	0,00	*<0.01*	*<0.01*	*<0.01*	0,02	0,01	*<0.01*	0,02	*<0.01*	*<0.01*
SrO	0	0,00	*<0.01*	*<0.01*	*<0.01*	0,02	*<0.01*	*<0.01*	*<0.01*	0,01	0,03
RbO2	0	0,00	*<0.01*	*<0.01*	*<0.01*	0,02	0,02	0,02	0,03	0,04	*<0.01*
NiO	0	0,01	*<0.01*	*<0.01*	*<0.01*	0,01	0,01	*<0.01*	*<0.01*	*<0.01*	*<0.01*
PbO	0	0,00	*<0.01*	*<0.01*	*<0.01*	*<0.01*	*<0.01*	*<0.01*	*<0.01*	*<0.01*	*<0.01*
LOI	0	0,10	5,01	4,05	5,43	4,81	4,42	4,22	4,98	4,57	3,58
TOTAL	100	99,95	**99,98**	**99,97**	**99,96**	**100,00**	**99,93**	**99,96**	**99,91**	**99,95**	**99,98**

FO1D 9-10	FO1D 10-11	FO1D 11-12	FO1D 12-13	FO1D 13-14	FO1D14-15	FO1D 15-16

63,60	60,50	60,50	67,20	73,20	60,20	60,20
9,54	9,98	10,10	7,64	6,14	8,96	9,73
13,70	15,70	16,00	14,10	10,80	16,90	15,80
0,87	0,79	0,97	1,01	0,74	1,05	0,88
3,61	4,22	4,37	2,31	0,66	4,62	4,71
<0.01	0,02	0,01	0,02	0,02	0,01	0,03
0,13	0,11	0,13	0,07	0,08	0,09	0,09
0,02	0,02	0,04	0,03	0,01	*<0.01*	0,05
0,12	0,11	0,13	0,09	*<0.01*	0,15	0,18
0,02	0,05	0,01	0,02	0,04	0,03	0,04
0,75	0,59	0,66	1,03	2,94	0,78	0,78
<0.01	*<0.01*	0,03	*<0.01*	0,01	*<0.01*	*<0.01*
1,32	1,62	1,36	0,81	0,14	1,14	1,49
<0.01	*<0.01*	0,11	0,01	0,07	*<0.01*	*<0.01*
<0.01	*<0.01*	*<0.01*	*<0.01*	*<0.01*	0,01	*<0.01*
0,04	*<0.01*	0,08	*<0.01*	*<0.01*	0,01	*<0.01*
0,16	0,18	0,11	*<0.01*	*<0.01*	0,15	0,12
1,67	0,76	0,73	2,39	3,45	1,06	0,70
<0.01	0,02	0,02	0,01	*<0.01*	0,01	0,03
0,01	*<0.01*	0,02	0,03	0,05	0,01	*<0.01*
0,02	0,03	0,03	*<0.01*	*<0.01*	0,03	0,03
<0.01	0,02	*<0.01*	*<0.01*	*<0.01*	*<0.01*	*<0.01*
<0.01	0,45	*<0.01*	*<0.01*	*<0.01*	*<0.01*	*<0.01*
4,37	4,79	4,60	3,19	1,57	4,71	5,02
99,96	**99,95**	**99,99**	**99,96**	**99,92**	**99,92**	**99,87**

	SARM49										
%	**Certified**	**Analysed**	**FO1D 16-17**	**FO2D 1**	**FO2D 2**	**FO2D 3**	**FO2D 4**	**FO2D 5**	**FO2D 6**	**FO2D 7**	**FO2D 8**
SiO_2	**99,6**	99,70	65,60	52,10	59,10	63,20	63,00	66,40	67,80	65,80	67,10
Fe_2O_3	**0,05**	0,01	6,67	30,80	17,60	13,50	13,00	10,70	9,22	10,80	10,00
Al_2O_3	**0,05**	0,01	11,30	7,79	12,90	14,10	14,10	13,70	14,20	13,60	13,60
TiO_2	**0,01**	0,00	0,71	0,74	0,91	0,90	0,98	0,85	0,74	0,84	0,76
K_2O	**0,01**	0,01	1,90	0,36	1,26	1,81	2,13	1,26	1,58	1,95	2,08
Cr_2O_3	**0**	0,00	0,01	0,22	0,04	0,04	0,03	0,03	0,03	0,03	0,02
MnO	**0,01**	0,00	0,05	0,20	0,67	0,20	0,14	0,15	0,12	0,17	0,12
V_2O_5	**0**	0,00	0,02	0,07	0,05	0,02	0,04	0,02	0,04	0,02	0,02

P_2O_5	**0**	0,03	0,07	0,07	*<0.01*	0,01	*<0.01*	*<0.01*	0,04	0,03	*<0.01*
ZrO_2	**0**	0,01	0,03	0,06	0,06	0,06	0,06	0,04	0,05	0,05	0,05
CaO	**0,01**	0,01	1,18	0,06	0,11	0,07	0,06	0,10	0,15	0,18	0,20
MgO	**0,05**	0,01	0,66	*<0.01*	0,31	0,26	0,45	0,21	0,43	0,43	0,55
WO3	**0**	0,00	*<0.01*	*<0.01*	*<0.01*	*<0.01*	*<0.01*	*<0.01*	*<0.01*	*<0.01*	*<0.01*
CuO	**0**	0,00	*<0.01*	*<0.01*	*<0.01*	*<0.01*	*<0.01*	*<0.01*	*<0.01*	0,01	*<0.01*
SO3	**0**	0,00	0,12	*<0.01*	0,08	*<0.01*	0,09	*<0.01*	0,06	0,06	*<0.01*
BaO	**0**	0,00	*<0.01*	*<0.01*	0,19	*<0.01*	*<0.01*	*<0.01*	*<0.01*	*<0.01*	0,09
Na_2O	**0,05**	0,02	2,44	*<0.01*	*<0.01*	*<0.01*	*<0.01*	*<0.01*	*<0.01*	0,26	*<0.01*
ZnO	**0**	0,00	*<0.01*	*<0.01*	*<0.01*	*<0.01*	*<0.01*	*<0.01*	*<0.01*	*<0.01*	*<0.01*
SrO	**0**	0,00	0,02	*<0.01*	*<0.01*	*<0.01*	*<0.01*	*<0.01*	*<0.01*	*<0.01*	*<0.01*
RbO2	**0**	0,00	*<0.01*	*<0.01*	*<0.01*	*<0.01*	*<0.01*	*<0.01*	*<0.01*	*<0.01*	*<0.01*
NiO	**0**	0,01	*<0.01*	*<0.01*	*<0.01*	*<0.01*	0,01	*<0.01*	*<0.01*	*<0.01*	0,01
CeO2	**0**	0,00	*<0.01*	*<0.01*	0,04	0,05	*<0.01*	*<0.01*	*<0.01*	*<0.01*	*<0.01*
LOI	**0**	0,10	9,17	7,47	6,60	5,66	5,83	6,43	5,51	5,71	5,35
TOTAL	**100**	**99,95**	**99,95**	**99,93**	**99,92**	**99,89**	**99,91**	**99,91**	**99,96**	**99,94**	**99,94**

FO2D 9	FO2D 10	FO2D 11	FO2D 12	FO2D 13	FO2D 14	FO3D 0-1
67,10	65,80	65,70	65,00	67,20	72,40	50,60
9,44	10,10	10,00	10,40	9,60	6,64	31,80
13,90	14,10	14,00	14,20	13,50	11,10	7,88
0,78	0,81	0,81	0,82	0,81	0,60	0,65
2,20	2,22	2,47	2,66	2,12	1,18	0,33
0,03	0,02	0,04	0,02	0,03	0,03	0,08
0,09	0,10	0,10	0,09	0,11	0,09	0,22
0,03	0,02	0,02	0,03	0,01	0,00	0,09
<0.01	0,01	*<0.01*	*<0.01*	0,04	0,06	0,04
0,05	0,04	0,05	0,05	0,02	0,01	0,05
0,27	0,26	0,31	0,31	0,57	2,15	0,04
0,61	0,68	0,69	0,83	0,56	0,42	0,01
<0.01	*<0.01*	*<0.01*	*<0.01*	*<0.01*	0,03	0,05
0,03	*<0.01*	*<0.01*	*<0.01*	*<0.01*	*<0.01*	0,02
<0.01	*<0.01*	*<0.01*	0,07	*<0.01*	*<0.01*	*<0.01*
<0.01	*<0.01*	*<0.01*	*<0.01*	*<0.01*	*<0.01*	*<0.01*
0,29	0,33	0,31	0,10	0,42	2,66	*<0.01*
<0.01	*<0.01*	*<0.01*	0,02	0,02	*<0.01*	*<0.01*

<0.01	<0.01	<0.01	<0.01	0,01	0,04	<0.01
<0.01	<0.01	0,02	<0.01	<0.01	<0.01	<0.01
0,02	<0.01	<0.01	<0.01	<0.01	<0.01	0,01
<0.01	<0.01	<0.01	<0.01	<0.01	<0.01	<0.01
5,14	5,48	5,42	5,39	5,00	2,49	8,12
99,98	**99,99**	**99,93**	**99,98**	**100,02**	**99,88**	**100,00**

	SARM49								
%	**Certified**	**Analysed**	**FO3D 1-2**	**FO3D 2-3**	**FO3D 3-4**	**FO3D 4-5**	**FO3D 5-6**	**FO3D 6-7**	**FO3D 7-8**
SiO_2	**99,6**	99,70	69,40	68,10	70,90	72,60	73,20	74,80	71,60
Fe_2O_3	**0,05**	0,01	12,60	14,30	11,90	9,06	7,66	6,42	7,37
Al_2O_3	**0,05**	0,01	10,60	10,00	9,58	11,20	11,40	10,90	12,40
TiO_2	**0,01**	0,00	0,57	0,64	0,62	0,64	0,55	0,57	0,66
K_2O	**0,01**	0,01	0,60	0,73	0,95	1,17	1,70	1,86	1,95
Cr_2O_3	**0**	0,00	0,04	0,04	0,07	0,03	0,03	0,01	0,04
MnO	**0,01**	0,00	0,21	0,18	0,13	0,11	0,19	0,16	0,17
V_2O_5	**0**	0,00	0,02	0,03	0,07	0,02	0,02	0,02	0,01
P_2O_5	**0**	0,03	<0.01	0,02	<0.01	0,03	<0.01	<0.01	0,02
ZrO_2	**0**	0,01	0,06	0,06	0,07	0,05	0,07	0,06	0,05
CaO	**0,01**	0,01	0,03	0,05	0,06	0,05	0,07	0,11	0,14
Co3O4	**0**	0,00	0,03	<0.01	0,00	<0.01	<0.01	<0.01	<0.01
MgO	**0,05**	0,01	0,09	0,03	0,07	0,11	0,17	0,27	0,40
WO3	**0**	0,00	0,08	0,04	0,11	0,02	<0.01	<0.01	<0.01
CuO	**0**	0,00	<0.01	<0.01	<0.01	<0.01	<0.01	<0.01	<0.01
SO3	**0**	0,00	0,12	<0.01	<0.01	<0.01	0,10	0,10	0,06
BaO	**0**	0,00	<0.01	<0.01	<0.01	<0.01	<0.01	0,05	0,11
Na_2O	**0,05**	0,02	<0.01	<0.01	<0.01	<0.01	<0.01	<0.01	<0.01
ZnO	**0**	0,00	<0.01	<0.01	<0.01	<0.01	<0.01	<0.01	<0.01
SrO	**0**	0,00	<0.01	<0.01	<0.01	<0.01	<0.01	<0.01	<0.01
RbO2	**0**	0,00	<0.01	<0.01	<0.01	<0.01	<0.01	<0.01	<0.01
NiO	**0**	0,01	<0.01	<0.01	0,02	<0.01	<0.01	<0.01	0,01
PbO	**0**	0,00	<0.01	<0.01	<0.01	<0.01	<0.01	<0.01	<0.01
CeO2	**0**	0,00	<0.01	<0.01	<0.01	<0.01	<0.01	<0.01	<0.01
MoO3	**0**	0,00	<0.01	<0.01	<0.01	<0.01	<0.01	<0.01	<0.01
LOI	**0**	0,10	5,53	5,70	5,41	4,86	4,75	4,59	4,96

TOTAL	**100**	**99,96**	**99,99**	**99,92**	**99,96**	**99,95**	**99,90**	**99,92**	**99,95**	

TRACE ELEMENT ANALYSES RESULTS:

	BHVO1										
ppm	**Certified**	**Analysed**	**FO1D 0-1**	**FO1D 1-2**	**FO1D 2-3**	**FO1D 3-4**	**FO1D 4-5**	**FO1D 5-6**	**FO1D 6-7**	**FO1D 7-8**	**FO1D 8-9**
As	**0,4**	0	40	10	19	4	12	8	0	27	26
Cu	**136**	125	39	25	20	28	25	15	29	13	19
Ga	**21**	23	11	12	21	23	20	22	24	25	19
Mo	**1,02**	2	3	4	3	3	3	4	3	2	3
Nb	**19**	13	5	8	10	13	12	12	13	12	12
Ni	**121**	101	44	27	32	62	46	35	55	44	27
Pb	**2,6**	0	37	18	30	17	16	21	12	23	21
Rb	**11**	10	24	45	126	153	126	129	155	131	75
Sr	**403**	384	10	7	37	93	83	85	70	103	146
Th	**1,08**	0	0	0	4	7	6	6	9	9	7
U	**0,42**	0	0	0	0	0	0	0	0	0	0
W*	**0,27**	1	377	176	84	33	325	121	50	73	200
Y	**27,6**	23	12	11	28	73	42	35	41	36	33
Zn	**105**	100	24	30	62	139	108	91	142	100	59
Zr	**179**	188	268	308	288	253	240	247	237	247	249

FO1D 9-10	**FO1D 10-11**	**FO1D 11-12**	**FO1D 12-13**
7	5	0	26
25	36	46	31
22	25	25	21
3	3	3	4
11	10	12	14
43	54	51	28
16	16	16	15
135	163	161	88
81	64	63	126
6	4	6	11

0	0	0	0
97	62	127	218
37	37	38	37
123	135	138	83
237	222	235	299

ppm	FO1D 13-14	FO1D 15-16	FO1D 16-17	FO2D 1	FO2D 2	FO2D 3	FO2D 4	FO2D 5	FO2D 6	FO2D 7	FO2D 7-8
As	37	0	2	0	0	0	0	1	0	1	7
Cu	29	68	39	66	58	45	47	47	48	50	31
Ga	15	25	17	14	21	22	23	18	18	20	16
Mo	5	1	3	1	4	2	4	3	3	2	3
Nb	14	12	12	2	8	11	12	11	11	12	11
Ni	12	51	22	56	44	35	32	38	37	40	25
Pb	31	8	11	32	82	28	23	36	21	32	10
Rb	25	167	79	23	71	89	104	71	88	91	88
Sr	366	61	120	0	4	6	8	7	12	11	14
Th	9	7	6	0	0	4	6	7	4	3	2
U	0	0	0	0	0	0	0	0	0	0	0
W*	521	59	101	165	63	73	57	39	39	78	119
Y	38	39	33	11	24	28	33	48	53	51	28
Zn	50	152	74	36	42	43	46	49	54	57	43
Zr	360	246	256	305	330	349	349	265	269	278	278

FO2D 8	FO2D 10	FO2D 11	FO2D 12
0	0	0	0
49	49	49	47
19	20	22	21
4	2	2	2
12	11	11	11
40	40	41	43
20	18	21	17
97	99	107	114
20	22	26	26
5	5	6	5

0	0	0	0
26	72	66	56
56	54	56	55
67	70	76	79
267	262	271	266

ppm	FO2D 13	FO2D 14	FO3D 0-1	FO3D 1-2	FO3D 2-3	FO3D 3-4	FO3D 4-5	FO3D 5-6	FO3D 6-7	FO3D 14-15
As	4	17	0	16	7	27	6	2	6	5
Cu	45	25	78	36	44	36	28	27	26	54
Ga	20	16	13	15	14	15	17	15	14	28
Mo	3	3	1	2	2	3	4	4	4	4
Nb	11	10	0	7	5	7	10	9	11	13
Ni	42	23	36	31	31	29	26	22	23	46
Pb	20	19	22	26	31	18	8	9	12	19
Rb	93	49	18	41	38	51	65	71	77	167
Sr	55	238	1	3	3	5	8	9	10	78
Th	5	6	0	0	0	0	2	0	4	10
U	0	0	0	0	0	0	0	0	0	0
W*	66	257	192	606	400	738	173	124	221	71
Y	47	34	9	18	14	20	22	21	23	43
Zn	72	53	29	32	37	35	36	34	36	129
Zr	260	234	245	281	269	270	288	300	311	278

If you have any further queries, kindly contact the laboratory.

Analyst: J.E. Strydom
XRF Analyst

APPENDIX 3: WATER QUALITY RESULTS

WATERLAB (Pty) Ltd
Reg. No.: 1983/009165/07 V.A.T. No.: 4130107891
23B De Havilland Crescent
Persequor Techno Park
Meiring Naudé Drive
Pretoria
P.O. Box 283
Persequor Park, 0020
Tel: +2712 – 349 – 1066
Fax: +2712 – 349 – 2064
e-mail: admin@waterlab.co.za
T0391

CERTIFICATE OF ANALYSES
GENERAL WATER QUALITY PARAMETERS

Date received: 2017 - 01 - 19 **Date completed:** 2017 - 02 – 10
Project number: 215 **Report number: 64529** **Order number: 0000481196**
Client name: University of Pretoria **Contact person: Mr. M. Dippenaar**
Address: Private Bag X20, Geology Department, Hatfield, 0028 **e-mail: matthysd@icloud.com**
Telephone: 082 826 5468 **Facsimile: -** **Mobile: 082 826 5468**

Analyses in mg/ℓ (Unless specified otherwise)	Method Identification	Sample Identification				
		BH2D 20/10/2016	Stream A 20/10/2016	Stream B 20/10/2016	Stream C 20/10/2016	Hydro-census BH14A 08/11/2016
Sample Number		26382	26383	26384	26385	26386
pH – Value at 25°C *	WLAB065	6.2	6.3	7.0	6.5	7.0
Electrical Conductivity in mS/m at 25°C	WLAB002	31.4	82.7	69.0	63.6	56.8
Total Dissolved Solids at 180°C *	WLAB003	250	660	556	454	398
Colour in PtCo Units *	WLAB006	61	18	25	39	11
Odour in T.O.N *	WLAB038	<5	<5	<5	<5	<5
Turbidity in N.T.U	WLAB005	1 752	4.0	1.0	4.1	0.4
Chloride as Cl	WLAB046	63	20	17	17	49
Sulphate as SO_4	WLAB046	9	276	243	217	68
Fluoride as F	WLAB014	<0.2	0.3	0.3	0.4	<0.2
Nitrate as N	WLAB046	1.1	0.2	0.3	0.1	9.0
Nitrite as N	WLAB046	<0.05	<0.05	<0.05	<0.05	<0.05
Total Organic Carbon as C *	WLAB060	1.0	5.3	5.1	6.2	1.4
Total Coliform Bacteria / 100 mℓ	WLAB021	1 400	64	170	33	77
Faecal Coliform Bacteria / 100 mℓ *	WLAB021	1	4	30	0	0
E. coli / 100 mℓ	WLAB021	0	3	13	0	0
Heterotrophic Plate Count / mℓ *	WLAB021	13 000	77	70	33	1 800
ICP-MS Scan *	WLAB050	See Attached Report: 64529-A				
% Balancing *	---	91.6	93.9	86.5	99.2	91.3

Analyses in mg/ℓ (Unless specified otherwise)	Method Identification	Sample Identification				
		Hydro-census BH5A	BH17 08/11/2016	Mun 1 08/11/2016	Mall BH1 08/11/2016	Mun 1 08/12/2016

		08/11/2016				
Sample Number		26387	26388	26389	26390	26391
pH – Value at 25°C *	WLAB065	6.4	6.1	6.5	6.7	6.5
Electrical Conductivity in mS/m at 25°C	WLAB002	28.6	14.1	92.4	13.9	76.1
Total Dissolved Solids at 180°C *	WLAB003	214	106	742	126	600
Colour in PtCo Units *	WLAB006	11	12	11	11	12
Odour in T.O.N *	WLAB038	<5	<5	<5	<5	<5
Turbidity in N.T.U	WLAB005	0.2	40	0.1	0.3	0.2
Chloride as Cl	WLAB046	21	12	27	2	23
Sulphate as SO_4	WLAB046	13	10	368	<2	260
Fluoride as F	WLAB014	<0.2	<0.2	0.5	<0.2	0.4
Nitrate as N	WLAB046	3.2	1.6	0.3	<0.1	0.5
Nitrite as N	WLAB046	<0.05	<0.05	<0.05	<0.05	<0.05
Total Organic Carbon as C *	WLAB060	<1.0	3.7	4.4	<1.0	4.0
Total Coliform Bacteria / 100 mℓ	WLAB021	0	1	0	1	3
Faecal Coliform Bacteria / 100 mℓ *	WLAB021	0	0	0	0	0
E. coli / 100 mℓ	WLAB021	0	0	0	0	0
Heterotrophic Plate Count / mℓ *	WLAB021	210	2 500	<10	3 200	140
ICP-MS Scan *	WLAB050	See Attached Report: 64529-A				
% Balancing *	---	90.4	98.2	98.2	99.2	98.9

Analyses in mg/ℓ (Unless specified otherwise)	**Method Identification**	**Sample Identification**				
		Hydro-census BH5A 08/12/2016	**Hydro-census BH14 08/12/2016**	**BH2D 08/12/2016**	**BH1D 08/12/2016**	**BH17 08/12/2016**
Sample Number		26392	26393	26394	26395	26396
pH – Value at 25°C *	WLAB065	7.9	7.7	6.3	6.1	6.8
Electrical Conductivity in mS/m at 25°C	WLAB002	22.9	28.2	29.4	7.6	5.2
Total Dissolved Solids at 180°C *	WLAB003	164	206	230	62	74
Colour in PtCo Units *	WLAB006	5	9	9	98	22
Odour in T.O.N *	WLAB038	<5	<5	<5	<5	<5
Turbidity in N.T.U	WLAB005	2.1	1.5	252	137	12
Chloride as Cl	WLAB046	16	15	59	3	2
Sulphate as SO_4	WLAB046	12	38	<2	8	<2

Fluoride as F	WLAB014	<0.2	<0.2	<0.2	0.3	<0.2
Nitrate as N	WLAB046	2.6	3.2	0.2	<0.1	0.1
Nitrite as N	WLAB046	<0.05	<0.05	<0.05	<0.05	<0.05
Total Organic Carbon as C *	WLAB060	<1.0	<1.0	<1.0	1.5	<1.0
Total Coliform Bacteria / 100 mℓ	WLAB021	0	22	16	62	1
Faecal Coliform Bacteria / 100 mℓ *	WLAB021	0	0	0	0	0
E. coli / 100 mℓ	WLAB021	0	0	0	0	0
Heterotrophic Plate Count / mℓ *	WLAB021	150	120	1 800	1 300	11 000
ICP-MS Scan *	WLAB050	See Attached Report: 64529-A				
% Balancing *	---	98.2	95.2	94.6	95.8	94.4

Analyses in mg/ℓ (Unless specified otherwise)	**Method Identification**	**Sample Identification**					
		BH1S 08/12/2016	**BH4 08/12/2016**	**Stream A 08/12/2016**	**Stream B 08/12/2016**	**Stream C 08/12/2016**	**Mall BH1 08/12/2016**
Sample Number		26397	26398	26399	26400	26401	26402
pH – Value at 25°C *	WLAB065	6.2	6.6	6.0	7.1	6.3	7.4
Electrical Conductivity in mS/m at 25°C	WLAB002	21.4	96.3	31.6	33.4	34.3	18.5
Total Dissolved Solids at 180°C *	WLAB003	164	704	262	274	270	136
Colour in PtCo Units *	WLAB006	20	21	16	17	17	4
Odour in T.O.N *	WLAB038	<5	<5	<5	<5	<5	<5
Turbidity in N.T.U	WLAB005	91	62	0.9	1.0	1.7	0.3
Chloride as Cl	WLAB046	7	145	12	13	13	2
Sulphate as SO_4	WLAB046	43	219	97	101	100	<2
Fluoride as F	WLAB014	0.2	0.2	0.2	0.2	0.2	<0.2
Nitrate as N	WLAB046	1.3	1.4	0.1	<0.1	0.1	0.1
Nitrite as N	WLAB046	<0.05	<0.05	<0.05	<0.05	<0.05	<0.05
Total Organic Carbon as C *	WLAB060	3.2	13	3.0	3.0	3.4	<1.0
Total Coliform Bacteria / 100 mℓ	WLAB021	390	12	4 500	650	370	0
Faecal Coliform Bacteria / 100 mℓ *	WLAB021	0	2	36	78	30	0
E. coli / 100 mℓ	WLAB021	0	0	0	44	17	0
Heterotrophic Plate Count / mℓ *	WLAB021	>100 000	41 000	3 000	200	230	<10
ICP-MS Scan *	WLAB050	See Attached Report: 64529-A					
% Balancing *	---	95.3	87.7	97.8	92.4	99.4	92.5

Analyses in mg/ℓ (Unless specified otherwise)	**Method Identification**	**Sample Identification**					
		Stream A 15/01/2017	**Stream B 15/01/2017**	**Stream C 15/01/2017**	**Mun 1 15/01/2017**	**BH1D 15/01/2017**	**BH2D 15/01/2017**
Sample Number		26403	26404	26405	26406	26407	26408
pH – Value at 25°C *	WLAB065	6.4	6.1	6.3	6.5	6.3	6.2

Electrical Conductivity in mS/m at 25°C	WLAB002	47.1	45.0	44.1	86.4	13.3	31.7
Total Dissolved Solids at 180°C *	WLAB003	348	374	362	692	90	186
Colour in PtCo Units *	WLAB006	21	20	24	20	16	6
Odour in T.O.N *	WLAB038	<5	<5	<5	<5	<5	<5
Turbidity in N.T.U	WLAB005	1.1	1.4	3.4	0.2	545	33
Chloride as Cl	WLAB046	20	18	18	23	4	59
Sulphate as SO_4	WLAB046	129	128	122	299	15	<2
Fluoride as F	WLAB014	0.3	0.3	0.3	0.5	0.3	<0.2
Nitrate as N	WLAB046	<0.1	0.1	0.1	0.7	<0.1	<0.1
Nitrite as N	WLAB046	<0.05	<0.05	<0.05	<0.05	<0.05	<0.05
Total Organic Carbon as C *	WLAB060	3.9	3.7	3.8	4.1	1.8	1.0
Total Coliform Bacteria / 100 mℓ	WLAB021	39 000	14 000	46 000	0	21 000	1 100
Faecal Coliform Bacteria / 100 mℓ *	WLAB021	36	820	1 100	0	0	3
E. coli / 100 mℓ	WLAB021	26	460	820	0	0	2
Heterotrophic Plate Count / mℓ *	WLAB021		2 500	1 100	110	28 000	770
ICP-MS Scan *	WLAB050	See Attached Report: 64529-A					
% Balancing *	---	89.8	96.2	93.6	99.2	98.9	91.1

*** = Not SANAS Accredited**
Tests marked "Not SANAS Accredited" in this report are not included in the SANAS Schedule of Accreditation for this Laboratory.

Bacteriological parameters analyzed on: 2017-01-19

WATERLAB (Pty) Ltd
Reg. No.: 1983/009165/07 V.A.T. No.: 4130107891
23B De Havilland Crescent
Persequor Techno Park
Meiring Naudé Drive
Pretoria
P.O. Box 283
Persequor Park, 0020
Tel: +2712 – 349 – 1066
Fax: +2712 – 349 – 2064
e-mail: admin@waterlab.co.za
T0391

CERTIFICATE OF ANALYSES
GENERAL WATER QUALITY PARAMETERS

Date received: 2017 - 02 - 13 **Date completed:** 2017 - 03 – 13
Project number: 215 **Report number: 65056** **Order number: 0000479885**
Client name: University of Pretoria **Contact person: Mr. M. Dippenaar**
Address: Private Bag X20, Geology Department, Hatfield, 0028 **e-mail: matthysd@icloud.com**
Telephone: 082 826 5468 **Facsimile: -** **Mobile: 082 826 5468**

Analyses in mg/ℓ (Unless specified otherwise)	**Method Identification**	**Sample Identification:**			
		Stream A	**Stream B**	**Stream C**	**BH14A**
Sample Number		28105	28106	28107	28108
pH – Value at 25°C *	WLAB065	8.5	8.2	8.3	8.4

Electrical Conductivity in mS/m at 25°C	WLAB002	51.9	43.8	50.0	57.2
Total Dissolved Solids at 180°C *	WLAB003	428	384	410	502
Colour in PtCo Units *	WLAB006	24	31	31	5
Odour in T.O.N *	WLAB038	<5	<5	<5	<5
Turbidity in N.T.U	WLAB005	0.6	2.2	2.6	0.6
Chloride as Cl	WLAB046	22	17	19	53
Sulphate as SO_4	WLAB046	121	103	133	79
Fluoride as F	WLAB014	0.3	0.3	0.3	<0.2
Nitrate as N	WLAB046	<0.1	<0.1	<0.1	10
Nitrite as N	WLAB046	<0.05	<0.05	<0.05	<0.05
Total Organic Carbon as C *	WLAB060	4.8	4.3	4.6	1.7
Total Coliform Bacteria / 100 mℓ	WLAB021	42 000	>100 000	30 000	19
Faecal Coliform Bacteria / 100 mℓ *	WLAB021	160	230	290	14
E. coli / 100 mℓ	WLAB021	160	230	290	14
Heterotrophic Plate Count / mℓ *	WLAB021	>100 000	>100 000	>100 000	27
ICP-MS Scan (Dissolved)*	WLAB050	See Attached Report: 65056-A			
% Balancing *	---	96.1	99.1	98.6	95.1

Analyses in mg/ℓ (Unless specified otherwise)	**Method Identification**	**Sample Identification:**		
		BH2D	**Mun 1**	**Athlone Dam**
Sample Number		28109	28110	28111
pH – Value at 25°C *	WLAB065	8.1	8.3	7.8
Electrical Conductivity in mS/m at 25°C	WLAB002	32.2	85.2	44.9
Total Dissolved Solids at 180°C *	WLAB003	280	702	368
Colour in PtCo Units *	WLAB006	18	11	37
Odour in T.O.N *	WLAB038	<5	<5	<5
Turbidity in N.T.U	WLAB005	304	0.4	12
Chloride as Cl	WLAB046	67	24	14
Sulphate as SO_4	WLAB046	<2	292	144
Fluoride as F	WLAB014	<0.2	0.4	0.2
Nitrate as N	WLAB046	0.1	0.4	<0.1
Nitrite as N	WLAB046	<0.05	<0.05	<0.05
Total Organic Carbon as C *	WLAB060	1.3	4.3	5.4
Total Coliform Bacteria / 100 mℓ	WLAB021	6 400	0	>100 000
Faecal Coliform Bacteria / 100 mℓ *	WLAB021	21	0	92 000
E. coli / 100 mℓ	WLAB021	21	0	82 000
Heterotrophic Plate Count / mℓ *	WLAB021	12 000	<10	>100 000
ICP-MS Scan (Dissolved)*	WLAB050	See Attached Report: 65056-A		

% Balancing *	---	94.4	95.0	94.7

*** = Not SANAS Accredited**
Tests marked "Not SANAS Accredited" in this report are not included in the SANAS Schedule of Accreditation for this Laboratory.

Bacteriological parameters analyzed on: 2017-02-13

APPENDIX 4: GEOLOGICAL LOGS

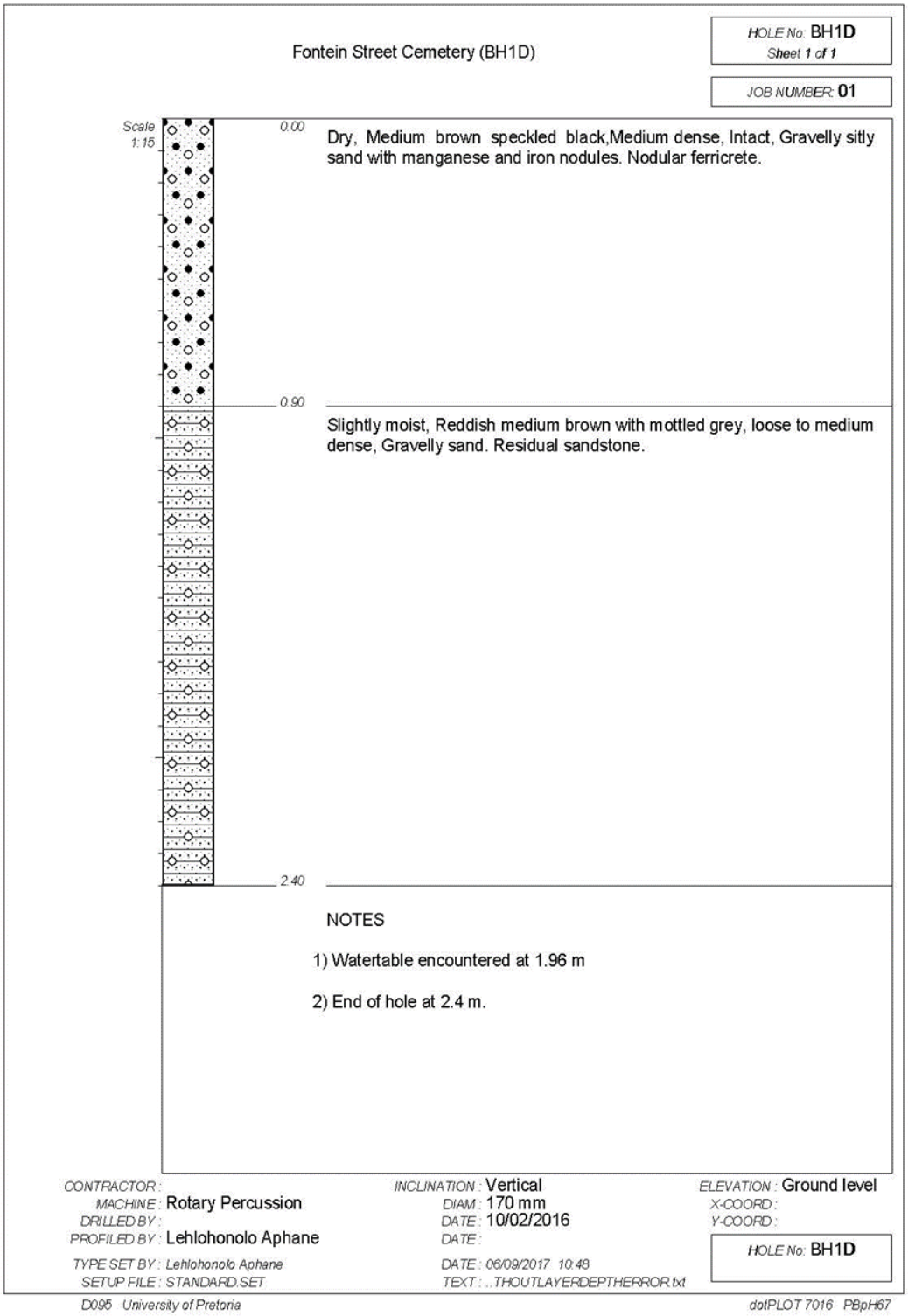

Fontein Street Cemetery (BH2D)

HOLE No: BH2D
Sheet 1 of 1

JOB NUMBER: 01

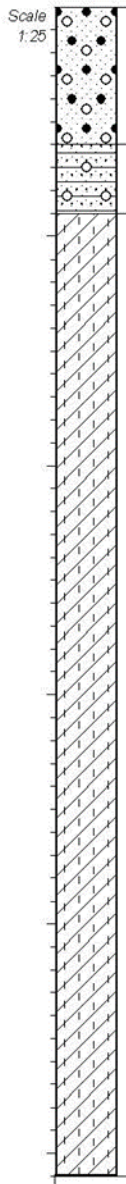

0.00 — Dry, Medium brown speckled black, Medium dense, Intact, Gravelly sitly sand with manganese and iron nodules. Nodular ferricrete.

0.60 — Slightly moist, Reddish medium brown with mottled grey, loose to medium dense, Gravelly sand. Residual sandstone.

0.90 — Very moist, Reddish grey, Muddy-dense, Fine grained, Silty Clay, Shale

5.10

NOTES

1) Watertable encountered at 4.06 m.

2) End of hole at 5.1 m.

3) Hole sunk to 8 m due to the muddy material.

CONTRACTOR :
MACHINE : Rotary Percussion
DRILLED BY :
PROFILED BY : Lehlohonolo Aphane
TYPE SET BY : Lehlohonolo Aphane
SETUP FILE : STANDARD.SET

INCLINATION : Vertical
DIAM : 170 mm
DATE : 10/02/2016
DATE :
DATE : 06/09/2017 11:12
TEXT : ..THOUTLAYERDEPTHERROR.txt

ELEVATION : Ground level
X-COORD :
Y-COORD :

HOLE No: BH2D

D095 University of Pretoria

dotPLOT 7016 PBpH67

Fontein Street Cemetery (BH3D)

HOLE No: BH3D
Sheet 1 of 1

JOB NUMBER: 01

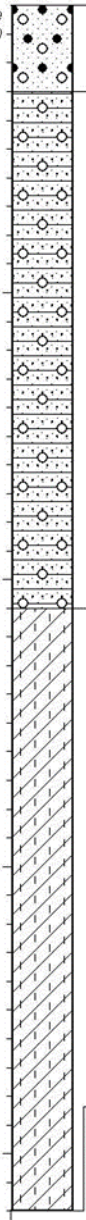

0.00 Dry, Medium brown speckled black, Medium dense, Intact, Gravelly sitly sand with manganese and iron nodules. Nodular ferricrete.

0.30 Slightly moist, Reddish medium brown with mottled grey, loose to medium dense, Gravelly sand. Residual sandstone.

2.10 Very moist, Reddish grey, Muddy-dense, Fine grained, Silty Clay, Shale

4.20

NOTES

1) No watertable encountered.

2) End of hole at 4.2 m.

CONTRACTOR :
MACHINE : Rotary Percussion
DRILLED BY :
PROFILED BY : Lehlohonolo Aphane
TYPE SET BY : Lehlohonolo Aphane
SETUP FILE : STANDARD.SET

INCLINATION : Vertical
DIAM : 170 mm
DATE : 10/02/2016
DATE :
DATE : 06/09/2017 11:08
TEXT : ..THOUTLAYERDEPTHERROR.txt

ELEVATION : Ground level
X-COORD :
Y-COORD :

HOLE No: BH3D

D095 University of Pretoria

dotPLOT 7016 PBpH67

Fontein Street Cemetery (BH3D)

LEGEND
Sheet 1 of 1

JOB NUMBER: 01

	GRAVELLY	{SA03}
	SAND	{SA04}
	SILTY	{SA07}
	CLAY	{SA08}
	SANDSTONE	{SA11}
	NODULAR FERRICRETE	{SA24}

CONTRACTOR :
MACHINE :
DRILLED BY :
PROFILED BY :

INCLINATION :
DIAM :
DATE :
DATE :

ELEVATION :
X-COORD :
Y-COORD :

LEGEND
SUMMARY OF SYMBOLS

TYPE SET BY : Lehlohonolo Aphane
SETUP FILE : STANDARD.SET

DATE : 06/09/2017 11:08
TEXT : ..THOUTLAYERDEPTHERROR.txt

D095 University of Pretoria

dotPLOT 7016 PBpH67